Prion Disease in Brain Slice Cultures

DISSERTATION

Zur

Erlangung der naturwissenschaftlichen Doktorwürde

(Dr. sc. nat.)

vorgelegt der

Mathematisch-naturwissenschaftlichen Fakultät

der

Universität Zürich

von

Jeppe Falsig Pedersen

aus

Dänemark

Promotionskommitee

Prof. Dr. med. Dr. sc. Adriano Aguzzi

Prof. Dr. phil. Dr. med. Martin E. Schwab

Prof. Dr. Michael O. Hengartner

Zürich, 2008

TABLE OF CONTENT

SUMMARY

Prion diseases or transmissible spongiform encephalopathies (TSEs) are lethal infectious diseases affecting humans and a variety of animal species. The prevailing hypothesis suggests that the infectious disease-causing particle termed "the prion" consist of a misfolded form of the normal cellular prion protein (PrP^{C}) that has been converted into a disease-associated form (PrP^{Sc}). It is believed that PrP^{Sc}, either as a monomer or as a highly order aggregate, catalyses the conversion of PrP^{C} into PrP^{Sc} and thus becomes self-propagating (i.e. infectious). The molecular composition of PrP^{Sc}, the mechanism of conversion and how the conversion leads to pathology is not clear. None-the-less, all familiar TSEs display mutations within the *Prnp* locus and ablation of *Prnp* confers resistance to TSEs in mice.

In the main part of the thesis I investigated the role of microglia in prion disease. In order to do so, I first established a novel assay allowing for prion replication in organotypic cerebellar slice cultures. These cultures are thin slices of living cerebellar brain tissue that can be kept alive for up to 26 weeks *ex vivo*. In prion infected cultures prepared from mice over-expressing PrP^{C}, PrP^{Sc} could be recovered as early as 3 weeks post-inoculation. I transmitted the prion-infected slices to a secondary prion transmission assay that allowed us to determine the amount of infectivity generated within the slices. The amount of infectivity recovered from organotypic cerebellar slices 5 weeks post-inoculation was equal to what could be recovered from a terminally scrapie-sick mouse 150 days post-inoculation. No infectivity was recovered from prion-exposed $Prnp^{o/o}$ slices. I could show that the localization and the replication properties of PrP^{Sc} in our cultures behaved similar to what is seen *in vivo.*

Next, I utilized a transgenic mouse model (CD11b-HSVTK) that allowed for the conditional depletion of microglia. Microglia could be ablated from CD11b-HSVTK slices within 2 weeks with no obvious consequences for other neural cells populations. A 15-fold increase in prion infectivity was observed 30 days post-inoculation in prion infected microglia-depleted slices relative to non-depleted slices. This increase in prion-infectivity could blocked by adding back exogenous macrophages to microglia-depleted tissue. In addition, depletion of microglia allowed for an infection of the tissue with an amount of prions that would normally not lead to

an infection. Our results strongly suggests that microglia play a role in inhibiting prion replication and could represent an important central nervous system (CNS) anti-prion defense.

For the second part of the thesis I developed a novel method to distinguish between the inoculum used to infect cells (input) and the newly synthesized prions that can be recovered from prion infected cells (output). This technique allows for the study of prion-replication in non-diving cells without the interference of persisting residual inoculum, which could interfere with the interpretation of the experiment. I use homogenates of prion-infected *C4/C4* mice that express a deletion mutant of the prion protein lacking the octa-repeat region (ΔPrP32-93). Brain homogenates from these mice can be used to infect cultures expressing the full-length prion protein. PrP^{Sc} is subsequently detected with an antibody recognizing a linear epitope in the octa-repeat region of PrP^{C}. This epitope is absent in the inoculum, but present in the newly generated PrP^{Sc}, allowing for a specific detection of *de novo* replicated PrP^{Sc}. This allows for the investigation of which post-mitotic or slowly dividing cells can be prion infected. I show with the technique that cerebellar granule neurons and astrocytes can be infected. I also show that I cannot infect microglia, most likely due to their low expression of PrP^{C}. I am currently testing which other CNS or peripheral nervous system (PNS)-derived cells can support prion replication.

Zusammenfassung

Prionenerkrankungen oder transmissible spongiforme Enzephalopathien (TSE) sind tödlich verlaufende, übertragbare Erkrankungen, die eine Vielzahl verschiedener Spezies befallen können. Eine vorherrschende Hypothese besagt, dass das infektiöse, die Erkrankung auslösende Agens – auch als „Prion“ bezeichnet – aus fehlgefaltetem normalem zellulärem Prionprotein (PrP^{C}) besteht, welches in die Erkrankungs-assoziierte Form (PrP^{Sc}) konvertiert worden ist. Man nimmt an, dass PrP^{Sc}, entweder als Monomer oder als Aggregat hoher Organisationsstufe, die Konversion von PrP^{C} zu PrP^{Sc} katalysiert und auf diese Weise im infektiösen Sinne selbst-replizierend wird. Weder die molekulare Zusammensetzung von PrP^{Sc} und der Mechanismus der Konversion, noch der Zusammenhang zwischen der Umfaltung und den zu beobachtenden pathologischen Veränderungen sind bekannt. Allerdings weisen alle familiären Fälle von TSE Mutationen im *Prnp* Lokus auf und die genetische Ausschaltung („knockout“) von *Prnp* bewirkt in Mäusen eine Resistenz gegen TSE.

Der Hauptteil der Doktorarbeit befasst sich mit der Rolle von Mikrogliazellen in Prionerkrankungen. Als Vorraussetzung hierfür musste zunächst ein neuer Assay entwickelt werden, um die Replikation der Prionen in organotypischen zerebellären Gewebskulturen („slice cultures“) zu untersuchen. Bei diesen Kulturen handelt es sich um dünne Schnitte aus lebendem zerebellärem Gewebe, welches ex vivo bis zu 26 Wochen am Leben erhalten werden kann. In prioneninfizierten slice cultures aus PrP^{C} überexprimieren Mäusen, konnte PrP^{Sc} bereits 3 Wochen nach Inokulation nachgewiesen werden. Die mit Prionen infizierten slice cultures wurden nachfolgend in einem weiteren Prionen Transmissionsexperiment untersucht, welches erlaubt die Menge an in den Kulturen erzeugter Infektiosität zu bestimmen. Die Menge an Infektiosität, welche nach 5 Wochen in den slice cultures nachgewiesen werden konnte, entsprach derjenigen einer terminal an Scrapie erkrankten Maus 150 Tage nach Inokulation. Dagegen fand sich keine Infektiosität in Prion exponierten Kulturen aus $Prnp^{o/o}$ Mäusen. Es zeigte sich, dass PrP^{Sc} in den Kulturen eine ähnliche räumliche Verteilung und Replikationseigenschaften wie in der *in vivo* Situation aufwies.

Im weiteren Verlauf wurde ein transgenes Mausmodell (CD11b-HSVTK) verwendet, in welchem eine getriggerte Depletion von Mikrogliazellen möglich ist.

Mikrogliazellen konnten aus Kulturen von CD11b-HSVTK Mäusen innerhalb von zwei Wochen ohne offensichtliche negative Konsequenzen für andere (neuronale) Zellpopulationen depletiert werden. In infizierten Mikroglia-depletierten Kulturen konnte 30 Tage nach Inokulation – im Vergleich zu nicht depletierten Kulturen – ein 15-facher Anstieg der Prion-Infektiosität beobachtet werden. Der Anstieg der Prion-Infektiosität konnte durch Zugabe von exogenen Makrophagen aufgehoben werden. Zusätzlich konnten durch die Depletion von Mikrogliazellen die Kulturen schon mit einer Prionendosis infiziert werden, die normalerweise nicht für eine Infektion ausreichen würde. Die Ergebnisse legen nahe, dass Mikrogliazellen an einer Hemmung der Replikation von Prionen beteiligt sind und einen wichtigen Abwehrmechanismus des ZNS gegen Prionen darstellen.

Im zweiten Teil meiner Doktorarbeit habe wurde eine neue Methode entwickelt, um zwischen dem für die Zellinfektion benutzten Inokulum (Input) und den neu synthetisierten Prionen, die in infizierten Zellen nachgewiesen werden können (Output), zu unterscheiden. Diese Technik erlaubt es, die Replikation von Prionen in postmitotischen Zellen ohne den Einfluss von noch vorhandenem restlichem Inokulum, welches die Interpretation des Experimentes beeinträchtigen könnte, zu untersuchen. Hierzu wurden Homogenate von Prionen infizierten C4/C4 Mäusen, welche eine Deletionsmutante des Prionproteins ohne die Oktarepeatregion (ΔPrP32-93) exprimieren, verwendet. Hirnhomogenate von diesen Mäusen können zur Infektion von Kulturen benutzt werden, welche das Volllängen Prionprotein exprimieren. In der Folge kann PrP^{Sc} mit einem Antikörper detektiert werden , der gegen ein lineares Epitop in der Oktarepeatregion von PrP^{C} gerichtet ist. Dieses Epitop fehlt im Inokulum, ist allerdings im neu entstandenen PrP^{Sc} enthalten, was einen spezifischen Nachweis von *de novo* erzeugtem PrP^{Sc} ermöglicht. Somit ist es möglich zu untersuchen, welche postmitotischen oder sich langsam teilenden Zellen mit Prionen infizierbar sind. Mit dieser Technik konnte gezeigt werden, dass Neuronen der Granularzellschicht des Kleinhirnkortex und Astrozyten mit Prionen infiziert werden können. Ausserdem wurde nachweisen, dass Mikrogliazellen nicht infizierbar sind, was am wahrscheinlichsten an den geringen Expressionsspiegeln von PrP^{C} in diesem Zelltyp liegt. Gegenwärtig wird untersucht, welche weiteren Zellen des ZNS oder des peripheren Nervensystems (PNS) die Replikation von Prionen unterstützen können.

DEFINITIONS

Prion: Agent of transmissible spongiform encephalopathy (TSE), with unconventional properties. The term does not have structural implications other than that a protein is an essential component.

'Protein-only' hypothesis: Maintains that the prion is devoid of informational nucleic acid, and that the essential pathogenic component is protein (or glycoprotein). Genetic evidence indicates that the protein is an abnormal form of PrP (perhaps identical with PrP^{Sc}). The association with other 'non-informational' molecules (such as glycosaminoglycans, or maybe even short nucleic acids) is not excluded.

PrP^{C}: The naturally occurring form of the mature *Prnp* gene product. Its presence in a given cell type is necessary, but not sufficient, for replication of the prion.

PrP^{Sc}: An 'abnormal' form of the mature *Prnp* gene product found in tissue of TSE sufferers, defined as being partly resistant to digestion by proteinase K (PK) under standardized conditions. It is believed to differ from PrP^{C} only (or mainly) conformationally, and is often considered to be the transmissible agent or prion.

Adapted from Aguzzi and Weissmann (Aguzzi and Weissmann, 1997)

ABBREVIATIONS

BSE	Bovine spongiform encephalopathy
CJD	Creutzfeldt-Jakob disease
CNS	Central nervous system
CWD	Chronic wasting disease
DPI	Days post-inoculation
DIV	Days *in vitro*
FFI	Fatal familial insomnia
GCV	Ganciclovir
GFAP	Glial fibrillary acidic protein
GPI	glycosylphosphatidylinositol
GSS	Gerstmann-Sträussler-Scheinker disease
IB_4	Isolectin-B_4
LPS	Lipopolysaccharide
MBP	Myeline basic protein
MIP-1β	Macrophage inflammatory protein-1 beta
OHSCs	Organotypic hippocampal slice cultures
PI	Propidium Iodide
PK	Proteinase K
PNS	Peripheral nervous system
POSCA	Prion organotypic slice culture assay
PrP^{C}	Cellular prion protein
PrP^{Sc}	Scrapie-associated prion protein
RML	Rocky Mountain laboratory strain
SCA	Scrapie cell assay
SCEPA	Scrapie cell assay in end point format
SCI50	Slice culture infectivity units
TCI50	Tissue culture infectivity units
TK	Herpes simplex virus thymidine kinase
TNF	Tumor necrosis factor
TSE	Transmissible spongiform encephalopathy
vCJD	Variant Creutzfeldt-Jakob disease

Introduction

Transmissible spongiform encephalopathies

Prion diseases are fatal neurodegenerative disorders, also known as transmissible spongiform encephalopathies, that affect humans and variety of captive and wild animals (Aguzzi, 2006). Known animal TSEs are restricted to a small number of species, including naturally occurring sheep and goat scrapie (Cuille and Chelle, 1939), but also chronic wasting disease (CWD) of mule deer and elk (Williams and Young, 1980), bovine spongiform encephalopathy (BSE) (Hope et al., 1989) and transmissible mink encephalopathy (Marsh and Hadlow, 1992). Human TSEs include variant and 'classical' Creutzfeldt-Jacob diseases (CJD) (Gibbs et al., 1968), fatal familial insomnia (FFI) (Medori et al., 1992), Gerstmann-Sträussler-Scheinker syndrome (GSS) (Gajdusek, 1977) and Kuru (Gajdusek et al., 1966).

TSEs can be classified as either familial dominantly inherited diseases, acquired diseases (acquired by exposure to infectious material) or as sporadic diseases if a genetic or infectious cause cannot be identified. Major neuropathological hallmarks of TSEs are extensive spongiosis, neuronal cell loss in the central nervous system, gliosis (DeArmond et al., 1993), and deposition of amyloid plaques or amorphous PrP aggregates (Bendheim et al., 1984; DeArmond et al., 1985; Manuelidis et al., 1997). The accumulation in the brain of the host-encoded prion protein PrP that is designated PrP^{Sc}, an abnormally folded form of the normal cellular prion protein (PrP^{C}) is the defining trait of TSEs. Although the exact structure and composition of the transmissible prion has not been unequivocally demonstrated, the major component of the prion agent (from *pr*oteinaceous *i*nfectious *on*ly) seems to be devoid of informational nucleic acids and is composed mainly of PrP^{Sc}.

Although many similarities to other neurodegenerative protein misfolding diseases such as Alzheimer's, Huntington's and Parkinson's disease has been described (DeArmond, 1993; Aguzzi and Haass, 2003), prion diseases are unique in that they are transmissible. Experimental disease models in species ranging from mice to cows and elk are mainly based on the observation that injection of homogenates of brain or

spleen tissue from affected individuals into another individual of the same species will typically reproduce the disease. This important fact was recognized more than half a century ago in the case of scrapie affecting sheep and goats (Cuille and Chelle, 1939).

Prion diseases in animals

Naturally occurring scrapie has been recognized in sheep and goats since the 18th century (Aguzzi, 2006). Initially the disease was dubbed "tremblante" in French because of the tremor syndrome developed by these animals. Recently several other widespread occurrences of TSEs have been observed in other wild or domesticated species of animals. Chronic wasting disease is a prion disease of captive and free-ranging mule deer and elk. The first cases of CWD were reported in the late 1960s in Colorado and the current status is that the disease has spread across most of the US and into Canada with no means of limiting the spread of disease (Sigurdson and Aguzzi, 2007). In the UK, a previously unrecognized neurological disease in cattle was first defined in 1986: the pathologic changes in brains were similar to those characteristic of TSEs. This new form of TSE, called bovine spongiform encephalopathy or more popularly, mad-cow disease, rapidly developed into a major epidemic, primarily in the UK but also in other neighboring European countries. The emergence of BSE was possibly caused by transmission of sheep Scrapie to cattle, through infected feed prepared from rendered carcasses (Wilesmith, 1988). An alternative hypothesis is that feed prepared from cattle with BASE, an atypical possibly sporadic form of BSE, could have been the cause of the UK outbreak (Capobianco et al., 2007). The routes for transmission of prions in scrapie and CWD remain elusive, but recently several possible routes of horizontal and lateral transmission has been described, such as transmission through urine in animals suffering from nephritis (Seeger et al., 2005), through milk in animals with mastitis (Ligios et al., 2005), and through saliva (Mathiason et al., 2006).

Prion diseases in humans

All prion diseases can be subdivided into inherited, sporadic and acquired forms. Several different human neurodegenerative conditions have been recognized as prion diseases: Creutzfeldt-Jakob disease, Gerstmann-Sträussler-Scheinker syndrome, Kuru, fatal familial insomnia and cases of sporadic fatal insomnia. Most cases of human

prion disease are sporadic CJD (roughly 85 %). Sporadic CJD occur at a rate of 1-3 cases per million inhabitants per year across the world, with an equal incidence in men and women. The etiology of sporadic CJD is unknown, but different hypothesis propose that sporadic CJD could be triggered by somatic *Prnp* mutations, or that a spontaneous conversion of PrP^{C} into disease associated PrP^{Sc} occurs as a rare event, leading to further generation of PrP^{Sc} and ultimately disease. Homozygosity at a common coding polymorphism at codon 129 of *Prnp* encoding either methionine or valine predisposes to the development of sporadic and acquired CJD. Acquired conditions include diseases transmitted by dietary infections, such as Kuru (caused by human-to-human transfer through ritual cannibalism) and variant CJD (vCJD) (likely caused by bovine-to-human transfer) or by other infection routes like iatrogenic contact with infected material during treatment with purified human hormones or during brain surgery. Retrospective studies in subjects suffering from Kuru, showed that prion diseases typically exhibit a very long latency period (up to 50 years) between the time of infection and the clinical manifestation: this is the reason why these diseases were originally thought to be caused by "slow viruses" (Collinge et al., 2006). About 15 % of human prion diseases are associated with autosomal dominant pathogenic mutations in the *Prnp* gene. Most pathogenic mutations in *Prnp is* thought to lead to an increased tendency of PrP^{C} to convert into PrP^{Sc}, but not all disease causing *Prnp* mutations are associated with PrP^{Sc} and infectivity.

The discovery of a variant form of CJD in the United Kingdom in 1996 was epidemiologically and experimentally linked to the widespread UK BSE epidemic in the 1980s and early 1990s. The indication that BSE is transmissible to different animal species, including humans, unlike previously characterized prion diseases such as sheep scrapie, has raised enormous public health concerns worldwide. Although it would appear that the annual new cases of vCJD has peaked (Aguzzi et al., 2007), all patients suffering from vCJD so far were homozygous for methionine at codon 129 of *Prnp*. Experiments in mice expressing different isoforms of human PrP^{C} show that valine at codon 129 of *Prnp* inhibits transmission of BSE. Mice homozygous for methionine at codon 129 replicate BSE efficiently. Mice that are heterozygous for methionine and valine at codon 129 show a delayed onset of disease, but still develop clinical disease nonetheless (Wadsworth et al., 2004). Whether this is an indication that we will see a delayed vCJD outbreak in humans heterozygous at codon 129 is

still unknown and only time will tell. To make matters worse, transmission of vCJD through donated blood from a donor, who went on to develop vCJD years after donating blood, to multiple recipients was recently described (Llewelyn et al., 2004; Wroe et al., 2006). This shows that vCJD transmit efficiently through blood and unfortunately no sensitive diagnostic method is available for detecting prions in blood, although many different assays are currently under development. The threat to public health and the emergence of new prion epidemics such as CWD and BSE has intensified research efforts to understand the molecular basis of prion diseases, understand their transmission between and within species, improve methods of diagnosis, and develop therapeutic strategies for treatment and prevention of disease.

Prion conversion reaction

The protein-only hypothesis, the prevailing hypothesis on the nature of the infectious prion, proposes that the infectious disease causing agent consists essentially of PrP^{Sc}, an abnormally folded, protease resistant, β-sheet rich isoform of the normal cellular prion protein, denoted PrP^{C} (Prusiner, 1991). The notion that a protein might be the infectious agent causing TSEs was first proposed by Griffith (Griffith, 1967). This idea was later substantiated by Stanley Prusiner who suggested that this protein (discovered and named by him) was the prion protein, work for which he was rewarded the Nobel price (Prusiner, 1982). Subsequently the prion concept was further refined by Charles Weissmann (Weissmann, 1991) to mean an infectious protein that does not contain any informational nucleic acids, and its infectivity propagates by recruitment and "autocatalytic" conformational conversion of cellular prion protein into disease-associated PrP^{Sc} (Aguzzi et al., 2007).

The amount of evidence speaking in favor of the prion-only hypothesis is abundant, but several key observation bears mentioning. First of, familial cases of human TSEs are all characterized by *Prnp* mutations linking *Prnp* to prion disease (Prusiner et al., 1998). Indeed knockout mice carrying a homozygous deletion of the *Prnp* gene that encodes PrP^{C}, fail to develop disease upon inoculation with infectious brain homogenate (Büeler et al., 1993). Excitingly, it has now been shown that *de novo* prion infectivity can be generated by sonicating a mixture of lipids, synthetic poly-anions, and native PrP^{C} purified from normal hamster brain (Deleault et al., 2007).

External confirmation of these results should lay to rest the debate about the validity of the prion-only hypothesis and shift the focus of research to the nature of the infectious prion agent.

Prion diseases are associated with abundant accumulation of PrP^{Sc} in the CNS. PrP^{Sc} and PrP^{C} were found to share a similar amino acid structure but no known covalent modifications has been found to differentiate the 2 proteins (Stahl et al., 1993). It is therefore proposed that PrP^{Sc} is a posttranslational derivative of PrP^{C} having acquired a different 3-dimensional (3D) conformational structure and that pathologic PrP^{Sc} operates as a template promoting further conversion of PrP^{C}. The resolution of the 3D structure by NMR of mouse, hamster and human PrP^{C} (Riek et al., 1996; James et al.,

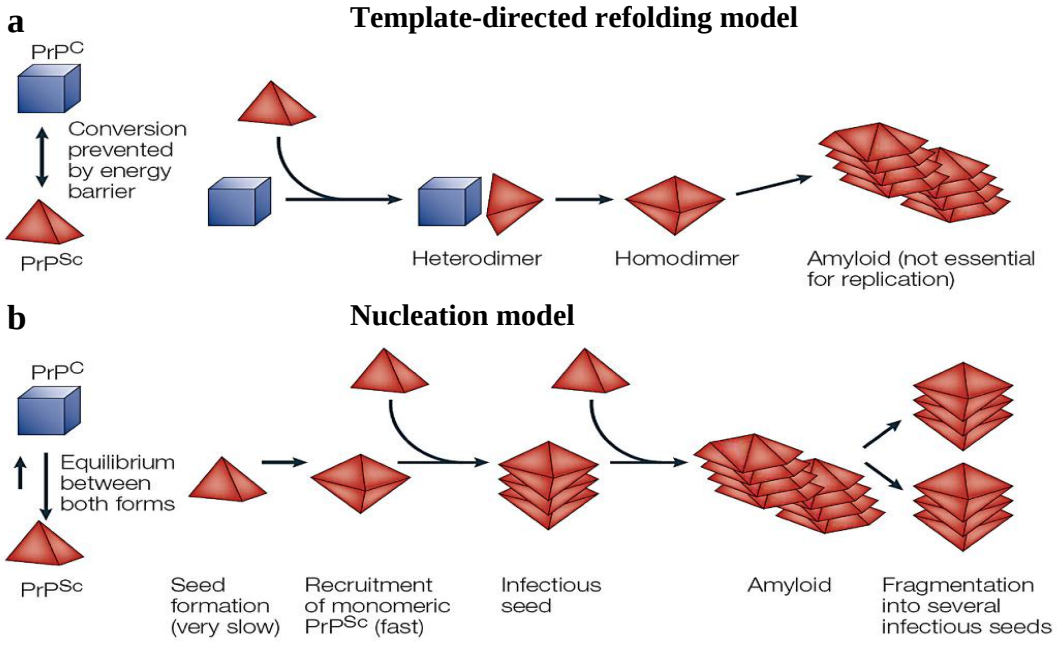

Figure 1. Models for the Conversion of PrP^{C} into PrP^{Sc}

(**a**) The 'Template-directed refolding model' postulates an interaction between PrP^{Sc} and PrP^{C}, which is subsequently induced to transform itself into PrP^{Sc}. A high energy barrier may prevent spontaneous conversion of PrP^{C} into PrP^{Sc}. (**b**) The 'nucleation-polymerization model' proposes that PrP^{C} and PrP^{Sc} are in a reversible thermodynamic equilibrium. Only if several monomeric PrP^{Sc} molecules form a highly ordered seed, can further monomeric PrP^{Sc} entities be recruited and eventually generate larger aggregates with an amyloid structure. Within such a crystal-like seed, PrP^{Sc} becomes stabilized. Fragmentation of PrP^{Sc} aggregates increases the number of nuclei, which can then recruit further PrP^{Sc} and thus replicate the prion agent (adapted from (Aguzzi and Polymenidou, 2004)).

1997; Hosszu et al., 1999) and the development of newer techniques to study amyloids such as hydrogen/deuterium exchange has provided some suggestions for a possible conversion mechanism (Lu et al., 2007). However, the high increase in β-sheet content of PrP^{Sc} (43 %) compared to PrP^{C} (only 3 %) has prevented the generation of a high resolution structure of PrP^{Sc} and the understanding of the conversion event itself. The structural transition is accompanied by profound changes in the physicochemical properties of the prion protein. While PrP^{C} is soluble in mild detergents and sensitive to proteinase K (PK) digestion, PrP^{Sc} forms insoluble aggregates and is partially resistant to PK (Bolton et al., 1982; Oesch et al., 1985; Meyer et al., 1986). Attempts to purify PrP^{Sc} by fractionation and correlating the mass of the purified (mainly) protein complexes to the infectivity of the samples, indicates that the most infectious prion particle has a mass corresponding to 14-28 PrP molecules (Silveira et al., 2005).

Nonetheless, 2 different hypothesis have been put forward to explain the pathological conversion of PrP^{C} into PrP^{Sc}. The first model, "the template-directed refolding model", postulates that a strong kinetic energy barrier prevents PrP^{C} from spontaneously misfold into PrP^{Sc}. Overcoming of the high energy barrier is only possible in the presence of a misfolded PrP^{Sc} template. Sporadic CJD may come about through a very rare spontaneous conversion of PrP^{C} to PrP^{Sc}, giving rise to a template-assisted conversion cascade. Possibly with the help of a chaperone (designated protein X) (Telling et al., 1995) or a non-protein molecule such as glucosaminoglycans or short nucleic acids (Priola et al., 2003).

The second hypothesis "the nucleation model" proposes that PrP^{C} and PrP^{Sc} exist in a natural equilibrium heavily shifted towards PrP^{C}, so that only minute amounts of PrP^{Sc} would coexist with PrP^{C}. PrP^{Sc} is stabilized by polymerizing onto a crystal-like seed, fibril or aggregate of PrP^{Sc}. Seed formation is an extremely slow event, but once a seed has been generated, monomers can add on rapidly. According to this "nucleation hypothesis" (Jarrett and Lansbury, 1993), the aggregated state and not necessarily the misfolded form of PrP, would be an intrinsic property of infectivity. Monomeric PrP^{Sc} would be harmless, but it would be prone to incorporation into nascent PrP^{Sc} aggregates leading to disease. However, both models fail to explain some aspects of TSEs, suggesting that component might be missing in the equation. Mainly, both models fail to explain that if spontaneous conversion of PrP^{C} to PrP^{Sc} or

the formation of a PrP^{Sc} seed is a rare, but random event, why then does sporadic TSEs occur exclusively in elderly patients? If it was a truly random event, sporadic CJD should occur both in young, as well as in elderly people, which is clearly not the case. The missing part of both models could be a cellular clearing mechanism capable of PrP^{Sc} removal. An age-related failure of this system combined with the stochastic generation of PrP^{Sc} could then lead to the formation of seeds and the pathological manifestation of disease. However, no genetic or experimental evidence exist for such a mechanism.

Because PrP^{C} can undergo disease-associated structural modifications that do not impart protease-resistance, the term PrP^{Sc} has more recently been used to denote protease-sensitive pathological PrP variants (Safar et al., 2002). In this thesis PrP^{Sc} refers exclusively to protease-resistant PrP and the term 'prion' is used to described the infectious prion agent (as measured by transmission experiments).

Prion pathogenesis

The mechanisms of prion pathogenesis leading to gliosis, spongiosis, neuronal cell loss and clinical signs are not yet understood. Mice devoid of PrP^{C} do not show any overt behavioral phenotype or signs of neurodegeneration (Büeler et al., 1992), suggesting that prion diseases are not caused by a loss-of-function associated with PrP^{C}. Indeed the absence of PrP^{C}, abolishes prion replication and clinical signs upon intracerebral inoculation with prions (Büeler et al., 1993).

Clearly PrP^{C} expression is crucial for prion replication, but does cerebral accumulation of PrP^{Sc} in the extracellular space suffice to damage nervous cells? To answer this question, Brandner *et al*. (Brandner et al., 1996) transplanted wild-type and PrP overproducing neuroectodermal grafts into brains of PrP knockout mice. After intracerebral inoculation with prions, the grafts accumulated high levels of PrP^{Sc} and infectivity and developed typical histopathological changes associated with scrapie pathogenesis. In the surrounding PrP-deficient tissue, no pathological changes were detected even when substantial accumulation of PrP^{Sc} occurred, indicating that neuronal cytotoxicity of PrP^{Sc} is dependent on the expression of cellular PrP^{C} by target cells. This was later confirmed in mice expressing a secreted form of PrP^{C} termed 'GPI-anchorless' (a secreted PrP molecule lacking the

glycosylinositolphospholipid-anchor (GPI)) (Chesebro et al., 2005). While the mice replicated PrP^{Sc} upon prion inoculation, the mice did not develop histopathological changes, illustrating that membrane attachment of PrP is required for cellular toxicity. In addition, it was recently described that early signs of prion pathogenesis such as spongiosis and behavioral symptoms can be can be reversed by conditionally removing PrP^{C} selectively in neurons after disease onset (Mallucci et al., 2003; Mallucci et al., 2007). All together this suggests that prion replication within neurons could be a target for anti-prion intervention strategies.

The cellular prion protein

PrP^{C} expression pattern

The cellular prion protein is highly conserved in mammals and has been identified in birds (Harris et al., 1993), in amphibian (Strumbo et al., 2001), in turtles (Simonic et al., 2000) and more recently in fish (Rivera-Milla et al., 2003), suggesting an important function of PrP^{C}. Despite the lack of a phenotype in PrP-deficient mice, no naturally occurring *Prnp* null alleles have been described despite the notion that a negative evolutionary pressure exist, stemming from the susceptibility of *Prnp*-expressing animals to prion disease (Mead et al., 2003).

PrP^{C} is highly expressed in the central nervous system, but it is also expressed at high levels in a broad range of peripheral tissues and cells including heart, skeletal muscle, kidney and lymphocytes (Dodelet and Cashman, 1998; Ford et al., 2002). Inflammatory conditions can induce ectopic PrP^{C} expression and prion replication competence in organs that only express very low amounts PrP^{C} under normal circumstances (Heikenwalder et al., 2005). In the central nervous system PrP^{C} is expressed to a high extend on neurons, although it is also expressed by other neural cell lineages including astrocytes and oligodendrocytes (Moser et al., 1995). In contrast, microglia express almost no, if any, PrP^{C} (Baker et al., 2002).

Biosynthesis of PrP^{C}

The newly transcribed unprocessed mouse PrP polypeptide consists of 254 amino acids. A 22 amino acids N-terminal hydrophobic signal sequence (in mice and hamsters) directs PrP to the membrane of the endoplasmic reticulum (ER), where the

signal peptide is removed. After ER translocation, 23 amino acids are removed from the C-terminus and replaced with a GPI-anchor (Stahl et al., 1987). Within the ER lumen, high mannose glycans are attached to the 25 kDa polypeptide on asparagines at residues 180 and 196 and processed to complex glycans during transport through the Golgi apparatus (Bolton et al., 1985). The mature form of PrP^{C} is transported within secretory vesicles to the external cell surface to which it is anchored by the GPI-moiety. The presence of 1 out of the 2 glycosylations is sufficient for an appropriate PrP-trafficking, but the deletion of both glycosylations causes intra-cellular accumulation of PrP^{Sc} (Cancellotti et al., 2005). In cell culture, most PrP^{C} molecules undergo endocytosis and degradation via the lysosome or proteasome pathway (Caughey et al., 1989), but about 10-30 % of PrP^{C} is shed into the medium (Borchelt et al., 1990).

The physiological function of PrP^{C}

The expression of PrP on the cell surface as a GPI-anchored extracellular molecule suggest a role in cell adhesion, cell-cell interaction or as a signalling molecule. Mice ablated of PrP^{C} was initially reported to lack any phenotype (Büeler et al., 1992). However, later reports suggested subtle alterations in hippocampal synaptic function (Collinge et al., 1994) and in circadian rhythm and sleep-pattern of PrP-deficient mice (Tobler et al., 1996). Post-developmental ablation of PrP^{C} was also reported to lead to subtle alterations in hippocampal synaptic function, identical to what was seen in PrP-null mice, excluding that compensatory developmental effects are masking a stronger PrP-related phenotype (Mallucci et al., 2002). Unfortunately, most of these results could not be reproduced by other groups (Herms et al., 1995; Lledo et al., 1996). PrP^{C} was recently suggested to be important for the self-renewal of long-term repopulating haematopoietic stem cells (Zhang et al., 2006) and a positive regulator of neural precursor proliferation during developmental and adult neurogenesis (Steele et al., 2006). The lack of understanding of the molecular action of PrP^{C} and even more the relative mildness of the described alterations in animals devoid of PrP^{C} renders it difficult to attribute a direct role to PrP in any of these functions. Furthermore, it begs the question as to why PrP^{C} is evolutionarily conserved if animals live fine without it.

PART I

Part I of my thesis is an extended version of the publication Falsig et al., Nature Neuroscience (2008). It also contains a modified figure from the publication of Heppner et al., Nature Medicine (2005), as well as unpublished data.

Introduction

Prion bioassays

The most common technique for measuring prions consists of inoculating test material intracerebrally into susceptible "indicator" animals. Precise titer determinations require determination of end-point dilutions, and therefore very large numbers of indicator animals. The incubation time is inversely proportional to the size of the inoculum, allowing for a simplified incubation-time bioassay which sacrifices precision yet requires much fewer animals (Prusiner et al., 1982). Conversely, these assays require observation periods that often span the entire natural life of indicator animals, as small amount of infectivity may go along with exceedingly long incubation times. This is impractical and very expensive. In addition, minimizing the numbers of animals used for titration would reduce the suffering wrought by experimental prion infections.

The introduction of the scrapie cell assay in end-point format (SCEPA) has eliminated some of the concerns listed above, and has allowed for a dramatic acceleration of infectivity assays (Klohn et al., 2003). Here, cells are exposed to end-point titrations of prions and are subsequently passaged several times. Prion titers are derived by counting PrP^{Sc}-positive tissue culture wells. Although the SCEPA does not require inoculation of animals, it is biologically equivalent to animal bioassays in that it detects actual transfer of prion infectivity from test materials to susceptible cells. However, the SCEPA suffers from 2 major limitations. Firstly, the infection of cultured cells reproduces only certain aspects of the *in vivo* situation. The reactions of the CNS to a prion infection involve multiple, highly diverse cell types such as neurons, astrocytes, oligodendrocytes, and microglia. This diversity cannot be reproduced in the SCEPA which is based on monoclonal, highly homogeneous cells.

Secondly, the spectrum of cell lines that have been identified as susceptible to prion infection *in vitro* is very limited. This presently restricts the applicability of the SCEPA to a small subset of mouse-adapted prion strains. These 2 limitations may be interdependent, since the molecular machinery necessary for overcoming strain and species barriers may reside in cells different from those replicating prions most efficaciously. Be as it may, infectivity titrations of any prion variant that does not efficiently infect cultured cells still require animal bioassays.

The prion strain phenomena

Prion strains are infectious isolates that when transmitted into identical hosts exhibits different prion disease phenotypes. The strain characteristics can differ in incubation times, histological lesion profiles, organ-tropism (e.g. lympho-tropism), biophysical characteristics and neuronal target areas (Aguzzi et al., 2007).

Strain-specific properties might be obtained by PrP^{Sc} adopting different specific disease associated conformations, all of which can transmit and cause disease, with the disease phenotypes being determined by the specific conformation of PrP^{Sc} in the donor inoculum. Circumstantial evidence indicates that strain phenotypes might be encoded within different PrP^{Sc} conformations with distinct properties. This is supported by evidence suggesting that different prion strains have different stability against chaotropic salts and heat (Safar, 1998) and susceptibility to digestion with PK. In addition, the site of protease digestion can vary with different prion strains. Various, naturally occurring, BSE and CJD cases exhibit distinct running patterns on western blots after digestion with PK (Casalone et al., 2004; Zanusso et al., 2004). Different strains can be cleaved with PK a different sites in the N-terminus (Zanusso et al., 2004), suggesting a difference in the accessibility of the N-terminal part of the PrP^{Sc} molecule, supporting the idea that PrP^{Sc} conformation can encode strain phenotypes. Of note, it has been shown that different strain phenotypes can co-exist within the same individual (Polymenidou et al., 2005; Yull et al., 2006). However, the final proof that conformational variants of PrP^{Sc} represent the biological basis of prion strains is still amiss. Other biochemical traits of strains can be differences in the glycosylation patterns (i.e. the ratio of un-, mono- and diglycosylated forms of PrP) (Collinge et al., 1996). It was recently suggested that the ratio of distinct glycoforms may determine the structure of the infectious seed and thus confer strain properties

(Collinge, 2005). In addition, certain aspects of the strain properties are encoded by host-encoded PrP^C (Nonno et al., 2006).

As described above, various prion cell culture assays, based upon clones of cells selected for an efficient prion replication, are highly selective in which experimental prion strains they can replicate (Klohn et al., 2003; Solassol et al., 2003). Recently, primary neuronal cell cultures have been reported to display a broader selectivity towards different strains, showing properties similar to transmission of prions into mice (Cronier et al., 2007). Screening the susceptibility of any new prion assay to a collection of different strains therefore is a crucial parameter.

The role of microglia in prion diseases

Microglia, a CNS cell of myeloid origin, is considered the main immune cell of the brain. One of the primary roles of microglia is to act as a sentinel, detecting and responding to early signs of cellular damage or infection in the brain (Nimmerjahn et al., 2005). When damage has been detected, microglia can differentiate into various phenotypically distinguishable microglia types, depending of the type of stimuli they encounter. The distinction between the microglia phenotypes are not well described and appear to be somewhat overlapping. In general, microglia can be phagocytic (microglia capable of eating damaged cells, protein aggregates or pathogens), pro-inflammatory (releasing large amounts of pro-inflammatory cytokines, chemokines and reactive oxygen species) and neuroprotective (releasing neurotrophic factors and supporting CNS regeneration) (Schwartz et al., 2006). It is believed that activated microglia contribute directly to the progression of prion pathology by releasing inflammatory and neurotoxic factors (Brown et al., 1996; Dandoy-Dron et al., 1998; Baker and Manuelidis, 2003; Baker et al., 2004; Kercher et al., 2007). However, anti-inflammatory properties of microglia have also been reported in certain prion models (Boche et al., 2006). Activation of microglia in prion infections is very extensive and precedes significant neurodegeneration (Manuelidis et al., 1997; Williams et al., 1997). Microglia are abundantly associated with prion plaques, and PrP^{Sc} can sometimes be found within microglia (Manuelidis et al., 1997; Andreoletti et al., 2002). Hence microglia may exert either precipitating or defensive effects in prion pathogenesis.

Outline of this work

Here I have investigated whether *ex vivo* cultures of tissues derived from wild-type or from genetically modified mice might help circumventing the limitations described above. I found that organotypic cerebellar slice cultures efficiently and rapidly amplify PrP^{Sc} after exposure to prions. This paradigm allows for dissecting CNS pathologies in a complex cellular environment which is morphologically very similar to the intact brain. The sensitivity of the prion organotypic slice culture assay (POSCA) was marginally lower than that of the SCEPA. While the POSCA makes use of animals as the original tissue donors, many genetically identical slices can be produced from each individual mouse. Thus, genetic background differences of mice can be controlled by comparing samples prepared from the same individual mouse. In addition, POSCA are capable of replicating a large variety of prion strain of scrapie and BSE origin, including strains that do not replicate in the SCEPA.

Since POSCA allows for the study of prion replication in a complex cellular environment the assay is ideally suited to study the function of microglia in prion diseases. I found that complete microglial ablation from slices generated from *CD11b-HSVTK* transgenic mice led to a dramatic increase in prion titers and PrP^{Sc} deposition. These data suggest that microglia plays a significant role in containing prion loads during the course of prion infections.

RESULTS

Prion Organotypic Slice Culture Assay

Culture establishment

In order to develop a slice culture based prion assay I utilized the membrane-insert based slice culture technique developed by Luc Stoppini (Stoppini et al., 1991). Various culturing conditions were tested, including the age of mice used for preparing slices, the method of slice preparation, culture medium compositions, as well as volume and frequency of media changing. The best results were consistently achieved when slices were prepared by vibratome sectioning, and were cultured on Millicell-CM Biopore^{TM} BTFE membranes. The full volume of medium was exchanged 3 times each week. Firstly, I assessed the morphological integrity of slices by standard light microscopy and immunohistochemistry. These studies uncovered that slices could be kept in culture without losing their defining morphological traits, including expression of neuronal, astrocytic, and myelin markers (Figure 2). Some

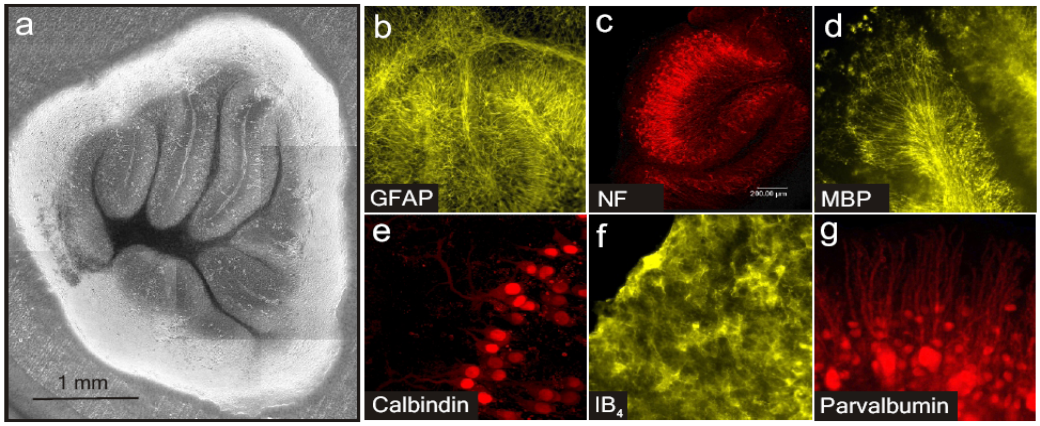

Figure 2. Morphological integrity of organotypic cerebellar slice cultures

(**a**) A composite phase contrast image of an organotypic cerebellar slice 5 weeks in vitro. The image was generated from 7 independent images (5x magnification). Major morphological features were visualized by fluorescent microscopy. Slices were stained with (**b**) rabbit α-glial fibrillary acidic protein (GFAP) polyclonal antibody (astrocytes), (**c**) rabbit α-neurofilament-M polyclonal antibody (axons of Purkinje neurons), (**d**) rat α-myelin basic protein (MBP) IgG_{2a} (myelin), (**e**) mouse α-calbindin IgG_1 (cell bodies of Purkinje neurons), (**f**) isolectin-B_4 (microglia), and (**g**) mouse α-parvalbumin IgG_1 (GABAergic interneurons).

morphological features were slightly altered in our culture system. After 2 weeks in culture approximately 1-2000 microglia and a few fibroblasts migrated out of the tissue and onto the membrane. An increased GFAP expression was seen after 1 week in culture and astrocytes extended a few processes outside the tissue, however no astrocytes could be found outside the tissue. The various cell layers displayed a progressive spreading over time, but in general the tissue appeared morphologically intact (Figure 2).

As prion infections are extremely slow processes *in vivo*, I reasoned that successful slice culture infection would crucially depend on the establishment of organotypic cultures with the greatest possible longevity, defined as the span of time during which cell death within slices does not rise above 5 %. Slice viability was assessed after 5 weeks of culturing by propidium iodide (PI) permeability and DEVDase activity assays (Figure 3a-c). These assays measure the total extent of cell death and the

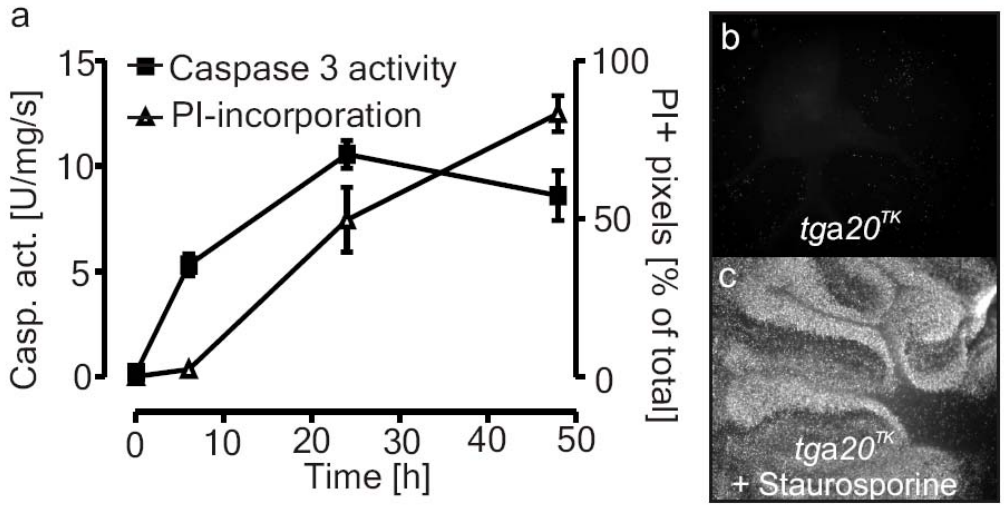

Figure 3. Viability of cerebellar slice cultures

(**a**) Time course of cell death induced by staurosporine treatment of cerebellar slice cultures cultured for 5 weeks *in vitro*. For generation of standardized positive controls, slices were cultured for 5 weeks and treated for different lengths of time with 5 µM staurosporine, a compound known to induce apoptotic death of neuronal cultures and PI incorporation (10 µg/ml) was measured (*n = 12*). Slices were harvested and caspase-3 enzymatic activity was measured and normalized to protein contents (*n = 3* pools of 4 slices). (**b-c**) Representative examples of images used for PI incorporation.

activation of executioner caspases. For control, slices were treated with staurosporine, which induces apoptotic death of granule neurons in culture. After 35 days *in vitro*, untreated slices showed 0.1 ± 0.02 % of the PI^+ cells (or < 0.1 ± 0.02 % of the total tissue surface area) and 2.1 ± 0.6 % of the DEVDase activity levels seen in staurosporine-treated slices. I conclude that acceptable slice viability was maintained during a period of up to 5 weeks. Morphological and immuno-histochemical analyses with various markers of CNS constituents (see Figure 9) supported the latter contention.

Prion infection of organotypic slice cultures

The most broadly used assays for assessing the presence of prion infections rely on the differential susceptibility of PrP^C and PrP^{Sc} to digestion with proteinase K (Bolton et al., 1982). The relative resistance of PrP^{Sc} to PK depends on prion strains, on the specific activity of PK, as well as on the composition and concentration of non-PrP contaminants. I therefore sought to determine the minimal conditions under which all PrP^C present in slices would be fully degraded by PK. Protein lysates were prepared from 5-week old slices, subjected to digestion with various concentrations of PK, and their PrP^C content was probed by western blotting (Figure 4a). Digestion of 20 µg protein lysate with 25 µg/ml PK (in a reaction volume of 20 µl, corresponding to 1 mg/ml total protein) was found to ensure complete, reproducible removal of PrP^C. These conditions were used in all subsequent experiments unless otherwise stated.

In a first set of experiments, I inoculated 3-day old pups *in vivo* with a relatively large inoculum intracerebellarly (3 µl, 1 % RML6) using a Hamilton syringe. Cultures were prepared from inoculated pups at 9 days post-inoculation (dpi) (illustrated in Figure 4b). Slices were cultured for 35 days *in vitro*, harvested, and assayed for PrP^{Sc}. No PK-resistant material was detected in any of 6 inoculated animals (Figure 4c). This outcome is consistent with multiple reports that prions undergo a long period of eclipse after intracerebral challenge, during which no infectivity can be recovered from the site of inoculation (Manuelidis and Fritch, 1996).

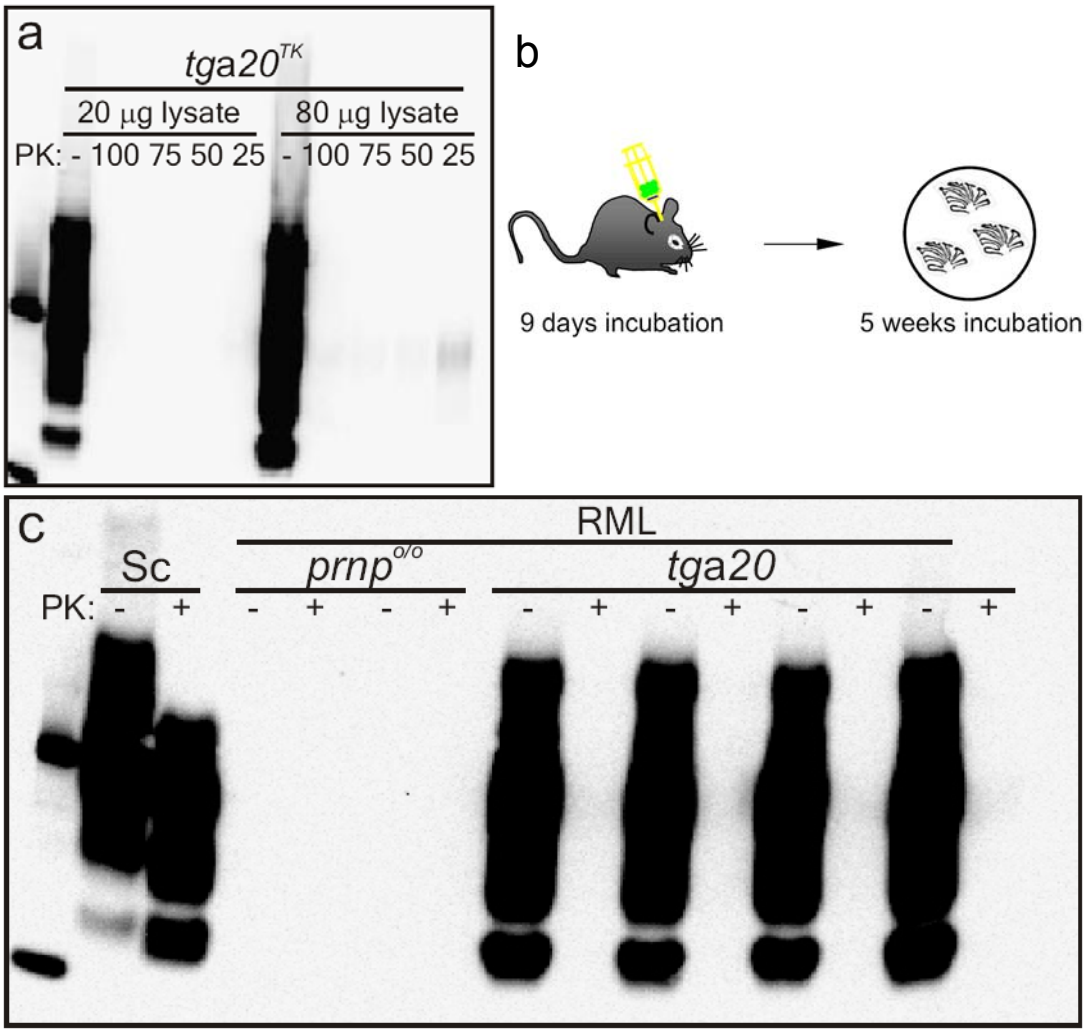

Figure 4. Cerebellar slice cultures prepared from infected mice

(**a**) Western blotting of PK-digested slice culture homogenates from cultures 5 weeks *in vitro*. Various PK concentrations (25-100 µg/ml) were used to digest 20 or 80 µg protein lysate and detected with mouse anti-mouse PrP^C IgG_1 (POM-1). 20 µg/ml PK represents the minimal PK-concentration needed to fully digest PrP^C in *tga20*^{TK} slices. (**b**) Scheme depicting set-up for slice cultures of prion inoculated mice. 3-day old *tga20* or *Prnp*$^{o/o}$ pups were inoculated with 300 ng RML6 (3 µl, 1% brain homogenate) injected into the cerebellum. Cerebellar slices were prepared from 12-day old *tga20* mice (9 days post-infection) and kept 35 days *in vitro*. (**c**) No PK-resistant material was observed in slices prepared from RML-treated *tga20* mice or RML-treated *prnp*$^{o/o}$ mice. Abundant PK-resistant material was found in brain homogenates from a terminal scrapie-sick *C57BL/6* mouse (Sc).

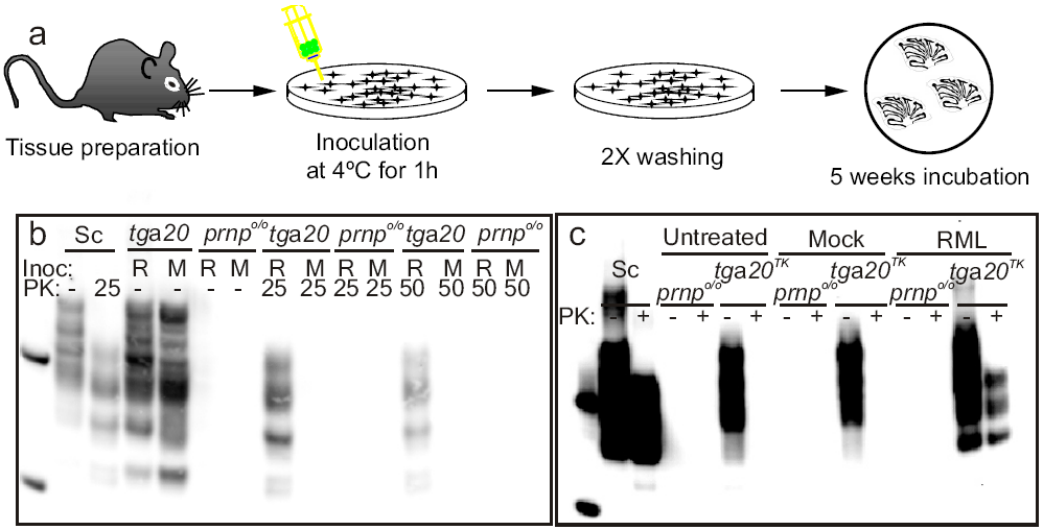

Figure 5. Establishment of in vitro prion infection

(**a**) Scheme depicting set-up for *in vitro* infection of cerebellar slice cultures. Slice cultures were prepared from 12-day old mice and incubated with 20 mg RML6 (**R**) or mock brain homogenate (**M**) and kept 5 weeks *in vitro*. (**b**) Inoculated tissue was digested with 25 or 50 µg/ml PK. (**c**) Western blotting was performed on 20 µg protein digested with 25 µg/ml PK (+) or 10 µg non-digested protein (-).

Next, I prepared organotypic cultures from non-inoculated 10-day old *tga20*^{TK} (the F1 offspring of *tga20*$^{+/+}$ males crossed to *CD11b-HSVTK* females) and *Prnp*$^{o/o}$ pups. Groups of 10 slices were incubated with 1 ml of medium containing 20 mg of RML6 homogenate (total brain homogenate from pooled, terminally sick CD-1 mice infected with RML prions). In order to minimize any potential toxicity stemming from cellular debris, exposure to the prion inoculum was carried out at 4°C in the presence of a non-selective glutamate receptor antagonist. The tissue was washed twice in 6 ml buffer and transferred to Millicell-CM Biopore^{TM} BTFE membranes (illustrated in Figure 5a).

After 5 weeks *in vitro,* slices were harvested and analyzed by western blot (Figure 5b). An equal amount of brain material from the same terminally scrapie sick C57BL/6 mouse (Sc) was loaded onto the first lanes of all blots as a positive control. In *tga20*^{TK} cultures infected with RML6, a characteristic triplet band pattern representing the di, mono and un-glycosylated forms of PrP^{Sc} was observed irrespectively of whether 25 or 50 µg/ml of PK was used. Levels were comparable to

those seen in the terminally scrapie sick C57BL/6 mouse (Figure 5b, lane 3,8,12). RML6-exposed slices deficient in PrP^C expression, as well as slices exposed to uninfected brain homogenate ("mock" inoculum), did not show any PK-resistant material Figure 5b-c, lanes 6,7,9-11,13-15). A strong high-molecular band was observed in undigested RML-infected *tga20*^{TK} samples, but not uninfected samples, showing an RML-induced shift in the post-translational modification of PrP^C (Figure 5b, lane 4,5).

Correlation of inoculum dilution and PrP^C template expression with PrP^{Sc}

I examined the possibility that the PK-resistant PrP signal I observed might be due to residual inoculum adhering to slice constituents. I therefore performed titration experiments using varying amounts of inoculum. PrP^{Sc} was clearly detected in *tga20*^{TK} cultures treated with as little as 1 µg RML6 homogenate per 10 slices (Figure 6a, lane 15). In RML-treated cultures deficient for PrP^C (n = 5) or in mock-treated cultures (n = 5) no PK-resistant material was observed even when the tissue was treated with 10 mg inoculum, showing that PrP^{Sc} was amplified at least 10^4-fold in *tga20*^{TK} slices (Figure 6a, lane 6). The differences in PrP^{Sc} levels were not due to changes in PrP^C expression (Figure 6b).

To illustrate that replication had taken place in *tga20*^{TK} cultures inoculated with 1 µg RML6, PrP^{Sc} levels were compared by Western blotting to a dilution curve of RML6 diluted in uninfected brain homogenate. The total amount of protein recovered from the RML-infected slices was 400 µg, of which only 20 µg (5 %) were loaded onto the blot (Figure 7, lane 10). In the unlikely event that 100 % of the inoculum used to infect the cultures (1 µg) was recovered 5 weeks post inoculation; maximally 50 ng (5 %) of inoculum could have been loaded onto the blot. The PrP^{Sc} band intensity for the RML-infected sample (containing at most 50 ng RML6) corresponded to the band intensity of a dilution containing 2000 ng RML6 (Figure 7, lane 5 compared to lane 10). Since I detect 40 times more PrP^{Sc} than what I initially treated the tissue with, I conclude that an amplification of PrP^{Sc} indeed has taken place.

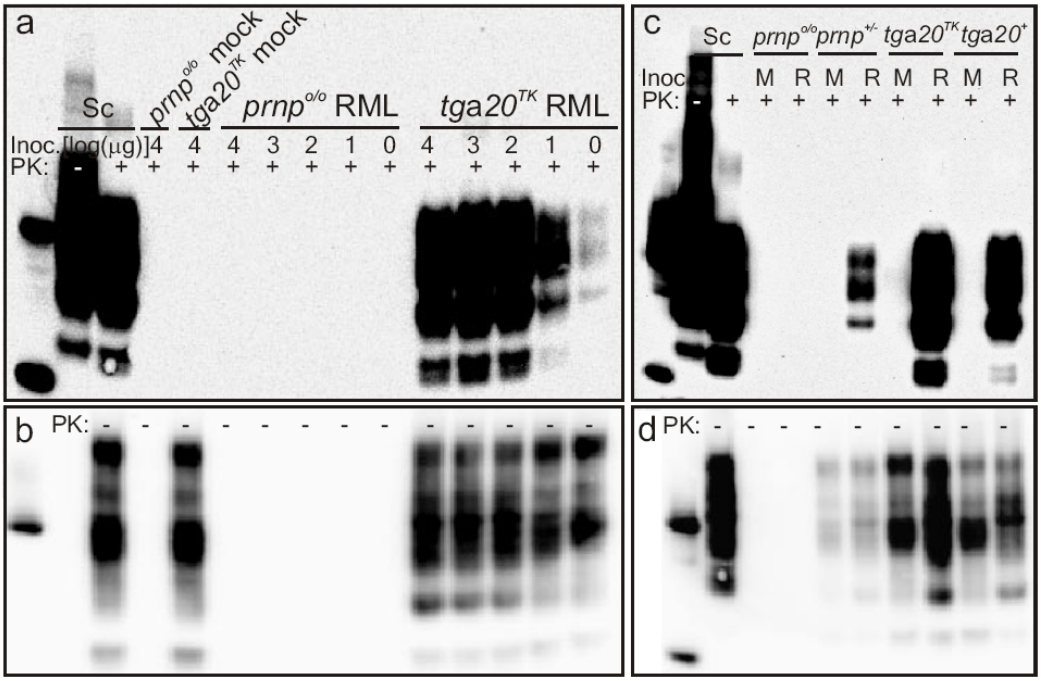

Figure 6. Titration of inoculum concentration and host PrP^{c} expression

Cultures from *tga20*^{TK} and *Prnp*$^{o/o}$ mice were inoculated with various concentrations of RML6 or mock brain homogenate and cultured for 35 days prior to harvesting the tissue. (**b**) Non-digested samples from blot **a**. (**c**) Cultures prepared from *tga20*^{TK}, *tga20*$^{+}$, *Prnp*$^{+/o}$ or *Prnp*$^{o/o}$ were inoculated with 1 mg RML6 or mock. The tissue was harvested after 35 days *in vitro*. (**d**) Non-digested samples from blot **c.**

The expression levels of PrP^{C} in host animals are negatively correlated to the incubation times *in vivo* (Büeler et al., 1993). In order to test for the impact of host PrP-expression levels on PrP^{Sc} replication I infected cultures from *tga20*^{TK} (heterozygous for *Prnp*$^{+/o}$ and *tga20*$^{+}$), heterozygous *Prnp*$^{+/o}$ mice, or *tga20*$^{+}$ mice. I then compared PrP^{Sc} levels after inoculating the cultures with 1 mg RML6. I observed a clear correlation between host expression of PrP^{C} (*tga20*^{TK} > *tga20*$^{+}$ > *Prnp*$^{+/o}$, Figure 6d) and the amount of PrP^{Sc} observed in the cultures 5 weeks post-inoculation (*tga20*^{TK} > *tga20*$^{+}$ > *Prnp*$^{+/o}$, Figure 6b).

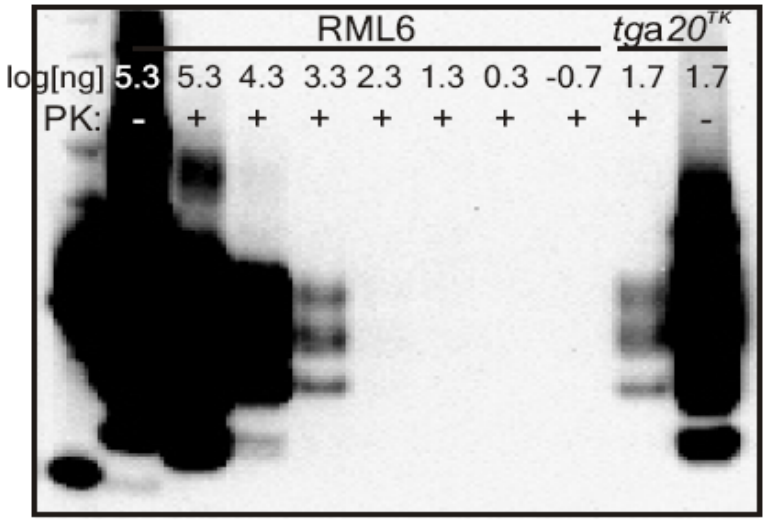

Figure 7. Sensitivity of western blot detection of PrP^{Sc}

Tga20^{TK} and *Prnp*$^{o/o}$ cultures were inoculated with 1 µg RML6 and after 35 DIV PrP^{Sc} levels were compared to a dilution curve of RML6 diluted in mock brain homogenate. Western blotting was performed on (+) 20 µg sample digested with PK (25 µg/ml) or (-) 10 µg undigested sample and detected with mouse anti-mouse PrP^{C} IgG_1 (POM-1). Legend for the RML-treated *tga20*^{TK} sample indicates the total amount of input inoculum that theoretically could be in the sample assuming 100% recovery of the input material.

Temporal increase in PrP^{Sc} deposition correlate with prion infectivity

To conclusively prove bona fide prion replication, a time course experiment was performed using 100 μg RML6 per 10 slices (Figure 8a-b). 1 hr post-inoculation no residual inoculum was detected (Figure 8a-b, lane 4,5). After 14 days *in vitro* no indication of prion replication was observed, but after 3 weeks a definite PrP^{Sc} signal could be observed (Figure 8a-b, lane 10). No difference in PrP^{C} expression was seen in the undigested cultures, showing that the difference in PrP^{Sc} levels were due to a difference in PK sensitivity rather than different expression of PrP^{C} (Figure 8b).

To test whether deposition of PrP^{Sc} goes along with prion replication, I assayed slice culture homogenates by SCEPA. Slices derived from *tga20*^{TK} or *Prnp*$^{o/o}$ mice upon infection with RML6 (100 μg) for up to 35 days were homogenized and transmitted to N2a-PK1 cells. *Tga20*^{TK} RML slice culture homogenates from the 4 and 5-week time points showed infectivity by SCEPA when transmitted at 10 and 1 μg protein/ml, but not at 0.1 μg protein/ml (in a volume of 300 μl/well, corresponding to 100 - 1 μg/ml RML6 homogenate) (Figure 8c). No infectivity was detected in *Prnp*$^{o/o}$ RML slice culture homogenates at any time point, or in *tga20*^{TK} RML slices prior to 4 weeks in culture. At 1 μg/well the 5-week time point showed a significantly higher signal than the 4-week sample (One-way ANOVA with Bonferroni's multiple comparison test, $p < 0.001$). The number of TCI_{50} units in RML-infected *tga20*^{TK} samples (1 TCI_{50} unit is the infectious dose required for infecting 50 % of the N2a-PK1 cultures) were 6.8 TCI_{50} units/g protein, identical to what was measured in a calibration experiment with serial dilutions of RML6 (6.8 TCI_{50} units/g protein) (Figure 8c). This confirmed that both PrP^{Sc} and prions were amplified to a level similar to what can be detected in terminally sick mouse brain (Figure 8c).

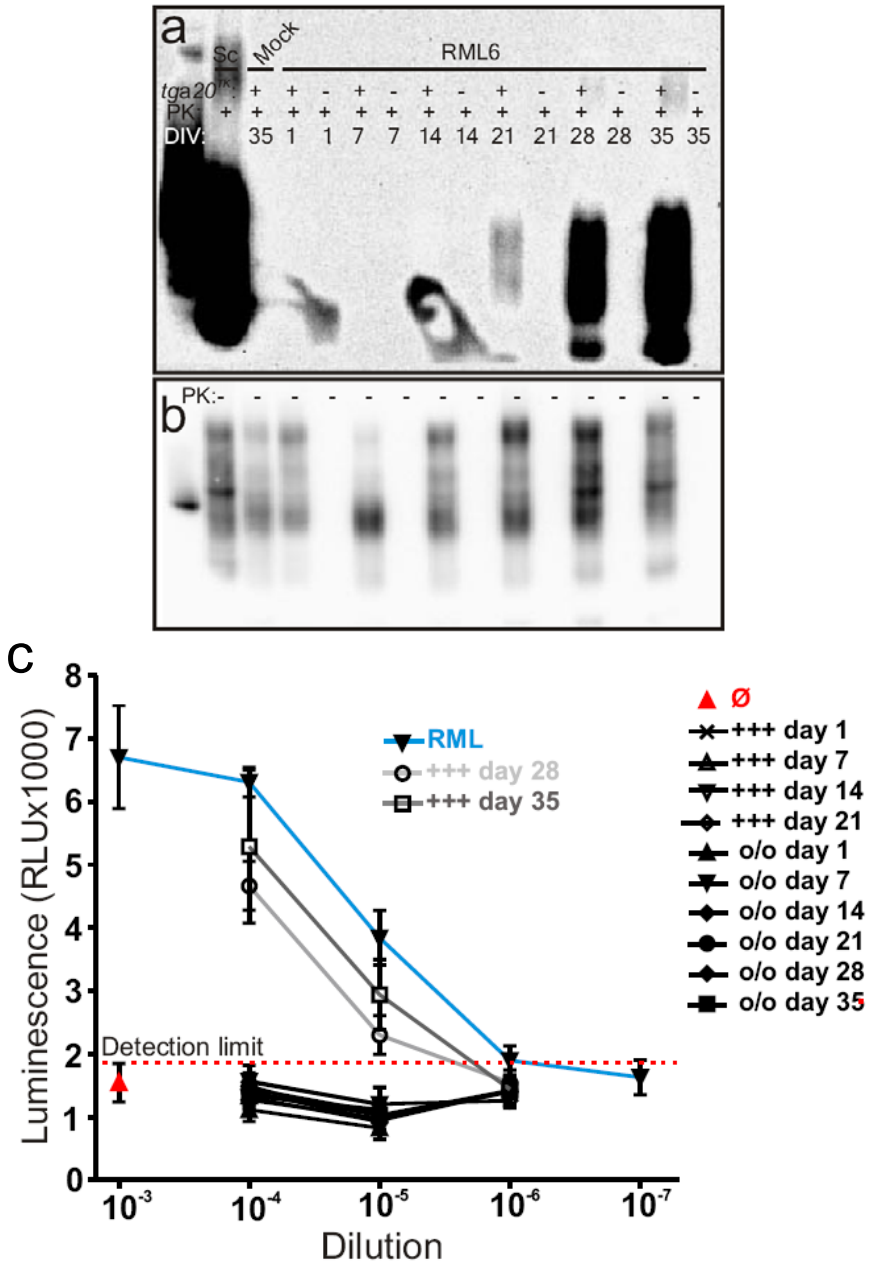

Figure 8. Time course analysis of prion replication

(**a**) Cultures from *tga20*^{TK} (+) and *Prnp*$^{o/o}$ (-) pups were inoculated with 100 µg mock or RML6 and seeded onto membrane inserts. Tissue was harvested 1 h, 7, 21 or 35 days after seeding. (**b**) Non-digested samples from blot **a**. (**c**) Time-dependent build up of prion titers in *tga20*^{TK} (+++) and *Prnp*$^{o/o}$ (o/o) slices. RML-infected (▼) or uninfected (Ø) brain homogenate and slice homogenates from the experiment reported in (**a**) were serially 10-fold diluted in uninfected brain homogenate, and infectivity was determined by transfer to PK1 cells. Exposure to 10 µg or 1 µg, but not 100 ng protein/ml from slices cultured for ≥28 days resulted in unambiguous replication of prion infectivity in PK1. In agreement with PrP^{Sc} determinations, no infectivity from any residual inoculum was detected as early as after 1 day of culture. Vigorous prion replication was detected in PK1 cells exposed to 10 µg/ml homogenate.

Localization of prion deposition and its impact on tissue integrity

Having validated PI as a suitable cell death marker in our cultures, I evaluated PI retention after 5 weeks of prion infection. Surprisingly, prion infection did not exert any significant effect on viability (one-way ANOVA with Bonferroni's multiple comparison test, $p > 0.05$, $n = 12$; Figure 9a-b).

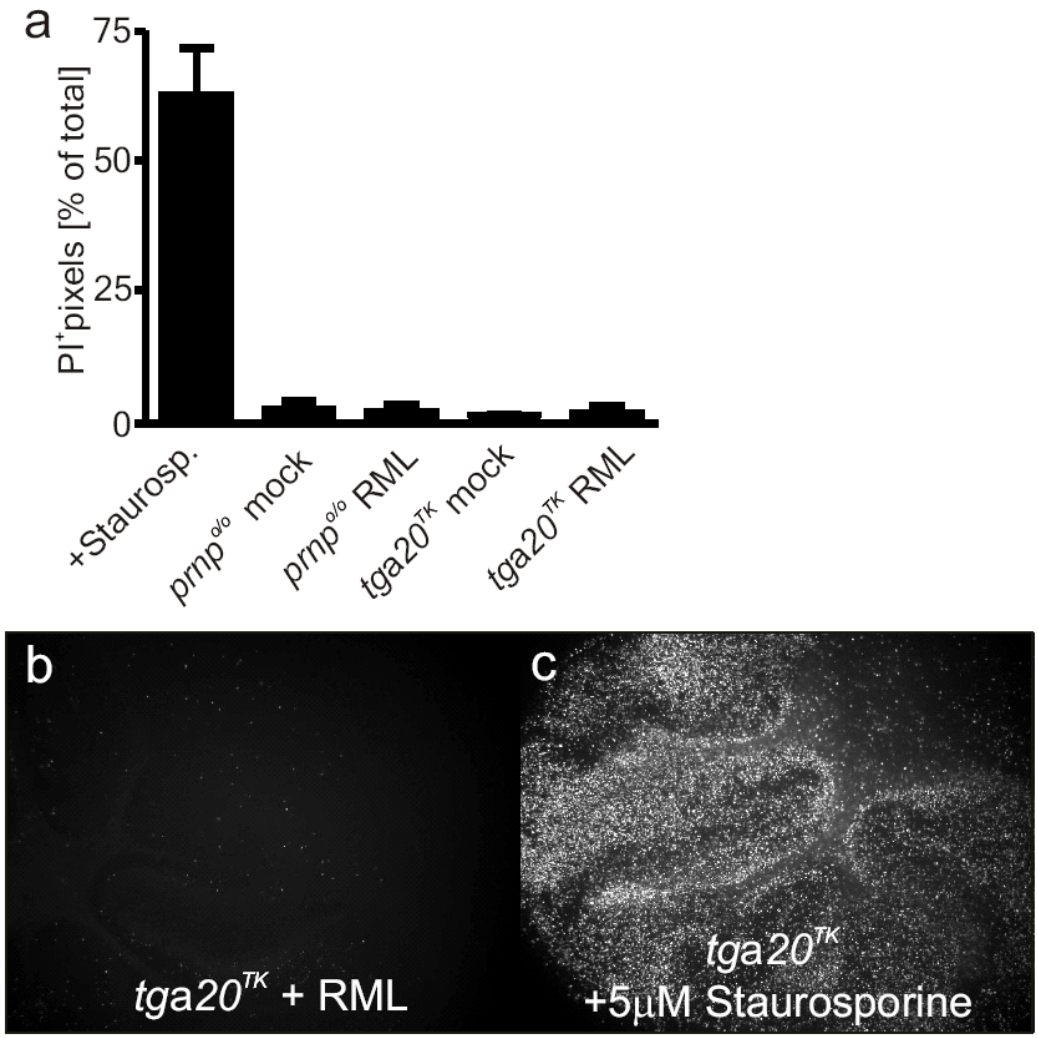

Figure 9. Impact of prion replication on tissue viability

(**a-c**) *Tga20*^{TK} (+++) and *Prnp*$^{o/o}$ (o/o) cultures were inoculated with 100 µg RML6 or Ø. 35 days post inoculation PI incorporation was analyzed. Data are presented as the average of 12 slices ± SD (**b-c**) Representative examples of images used for PI incorporation.

I assessed the morphological integrity of slices by standard light microscopy and immunohistochemistry at 1, 7, 21 and 35 days post inoculation. Neurons (calbindin), astrocytes (GFAP) and myelin (MBP) appeared intact. However, progressive broadening of cell layers became evident at 7-35 days of culture (Fig. 11a-c). Isolectin-B_4 (IB_4) and $CD68^+$ microglia/macrophages increased over time, confirming slices underwent progressive microgliosis (Figure 10d-e, see also Figure 15 and 18). However, no difference in any of the above parameters was detected between RML-treated *Prnp*$^{o/o}$, RML-treated *tga20*^{TK} or *tga20*^{TK} slice cultures treated with uninfected brain homogenates at any given time point (Figure 10a-e).

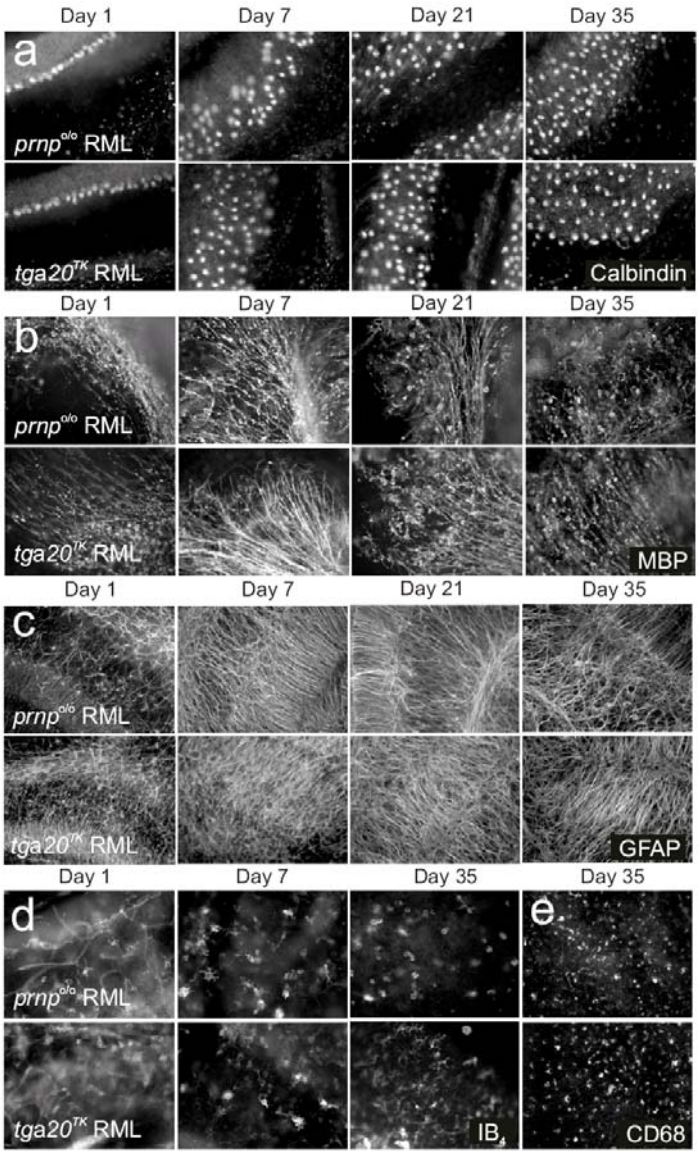

Figure 10. Impact of prion replication on tissue morphology
(**a-e**) *Tga20*^{TK} (+++) and *Prnp*$^{o/o}$ (o/o) cultures were inoculated with 100 µg RML or Ø. 1, 7, 21 or 35 days post inoculation, the tissue was fixed in PFA and stained with (**a**) mouse α-Calbindin IgG_1, (**b**) rat α-MBP IgG_{2a}, (**c**) rabbit α-GFAP polyclonal antibody, (**d**) IB_4-Alexa^{488} or (**e**) rat α-CD68 IgG_{2a}. No difference was detected between RML-treated *Prnp*$^{o/o}$, RML-treated *tga20*^{TK} or mock-treated *tga20*^{TK} cultures at any given time point (**a-c**), data not shown).

The sites of PrP^{Sc} replication/deposition were evaluated using the histoblot technique (Taraboulos et al., 1992). Proteins were transferred from slice cultures to nitrocellulose membranes, and membranes were digested with 50 µg/ml PK. PrP^{Sc} was detected by immunoblotting (Figure 11a-c). To determine the localization of PrP^{Sc}, the major neuronal populations and the white matter was visualized by immunohistochemistry (Figure 11b). A strong PrP^{Sc} signal was observed in the molecular layer and in the Purkinje cell layers consistent with a high PrP^{Sc} deposition in granule cell axons, in Purkinje neurons and possibly in astrocytes. An intermediate

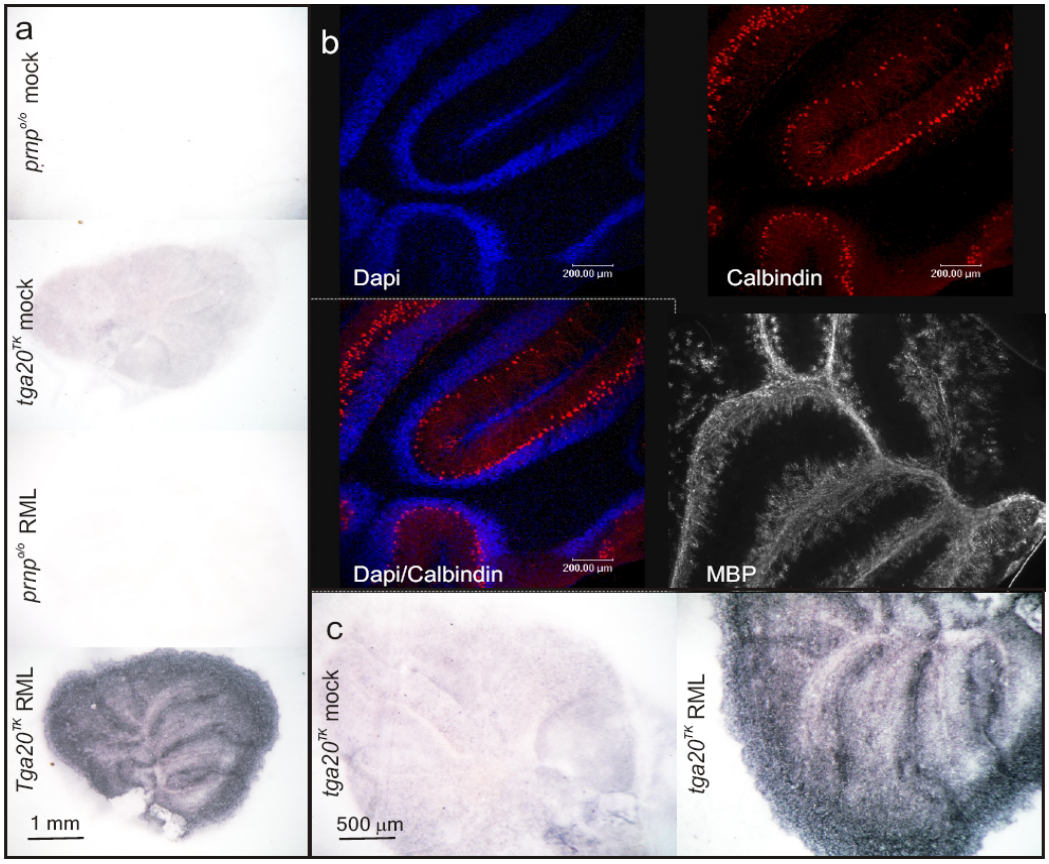

Figure 11. Localization of prion replication

(**a**) *Tga20*^{TK} and *Prnp*$^{o/o}$ cultures were inoculated with 100 µg RML6 or mock homogenate. After 35 days *in vitro* slice culture proteins were blotted onto a nitrocellulose membrane. The membrane was digested with 50 µg/ml PK and PrP^{Sc} was detected as described in materials and methods using the POM-1 antibody. (**b**) Uninfected cultures were stained with dapi (a chromatin-binding dye, blue) and antibodies against calbindin (Purkinje neurons, red) or myelin basic protein (myelin, white) to visualize the major morphological features of the cultures. (**c**) A larger magnification of (**a**) detailing the deposition of PrP^{Sc}.

signal was observed in the granule cell layer, and a weak signal was present in the white matter (Figure 11c).

Assay sensitivity

To determine the infectious dose required for infecting 50 % of the slice cultures, I performed multiple infections at 1 and 0.1 µg RML6 per 10 slices. All cultures infected with 1 µg RML6 showed PK-resistant PrP^{Sc}, whereas no PK-resistant material was observed in cultures infected with 0.1 µg RML6 (Table 1, Figure 12 and data not shown). The dose at which 50 % of the slice cultures were infected (SCI_{50}) was determined and 1 ml of 10 % RML6 (100 mg homogenate) contain > 5.7 log SCI_{50} calculated according to Kärber meaning that 1g brain yielded more than 6.7 log SCI_{50} (Kaerber, 1931).

In order to compare our assay sensitivity with that of the commonly used bioassays we transmitted dilution series of RML6 into *tga20* and *CD-1* mice by intracerebral

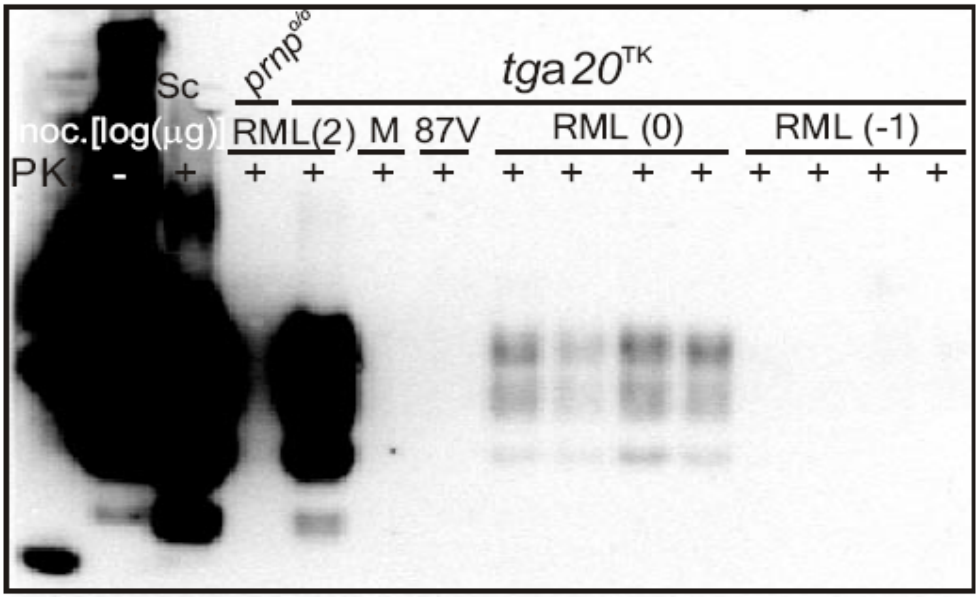

Figure 12. Determination of SCI_{50}

Tga20^{TK} and *Prnp*$^{o/o}$ cultures were inoculated with 100 µg of scrapie strain 87V, 100 µg, 1 µg (*n = 4*) or 0.1 µg (*n = 4*) of RML6 and incubated for 35 DIV. Western blotting was performed on (+) 20 µg sample digested with PK (25 µg/ml) or (-) 10 µg undigested sample and detected with mouse anti-mouse PrP^{C} IgG_1 (POM-1). PrP^{Sc} was observed in all *tga20*^{TK} samples treated with 1 µg or more RML6 and in none of the samples treated with 0.1 µg RML.

inoculation or into the SCEPA (Table 1). The *tga20* bioassay measured 9.9 log ID_{50} units and *CD-1* mice 9.3 log ID_{50} units/g brain homogenate. In comparison, the SCEPA showed a sensitivity of 7.7 log ID_{50}/g (Figure 8c).

Dilution	Sick/total	Incubation time days ± SD	Sick/total	Incubation time days ± SD	SCEPA (Pos/total)	POSCA (Pos/total
i.c. inoculation	tga20		CD1			
10^{-1}	4/4	54 ± 1	7/7	119 ± 1	Not done	5/5
10^{-2}	4/4	59 ± 2	7/7	124 ± 1	6/6	5/5
10^{-3}	3/3	69 ± 1	7/7	126 ± 1	6/6	15/15
10^{-4}	4/4	77 ± 2	6/6	132 ± 4	12/12	5/5
10^{-5}	6/6	86 ± 2	5/5	135 ± 3	12/12	9/9
10^{-6}	6/6	93 ± 2	5/5	159 ± 4	12/24	0/9 (2/2*)
10^{-7}	6/6	119 ± 4	2/5	167 ±16	5/24	0/3
10^{-8}	1/6	121, >236	1/5	202, >239	0/24	
10^{-9}	0/5	>236	0/5	>239		
log ID_{50}/g ± SE	9.9 ± 0.2		9.3 ± 0.9		7.7 ± 0.5	>6.7 ± 0.1

*microglia depleted slices

Table 1: Comparison of prion assay sensitivity. The assay sensitivity of the *tga20* and *CD1* bioassay, SCEPA and POSCA was compared by performing endpoint titrations of RML6 in the various assays. The number of ID_{50} units (i.e. LD_{50} for *tga20* and *CD1* mice) per g of brain material were determined according to Kärber et al. Data points are presented as the number of infected animals/cultures out of the total number of animals/cultures treated with the inoculum.

The POSCA is applicable to a broad range of prion strains

Theoretical considerations led us to predict that the POSCA may be applicable to a much broader range of prion strains than the current versions of the SCEPA. We tested this prediction by exposing POSCA slices to a variety of prion strains from different sources. Slices from *tga20*$^{+/+}$ pups were treated with homogenates of the 2 mouse-adapted scrapie strains, 79A and 139A (100 µg brain homogenate per 10 slices), which are known to replicate in N2a-PK1 cells (data not shown). Infection of the tissue with either 79A or 139A led to an abundant accumulation of PrP^{Sc} in the tissue 5 weeks post inoculation, the extent of which was comparable to, or even higher than that seen in RML6-exposed slices (Fig. 12a, lane 11-13). Other less adapted scrapie strains 5193/1 and 5192/2 (brain homogenate from a terminally scrapie sick sheep from a flock in Colorado, USA passaged twice in *tga20* or *wt* mice respectively) (C.J. Sigurdson et al, unpublished data) also replicated in *tga20*$^{+/+}$ slices, but showed less abundant PrP^{Sc} accumulation after 5 weeks (Fig. 12b, lane 14-15).

In addition, a murine adapted BSE strain reported not to replicate in N2A-PK1 cells, 301C, replicated in *tga20*$^{+/+}$ slices (Fig. 12b, lane 12). N2a-PK1 cells are also known to be resistant to an infection with the mouse adapted scrapie strain, ME7 (Klohn et al., 2003). In slices derived from *tga20*$^{+/+}$ pups infected with ME7 (100 µg), a faint PrP^{Sc} signal could be found 5 weeks post inoculation (Fig. 12b, lane 13). We infected slices with an increased amount of ME7 (1 mg) and after 5 weeks a clear PrP^{Sc} signal was found in all ME7-treated *tga20*$^{+/+}$ cultures (Figure 13c, lane 13-15), showing that POSCA exhibit a broad specificity.

However, not all strains tested replicate in the POSCA after 5 weeks. Four murine-adapted scrapie strains; 87A, 87V, 22F and 301V all failed to infect slice cultures 5 week post inoculation (100 µg brain homogenate per 10 slices) (Figure 12, data not shown). These strains all exhibited long incubation times after intracerebral inoculation of 30 µl 10 % brain homogenate into C57BL/6 mice (>290 days, fig. 12d) (Carlson et al., 1994). In comparison, all strains that replicate in POSCA showed incubation times between 150-200 days (RML6, 79A, 139A, ME7, 5193/1 and 301C) (Fig. 12d). The only exception was 5192/2 that showed an incubation time of 270 days (fig. 12d).

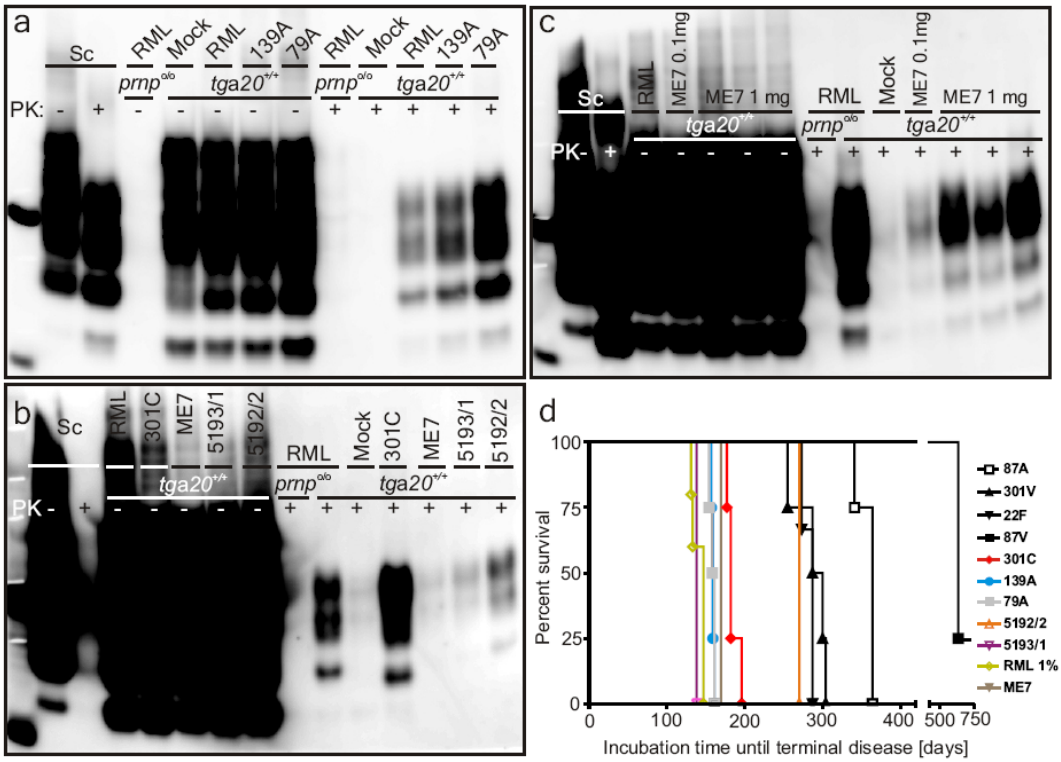

Figure 13. Versatile strain replication

Strain selectivity of POSCA. (**a-b**) Cultures were prepared from 10-day old *tga20*$^{+/+}$ and *Prnp*$^{o/o}$ pups, inoculated with 100 µg of infectious or mock brain homogenate and cultured for 35 days prior to harvesting the tissue. (**a**) Transmission of murine-adapted scrapie strains RML6, 139A, 79A and mock brain homogenate. Western blotting was performed on 20 µg protein digested with 25 µg/ml PK (+) or 10 µg non-digested protein (-) and detected with mouse anti-mouse PrP^C IgG_1 (POM-1). (**b**) Transmission of murine-adapted BSE 301C, murine adapted scrapie strains 5193/1, 5192/2, ME7, RML6 and mock brain homogenate. The RML6-infected slice culture sample was diluted 10-fold in mock brain homogenate prior to PK-digestion to decrease the PrP^{Sc} signal on the western blot. Western blotting was performed on 30 µg protein digested with 20 µg/ml PK (+) or 10 µg non-digested protein (-) and detected with mouse anti-mouse PrP^C IgG_1 (POM-1). (**c**) Cultures were prepared from 10-day old *tga20*$^{+/+}$ and *Prnp*$^{o/o}$ pups, inoculated with 0.1 and 1 mg of RML6, ME7 or mock brain homogenate and cultured for 35 days prior to harvesting the tissue. Western blotting was performed as indicated in (**b**). (**d**) Kaplan-Meyer plot comparing the incubation time until terminally disease of C57BL/6 mice inoculated intracerebrally with 30 µl, 10 % brain homogenate of various strains. Colored lines and symbols indicates strains that replicated in the POSCA and black lines and symbols indicate strains that did not.

This suggests a correlation between incubation times upon intracerebral inoculation into C57BL/6 mice and the ability of scrapie and BSE strains to replicate in the POSCA.

We also tested a strain of mule-deer CWD from a Colorado flock adapted in *tga20* mice (Sigurdson et al., 2006). *Tga20* mice inoculated intracerebrally with brain homogenate of a terminally sick mule-deer (30 µl, 10 % homogenate) came down with disease 400 days post inoculation upon 1st passage, 228 days post inoculation upon 2nd passage and 138 days post inoculation upon 4th passage. Despite the 2nd and 4th passage showing short incubation times *in vivo*, murine-adapted CWD inoculums did not appear to replicate in *tga20* slices 5 weeks post inoculation (100 µg brain homogenate per 10 slices, data not shown). All data are summarized in Table 2.

Original inoculum	Strain	Mouse genotype (last passage)	Number of passages in mice	Incubation time (days ± sd)	POSCA replication
Sheep scrapie	5193/1	*Tga20*	2	138*	+
	RML6	CD-1	>4	141±8	+++
	79A	C57BL/6	>4	159±3	+++
	139A	C57BL/6	>4	159±2	+++
	ME7	129/Sv	>4	180*	+
	5192/2	C57BL/6	2	270*	+
	5114/2	*Tga20*	1	414	+
	22F	C57BL/6	>4	282±8	-
	301V	C57BL/6	>4	287±22	-
	87A	C57BL/6	>4	358±12	-
	87V	C57BL/6	>4	635±0**	-
Cow BSE	301C	C57BL/6	>4	184±8	++
Deer CWD	5194	*Tga20*	4	138*	-
	5005	*Tga20*	2	228*	-
	5002	*Tga20*	1	400*	-

Table 2. Synopsis of the various prion strains used for infection of POSCA slices

Original inocula were derived from scrapie affected sheep, BSE-affected cows, and CWD-affected deer. The columns display the number of mouse passages undergone by the inoculum (> 4 passages are considered fully adapted), the genotype of the mice in which the inoculum was last passaged, and the average time until terminal disease (± SD) in the mice used to generate the inoculum.

* Inoculum was generated from a single mouse

** Only 3 out of 4 mice came down with scrapie

*** No replication (-), weak replication (+), intermediate replication (++), strong replication (+++) as estimated by approximate density of PrP^{Sc} western blot signals.

Conditional microglia depletion using CD11b-HSVTK transgenic mice

Conditional inhibition of microglia function in *CD11b-HSVTK* slices

CD11b-HSVTK mice which allow for the conditional inhibition of microglia function *in vivo* and *in vitro* by treatment with the DNA-analogue ganciclovir (GCV) was previously generated (Heppner et al., 2005). In brief, transgenic animals expressing the *herpes simplex* virus thymidine kinase (*tk*) enzyme under the *Itgam* promoter (the

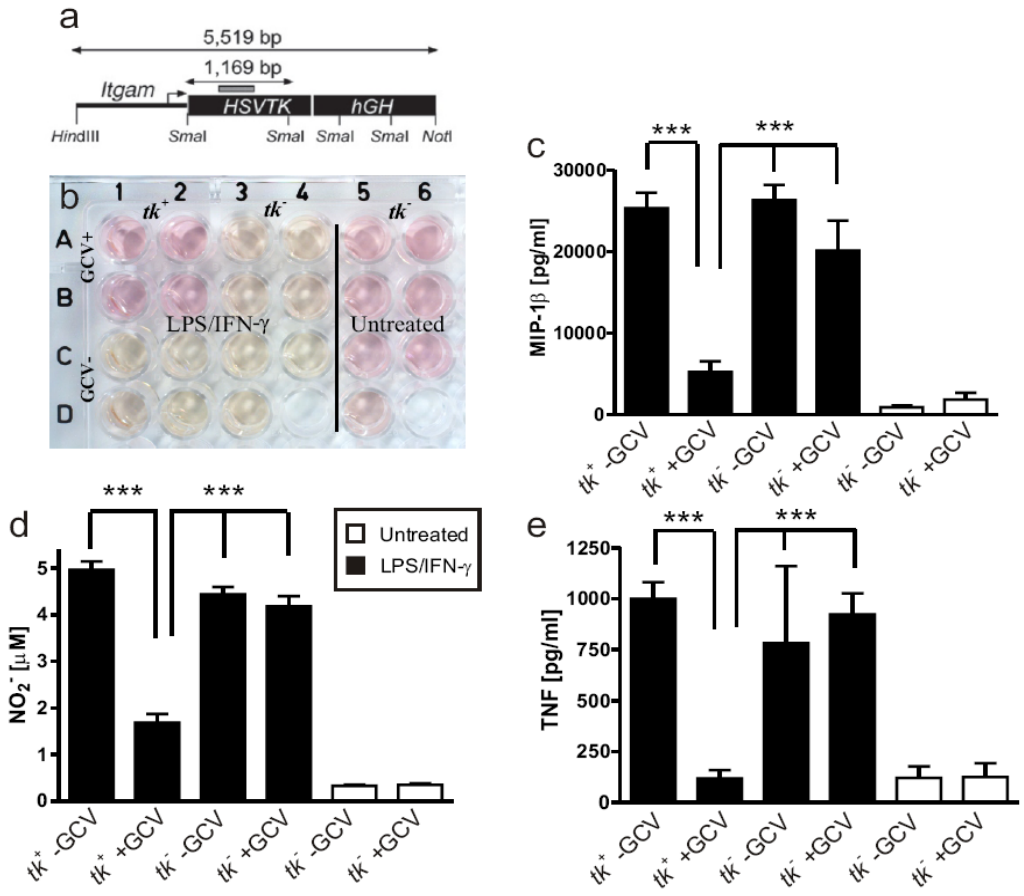

Figure 14. GCV-mediated inhibition of microglia activation in *CD11b-HSVTK*$^+$ slices

(**a**) LPS/IFN-γ-induced microglial activation in brain slices was accompanied by a pH change of cell culture supernatant within 48 h (yellowish color in wells C1–4, D1–3, A3–4, B3–4). Pretreatment of slice cultures derived from *CD11b-HSVTK* mice with GCV, inhibited such activation-associated pH changes (A1–2, B1–2). GCV-treatment abrogated the LPS/IFN-γ-induced (black bars) release of microglial TNF-α (**b**), nitrite (**c**) and MIP-1β (**d**) in *tk*$^+$ OHSCs. White bars, non-stimulated OHSCs. Statistical significance was assessed by a one-way ANOVA test. ***: $p < 0.001$.

promoter driving CD11b-expression) was generated. Administration of GCV to transgenic CD11b-positive cells, leads to the phosphorylation and activation of the pro-drug by the *tk* enzyme. Subsequent incorporation of p-GCV into genomic and mitochondrial DNA causes death or cell cycle arrest of the cell (Rubsam et al., 1998; Heppner et al., 2005). I assessed the functional consequences of microglia paralysis in organotypic hippocampal slice cultures (OHSCs). OHSCs derived from *CD11b-HSVTK* mice were stimulated with lipopolysaccharide (LPS) and interferon-gamma (IFN-γ), and microglia activation in the presence or absence of GCV (5 μg/ml) was determined. GCV treatment of stimulated OHSCs inhibited microglia activation-dependent acidification of the cell culture supernatant (Figure 14b) and abrogated the release of nitrite, tumor necrosis factor (TNF) and macrophage-inflammatory protein-1β (MIP-1β), suggesting a profound inhibition of microglia function (Figure 14c-e) (Heppner et al., 2005).

Conditional depletion of microglia in organotypic *CD11b-HSVTK* slices

I generated organotypic cerebellar slices derived from 10-day old *CD11b-HSVTK* mice, and added GCV to the medium. After 14 days, GCV treatment led to an almost complete loss of Isolectin-B_4 $(IB_4)^+$ and $CD68^+$ cells in *CD11b-HSVTK*$^+$ (*tk*$^+$) slices (Figure 15a-d). Remaining IB_4^+ cells appeared mostly fragmented (i.e. necrotic) or associated to IB_4^+ blood vessels (Figure 15a). Furthermore, time-lapse microscopy performed on IB_4-labelled GCV-treated *tk*$^+$ slices from 9-14 days *in vitro* confirm that microglia undergo an active form of cell death (See time-lapse video 1) and subsequently are taken up by neighboring (and still viable) microglia. Microglia depletion was quantified from images acquired by confocal laser scanning microscopy 35-40 μm below the tissue surface (i.e. underneath the glial scar). *tk*$^+$ slices showed a reduction in microglia of 97 %, 98 % and 99 % after 14, 28, and 42 days of GCV treatment, respectively (one-way ANOVA with Bonferroni's multiple comparison test, $p < 0.001$, $n = 4$; Figure 15c). Very few if any microglia were found outside the tissue in treated *CD11b-HSVTK*$^+$ slices (Figure 15d).

Quantification of mRNA transcript levels by quantitative RT-PCR showed a significant ($p < 0.001$, $n = 3$) 98 % reduction in CD11b expression in *TK*$^+$ slices treated with GCV for 14 days, whereas GFAP, MBP and neurofilament heavy-chain transcripts (markers for astrocytes, oligodendrocytes and neurons respectively) were

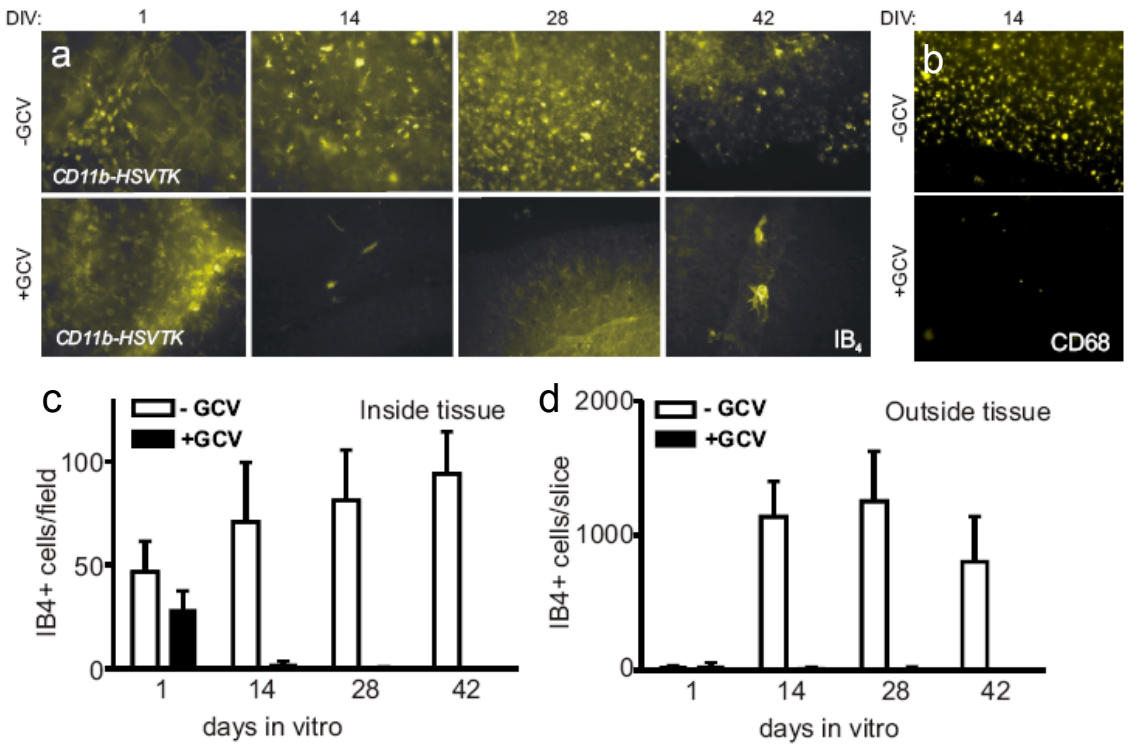

Figure 15. Microglia depletion in organotypic slice cultures

Cultures were prepared from 10-day old *CD11b-HSVTK* mice and cultured for 1, 14, 28 or 42 days, either untreated (-GCV) or in the presence of GCV (+GCV). Cultures were fixed in 2% PFA and stained with (**a**) IB_4-Alexa^{488} or (**b**) rat α-CD68 IgG_{2a} (only after 14 days *in vitro*). (**c**) Confocal images of IB_4^+ cells within the tissue were quantified. (**d**) Images were also acquired using a fluorescent microscope and IB_4^+ cells migrating out of the tissue was quantified (*n = 3* replicas, each the average of 4 individual 40X images).

unaffected (one-way ANOVA with Bonferroni's multiple comparison test, $p > 0.05$) (Figure 16a). Importantly, GCV treatment had no effect on *wt* slices (Figure 16a). GFAP protein expression increased over time and multiple lower-running isoforms could be observed after 7-21 days in culture (Figure 16). Depletion of microglia did not affect GFAP expression suggesting that the observed astrogliosis was independent of microglia activation. PrP^C protein expression levels were unaffected in microglia-depleted cultures (Figure 16b-c).

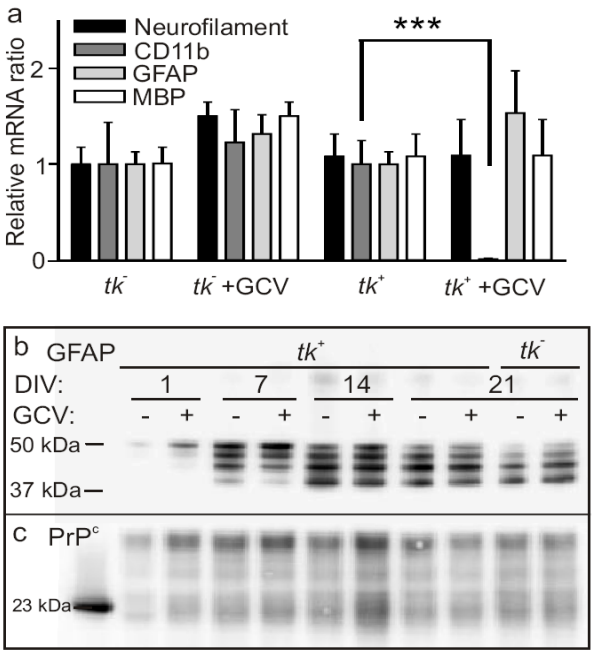

Figure 16. Specificity of microglia depletion in organotypic slice cultures

(**a**) Cultures were prepared from 10-day old *CD11b-HSVTK*$^+$ (*tk*$^+$) and *CD11b-HSVTK*$^-$ (*tk*$^-$) mice and cultured for 14 days with or without GCV. Total RNA was purified and cDNA was synthesized from 1 µg total RNA. Real-time quantitative PCR was performed and fold regulation was calculated relative to untreated *wt* mice after normalization to the β-actin signal (*n = 3*). (**b-c**) Cultures were prepared from 10-day old *tk*$^+$ and *tk*$^-$ mice and cultured for different days *in vitro* with or without GCV. Western blotting was performed on 10 µg protein and detected with (**b**) mouse anti-GFAP IgG_1 (Clone GA5) or (**c**) mouse anti-mouse PrP^C IgG_1 (POM-1).

Specific conditional microglia depletion does not affect tissue viability

Phosphorylated GCV released from dying microglia may be taken up by neighboring cells and cause toxicity ("bystander cell death"). The viability of *CD11b-HSVTK* slices treated with GCV for 14 days were assessed with respect to PI incorporation and DEVDase activity. Microglia-depleted slice cultures displayed a small, but significant increase in PI^+ cells from approximately 1 % up to 2 % of the total area (One-way ANOVA with Bonferroni's multiple comparison test, $p < 0.001$, $n = 12$) (Figure 17a). No difference in caspase activity was observed ($n = 3$, pools of 4 slices) (Figure 17a). Reconstitution of slices with intra-peritoneal *wt* macrophages partially rescued the GCV-induced increase in PI^+ cells (Figure 17b).

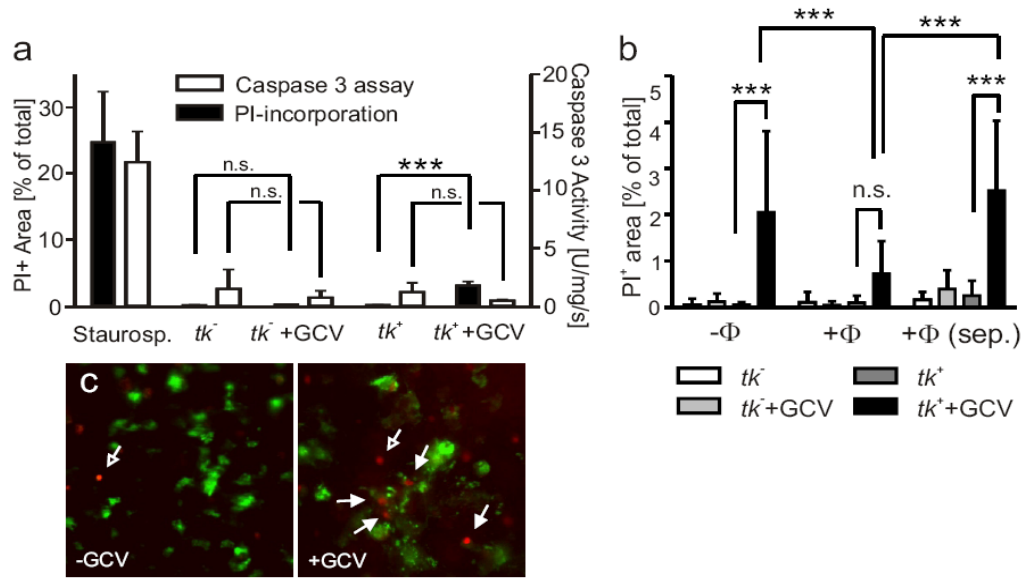

Figure 17. Minor impact of microglia depletion on tissue viability

(**a**) Cultures were prepared from 10-day old tk^+ and tk^- mice and treated with GCV for 5 weeks, including a positive control of *wt* tissue treated with 5 µM staurosporine for 24 h and PI incorporation was measured (*n = 12*). Slices were harvested and caspase-3 enzymatic activity was measured and normalized to protein contents (*n = 3* pools of 4 slices). (**b**) Slices were reconstituted with 250.000 macrophages either by adding macrophages directly onto the tissue (+Φ) or separated by a membrane (sep.) (*n = 12*). (**c**) tk^+ slices were treated with GCV for 10 days and living tissue were incubated with IB_4 (green) and PI (red). Images were acquired on a wide-field microscope. Open arrows indicate IB_4^-/PI^+ cells and closed arrows indicate IB_4^+/PI^+ cells.

I speculated that the increased number of PI^+ cells might be due to dying/dead *CD11b-HSVTK*$^+$ microglia. To test this, I performed dual-labelling of unfixed GCV-treated *CD11b-HSVTK* slices with PI and IB_4. In GCV-treated slices most PI^+ cells were co-stained with IB_4, indicating that the increase in PI^+ cells was due to dead microglia (Figure 17c). Phosphorylated GCV released from dying cells cannot only cause bystander cell death, but also cell cycle arrest (Rubsam et al., 1998). To test for adverse GCV-mediated effects in the most sensitive way, I performed a BrdU-incorporation experiment to label dividing cells. GCV-treatment of tk^+ slices for 14 days decrease greatly the number of $BrdU^+$ cells in the tissue (Figure 18a). Co-staining of slices with antibodies against BrdU and CD68 showed that GCV-treatment of tk^+ slices abolished $BrdU^+/CD68^+$ cells as expected (Figure 18c). No significant effect was seen on the number of $Brdu^+/CD68^-$ cells ($BrdU^+$ cells characterized by a

large nuclei) (Figure 18b-c). Also, no significant effect was seen by GCV-treatment of tk^+ slices. Therefore, depletion of $CD68^+$ cells is selective and transgene-dependent without significant bystander cell death.

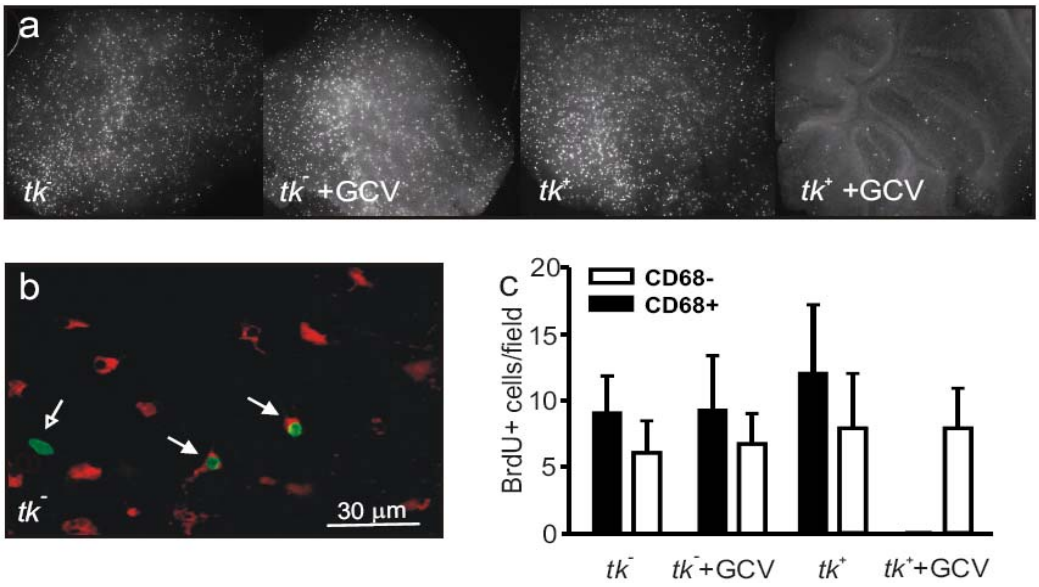

Figure 18. Microglia depletion does not affect proliferation of non-microglia cells

(**a**) Cultures were prepared from 10-day old tk^+ and tk^- mice and treated with GCV. After 13 DIV BrdU incorporation was performed and the tissue was stained with rat α-bromodeoxyuridine IgG_1. (**b**) Tissue was co-stained with α-bromodeoxyuridine (green) and α-CD68 IgG_{2a} (red). Example of $CD68^+$ (red) and $BrdU^+$ (green) cells. Closed arrows represent $CD68^+/BrdU^+$ cells and open arrows represent $BrdU^+/CD68^-$ cells. (**c**) $CD68^+/BrdU^+$ and $CD68^-/BrdU^+$ cells were counted ($n = 6$, each the average of 5 individual 40X images). Images analysis software analySIS© vs5.0 were used for all quantification purposes. Data is presented as the average of n replicas ± standard deviation (SD).

Impact of conditional microglia depletion on prion replication

Microglia depletion leads to increased prions accumulation

To address the contribution of microglia to prion formation/replication, I prepared slices from *tga20*^{TK} *CD11b-HSVTK*$^{-}$ (*tga20*^{TK}) and *tga20*^{TK} *CD11b-HSVTK*$^{+}$ pups (*tga20*$^{TK+}$). Slices infected with RML6 (100 µg RML6, i.e. 2.7 log SCI_{50}), were split into 2 pools and half the cultures were treated with GCV. After 30 days an equal amount of PrP^{Sc} was observed in all conditions except in GCV-treated *tga20*$^{TK+}$ slices.

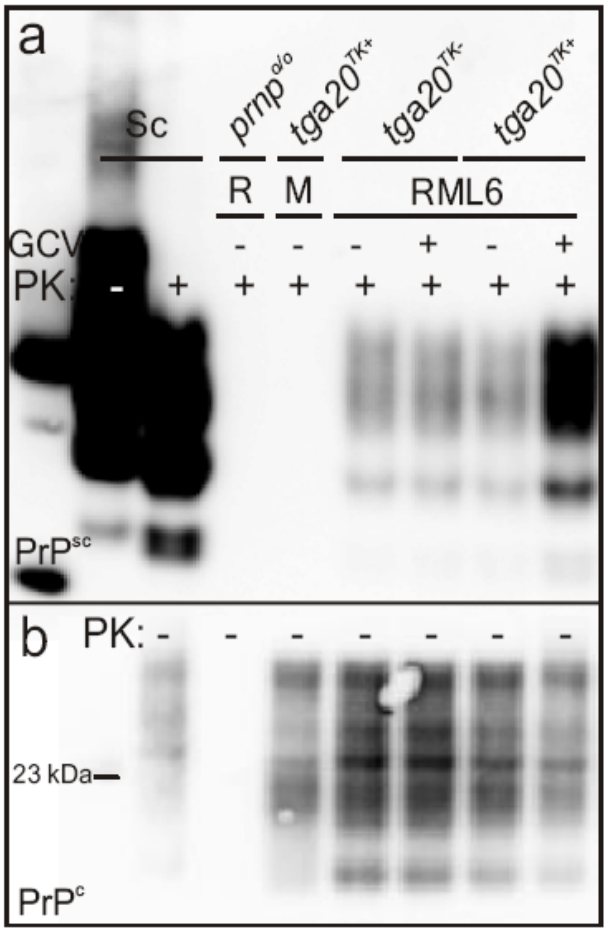

Figure 19. Impact of microglia depletion on prion replication

Cultures were prepared from 10-day old *tga20*^{TK} or *Prnp*$^{o/o}$ mice either *CD11b-HSVTK*$^{+}$ (*tga20*$^{TK+}$ or *Prnp*$^{o/o/TK+}$) or *CD11b-HSVTK*$^{-}$ (*tga20*^{TK}) mice. After treatment with RML6 (2.7 log SCI_{50}), *tga20*^{TK} and *tga20*$^{TK+}$ slices were separated into 2 pools each and 1 insert out of each pool were treated with GCV. (**a**) Western blotting of 20 µg sample digested with PK (25 µg/ml) (**b**) or 10 µg sample undigested detected with mouse anti-mouse PrP^{C} IgG_1 (POM-1).

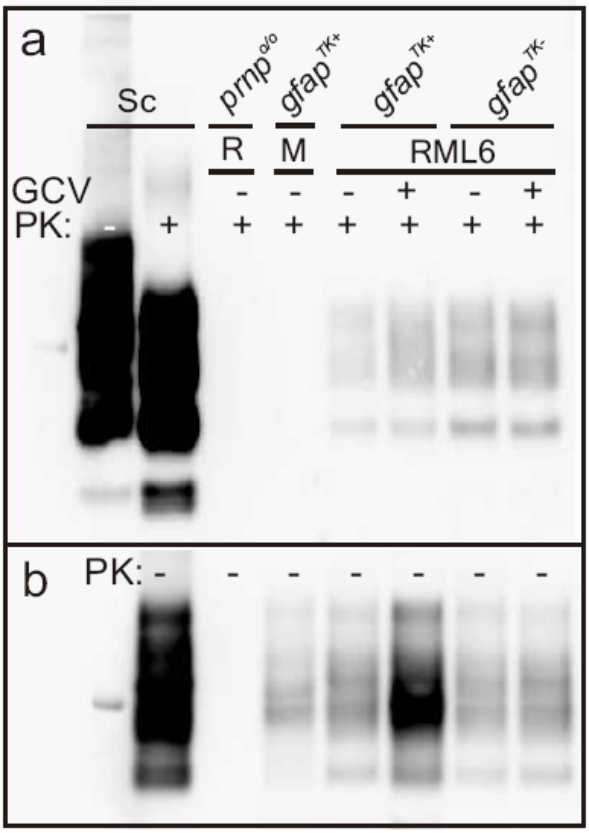

Figure 20. Impact of astrocyte depletion on prion replication

Cultures were prepared from 10-day old *GFAP-HSVTK*$^{+}$ (*gfap*$^{TK+}$), *GFAP-HSVTK*$^{-}$ (*gfap*^{TK}) or *Prnp*$^{o/o}$ mice and treated with RML6 (2.7 log SCI_{50}), *gfap*$^{TK+}$ slices were separated into 2 pools and 1 insert was treated with GCV. Western blotting was performed on (**a**) 20 µg sample digested with PK (25 µg/ml) (+) or (**b**) 10 µg undigested sample (-).

Microglia depletion resulted in a 5-fold increase in PK-resistant PrP^{Sc} (Figure 19a, lane 9). Since this increase was independent of PrP^{C} expression (Figure 19b), microglia either directly affected the conversion of PrP^{C} into PrP^{Sc} or – more likely – affected the half-life of PrP^{Sc} by phagocytosing and degrading prions. To test whether the observed increase in PrP^{Sc} was associated only with microglial expression of HSVTK I infected slices prepared from 10-day old *GFAP-HSVTK* mice that allows for conditional ablation of astrocytes (Bush et al., 1998). In contrast to *CD11b-HSVTK*$^{+}$ cultures, GCV-treatment of *GFAP-HSVTK*$^{+}$ cultures had only a small or no effect on PrP^{Sc} levels (Figure 20a-b). Hence increased PrP^{Sc} levels are selectively associated with microglia depletion.

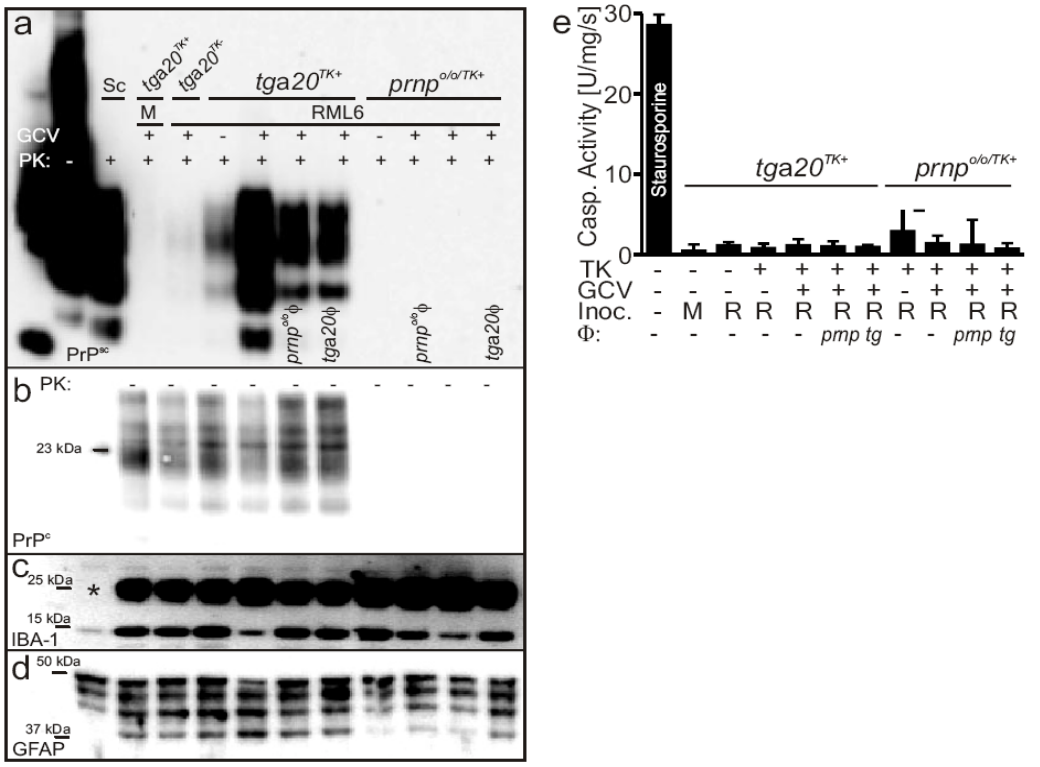

Figure 21. Rescue of microglia depletion and impact on prion replication

After treatment with RML6 (2.7 log SCI_{50}), *tga20*$^{TK+}$ and *Prnp*$^{o/o/TK+}$ were separated into 4 pools each and 3 pools/condition were treated with GCV. 250.000 *tga20* or *Prnp*$^{o/o}$ macrophages (*tga20*Φ and *Prnp*$^{o/o}$Φ respectively) were added to 2 GCV-treated cultures and after 30 days in vitro the tissue was harvested and analyzed. Western blotting was performed on (**a**) 20 µg sample digested with PK (25 µg/ml) or (**b**) 10 µg undigested sample detected with mouse anti-mouse PrP^C IgG_1 (POM-1), (**c**) rabbit anti-human Iba1 (* indicate an unknown protein cross reacting with the Iba1 antibody as described by the supplier) or (**d**) mouse anti-GFAP IgG_1 (Clone GA5). (**e**) Caspase-3 enzymatic activity was measured and normalized to protein contents. Data is presented as the average of 4 biological replicas ± standard deviation (SD). One-way ANOVA with Bonferroni post-test for selected pairs of columns was used for statistical analysis (n.s. = $p > 0.05$).

Macrophage reconstitution rescues effects caused by microglia depletion

To further study whether the observed effect was due to GCV-mediated removal of microglia I performed a macrophage-rescue experiment. *Tga20*$^{TK+}$ or *Prnp*$^{o/o/TK+}$ slices were incubated with RML6 and treated with GCV to deplete microglia. Microglia-depleted tissue was reconstituted with intra-peritoneal macrophages from *Prnp*$^{o/o}$ and

tga20$^{+/+}$ mice respectively. After microglia-depletion a clear increase in PrP^{Sc} was observed as expected (Figure 21a, lane 6-7). This increase in PrP^{Sc} could be almost completely rescued by reconstituting the tissue with macrophages, irrespectively of whether the macrophages expressed PrP^{C} (Figure 21a, lane 8-9). Microglia depletion/reconstitution was verified by analyzing the expression levels of the macrophage marker Iba1 (Figure 21c). PrP^{C} levels were equal in all samples (Figure 21b) and no differences in caspase activity (Figure 21e) or GFAP expression (Figure 21d) were observed in either of the prion infected tissues.

Microglia depletion leads to a significant increase in prion infectivity

Next, we used SCEPA to analyze *tga20*$^{TK+}$ samples, untreated or treated with GCV for 30 days from 3 independent biological experiments performed on different days (Figure 22a). Microglia-depleted cultures showed a significant 14.5 ± 13.2 fold increase over non-depleted cultures in their prion titers (2-tailed paired student T-test, $p = 0.458$, $n = 3$), which corresponds well to the difference observed by western blot analysis of the samples analysis of microglia-depleted samples (a 9 ± 11.8 fold increase over non-depleted slices, $n = 6$) (Figure 22a-b, data not shown). Despite a high inter-experimental variance, all 6 independent replicas displayed a clear increase in PrP^{Sc} accumulation after microglia-depletion (a 2-33 fold increase). No residual inoculum was observed in *Prnp*$^{o/o/TK}$ culture irrespectively of microglia status (Figure 22b). These result confirm that microglia regulate both PrP^{Sc} and prion formation in a negative fashion.

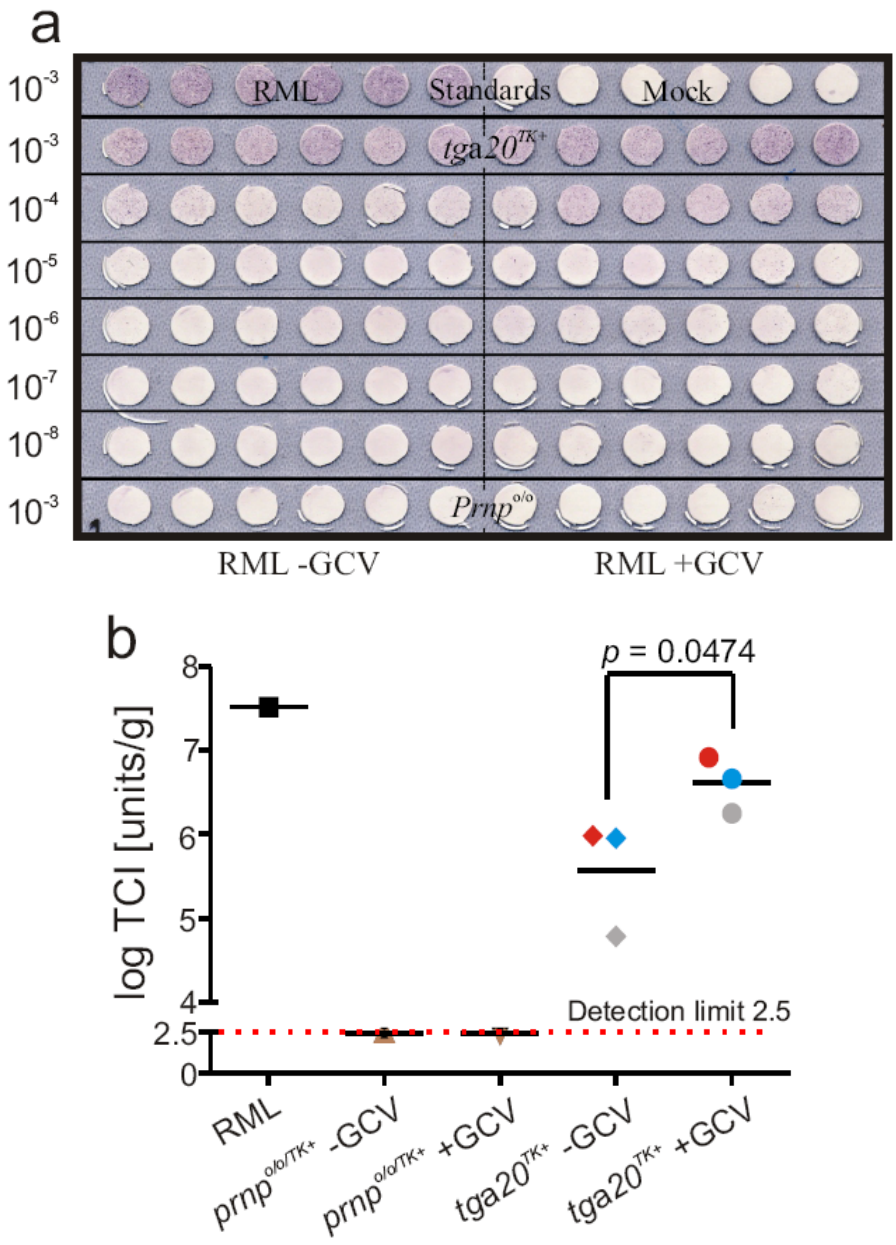

Figure 22. Microglia depletion leads to accumulation of prion infectivity

Homogenates of *tga20*$^{TK+}$ or *Prnp*$^{o/o/TK+}$ slices infected with RML6 (2.7 log SCI_{50}) for 5 weeks either in the absence (-GCV) or presence of GCV (+GCV) were transmitted into the scrapie cell assay in endpoint format (SCEPA). (**a**) Micrograph of a representative plate containing one -GCV and one +GCV sample. (**b**) 3 independent biological replicas of *tga20*$^{TK+}$ and single replicas of *Prnp*$^{o/o/TK+}$ slices or RML6 were analyzed in 10-fold dilution steps from 100 µg/ml – 1 ng/ml using 6-12 replica wells per dilution (300 µl/well).

Microglia depletion leads to an increased susceptibility to a prion infection

Microglia-depleted tissue accumulates prions to a higher degree, begetting the question whether GCV-treated *tk*$^{+}$ slices would be more sensitive to a prion infection. I therefore performed an end-point titration experiment with RML6 on *tga20*$^{TK+}$ slices. *Tga20*$^{TK+}$ slices were infected with various concentrations of RML6 and separated into 2 pools. One pool was left untreated and the other was treated with GCV. After 5 weeks *in vitro*, PK-resistant material was observed in microglia-depleted tissue at a 10-fold lower RML6-dilution (-0.3 log SCI_{50}), showing that microglia-depleted tissue indeed is more sensitive to a prion infection (Figure 23a-b).

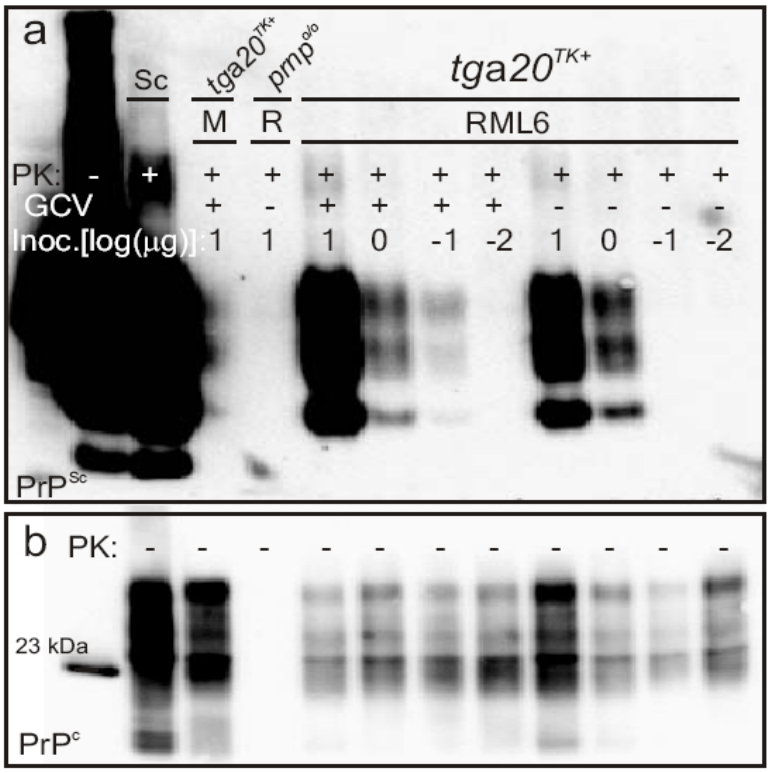

Figure 23. Impact of microglia on tissue susceptibility to a prion infection

Cultures were prepared from 10-day old *tga20*$^{TK+}$ or *Prnp*$^{o/o/TK+}$ mice and treated with RML6 in 10 fold dilution steps from 1.7 to -1.3 log SCI_{50}. Each samples was divided in 2 pools. One pool was treated with GCV and one pool was left untreated. The tissue was harvested after 35 days *in vitro*. (**a**) Western blotting of 20 µg sample digested with PK (25 µg/ml) or (**b**) 10 µg sample undigested detected with mouse anti-PrP^{C} IgG_1 (POM-1).

DISCUSSON

POSCA

In order to study the role of microglia in prion disease, I have developed the POSCA, a novel assay system which allows for prion infectivity determination and for studying prion replication *ex vivo* in a complex cellular environment. I have evaluated the operating characteristics of the POSCA against the 2 most commonly used prion titration assays: the SCEPA (Klohn et al., 2003) and the mouse endpoint bioassay (Fischer et al., 1996).

The SCEPA is a cell-culture based prion replication assay using a neuroblastoma subclone, N2a-PK1. Alternative primary cell culture assays have recently been reported. Primary cultures of neurons, astrocytes, neural stem cells and neurospheres has been shown to be infectible *in vitro* (Cronier et al, 2004; Giri et al., 2006; Milhavet et al., 2006). However, in these culture systems residual prion inoculum persisted in *Prnp*-deficient cultures after 24-28 days. SCEPA measured approximately 8 log LD_{50} per g brain material and the neurosphere assay measured approximately 5 log LD_{50}/g (Klohn et al., 2003; Giri et al., 2006). The POSCA assay measures approximately 6.9 LD_{50}/g. When I depleted microglia I could even detect a 10-fold lower dilution of RML6, therefore approaching the sensitivity of the SCEPA. Importantly, residual inoculum does not constitute a problem for the POSCA.

As a research tool, cell line based assays have the disadvantage that there is a limited number of cell lines available, especially PrP-deficient cell lines, making it difficult to control experiments stringently. *Ex vivo* organotypic brain slice cultures can be prepared from mice of any desired genotype and the tissue can easily be manipulated. This gives us a flexible and robust experimental system to study prion infection in. Importantly, cells retain the cellular connections of a normal brain, allowing for the study of the role of different cell types in prion replication and pathogenesis.

Many cell lines also show a high selectivity in which prion strain the cells can replicate. As compared to tumor cell lines, certain transgenic mouse lines are more ‘promiscuous’ in their inoculum compatibility. In contrast to the SCEPA, the POSCA can avail itself of the large repository of genetically modified mouse lines susceptible to prions of human, bovine, ovine, and cervid origin. This can allow us to study the

phenomenon strain adaptation and strain propagation (Weissmann, 2004). This can be done in a well-controlled fashion over multiple passages in a relative short period of time. I have successfully infected slice cultures using inoculum passaged in our slice cultures (data not shown).

Compared to *in vivo* models, the slice culture system has a very short incubation time. I observe prion replication already after 20 days in *tga20*^{TK} cultures (10^{-3} RML6). *Tga20* mice inoculated intra-cerebrally with a high dose of RML6 take 60-150 days to come down with clinical disease (Klohn et al., 2003). Furthermore, I observe prion replication in *Prnp*$^{+/o}$ slices after 35 days. *In vivo*, *Prnp*$^{+/o}$ mice have an incubation time of 225-300 days before coming down with clinical disease after intra-cerebral inoculation (Büeler et al., 1993). The reason why I see such a rapid replication in our *in vitro* system is unknown, but useful none-the-less. An additional feature of our model is that prions are replicated to a very high extend. I observed similar amounts of prions in homogenates from prion infected slice cultures and in brains of terminally sick mice, both by PK western blotting and by transmission into the SCEPA.

Microglia involvement in prion disease

Microglia activation is an early and extensive hallmark of most prion diseases. Numerous studies show that microglia can release inflammatory and neurotoxic factors typically associated with neurodegenerative diseases (Dandoy-Dron et al., 1998; Baker and Manuelidis, 2003; Baker et al., 2004). It has even been claimed that prion neurotoxicity is crucially mediated by microglia (Brown et al., 1996; Kercher et al., 2007). Mice devoid of a microglia-borne factor, Interleukin-1 were reported to experience a modest increase in survival time as compared to *wt* mice, which suggests and indirect link between microglia-mediated inflammation and neurodegeneration (Schultz et al., 2004).

The suggestion that microglia could play a role in prion turnover stem from the observation that microglia often are associated with prion plaques and that infectivity can be recovered from microglia purified from terminally sick mice (Manuelidis et al., 1997; Andreoletti et al., 2002; Baker et al., 2002). It was hypothesized that microglia acts as a carrier of prions within the brain and thus could play a role in the dissemination of prions within the CNS (Baker et al., 2002). In mice reconstituted with eGFP-labelled bone marrow, microglia turnover and CNS engraftment by

peripheral monocytes was increased dramatically upon prion infection. This suggested that *wt* monocytes engrafting the brain of *Prnp*$^{o/o}$ mice are neither able to transport prions to the CNS nor to replicate prions (Priller et al., 2006). This is in agreement with observations that other peripheral macrophage populations are capable of reducing prion infectivity *in vitro* and PrP^{Sc} accumulation in the spleen *in vivo* (Carp and Callahan, 1982; Michel et al., 1987; Beringue et al., 2000).

Selective manipulation of microglia *in vivo* is hampered by their similarities to macrophages. Here I used *CD11b-HSVTK* mice (Heppner et al., 2005) for pharmacogenetic ablation of microglia. I found that microglia can be completely ablated from cerebellar slice cultures derived from *CD11b-HSVTK*$^{+}$ mice, and this ablation has no obvious implications for the viability of other cell populations. I then show that microglia removal dramatically unleashes prion replication in organotypic slices. This points to a role for microglia in containment of prion infections. Microglia may exert this role by phagocytosing and degrading prions *in situ* (Carp and Callahan, 1982; Michel et al., 1987; Beringue et al., 2000; Priller et al., 2006), This may explain the presence of prions in microglia acutely isolated from scrapie-sick mice (Baker et al., 2002) despite the inability of microglia to replicate prions (Priller et al., 2006).

There may be eminently practical ramifications to the phenomena described above. One ID_{50} unit of prions measured upon intracerebral challenge has been reported to be equivalent to 10^4-10^5 PrP molecules (McKinley et al., 1983). This is in sharp contrast to many viral diseases in which 1-10 particles are equivalent to 1 ID_{50}, and has even been taken to cast doubts on the identity of the prion with PrP^{Sc} (Manuelidis et al., 1987). The priolytic activity of microglia uncovered in the present study may contribute to increasing the minimal amount of PrP^{Sc} needed to infect individual organisms. One hypothesis for the etiology of sporadic CJD states that PrP^{Sc} formation could be a stochastic event, which under normal circumstances are cleared from the brain. Changes compromising the brains capacity to clear PrP^{Sc}, such as the loss of microglia seen in other neurodegenerative disease (Ma et al., 2003) could then lead to an uncontrolled replication/deposition of PrP^{Sc} and neurodegeneration (Safar et al., 2005). We show in the current study, that microglia constitute exactly such a brain-specific clearing mechanism. As it has previously been shown that aging microglia show a decrease capacity to phagocytose amyloids (Floden et al., 2006), one might speculate whether microglia dysfunction associated with aging could be an

underlying cause for sporadic CJD. By extension, one might also speculate that medical conditions and iatrogenic interventions which affect the function of microglia may heighten the susceptibility to prion infections.

OUTLOOK

POSCA

Many cell lines show a high selectivity in which prion strain the cells can replicate. Researchers in many different laboratories world-wide are currently working with primary strains of scrapie for which there is no compatible cell-based prion assay. Recently, it was reported that bank voles (*Clethrionomys glareolus*), a wild rodent species, are susceptible to prions from a range of sources including various strains of scrapie, BSE and CJD (Nonno et al., 2006). Transgenic mice expressing the bank vole prion protein was generated in the lab of Juan M. Torres (unpublished data). We have received these mice and we are hoping to establish a slice culture based assay of broad specificity based on slices prepared from 'bank volized' mice.

Microglia in prion diseases

The role of microglia in neurodegenerative diseases is multi-faceted. In Alzheimer's disease microglia and infiltrating monocytes appear to play a neuroprotective role by antagonizing amyloid deposition (Simard et al., 2006), while at the same time contribute to pathology via the production of neurodegenerative factors such as reactive oxygen species, cytokines and complement factors (Heneka et al., 2007). Overall, it would appear that microglia play a neuroprotective role in Alzheimer's disease (Khoury et al., 2007) and therefore pharmacological intervention should focus on shaping, not blocking, a disease-associated microglia response. Indeed it has been shown in several independent studies that anti-inflammatory drugs modulating microglia function has pharmacological potential, making microglia a potentially important drug target in neurodegenerative protein-misfolding diseases (McGeer et al., 2006).

Analogues to what is seen in Alzheimer's disease, I observe that microglia antagonizes prion formation in organotypic brain slices. Our results indicate a protective role for microglia in prion disease. However, mRNA profiles of microglia purified from prion-infected animals suggests a pro-inflammatory and potentially neurotoxic function of microglia (Almond et al., 1995; Dandoy-Dron et al., 1998; Baker et al., 2002; Baker and Manuelidis, 2003; Baker et al., 2004). A possible

neurodegenerative function of microglia was not explored in the POSCA in detail. I am currently investigating whether longer incubation times will allow us to observe prion-induced neurodegeneration in POSCA. If that is so, I plan to explore the contribution of microglia to prion-induced cell death. Furthermore, I plan to explore the inflammatory response of microglia in prion-infected slices by quantitative PCR.

In addition, I am currently evaluating if pharmacological intervention or treatment with cellular factors can stimulate or inhibit prion removal. In short, prion-infected cultures are treated with recombinant cytokines and pharmacological agents that have been reported to affect microglia function. Factors that affect prion replication will be screened in microglia-depleted tissue to confirm whether the prion-modulatory effect is microglia-dependent.

PART II

Part II of my thesis consists exclusively of unpublished data.

INTRODUCTION

Prion replication in mono-cultures.

In order to understand prion replication and prion-induced pathology, a simplified cell culture system can be an important tool to dissect the molecular mechanisms behind it. It has been known for more than 35 years that prions can survive in cell culture. Explant cultures from chimpanzees experimentally infected with Kuru, a human iatrogenic form of CJD, persisted in harboring infectivity for up to 250 days *in vitro* (Gajdusek et al., 1972). Whether infectivity was amplified *in vitro* or if infectivity only persisted was not investigated. In the above mentioned studies cultures were prepared from monkey infected more than a year earlier. An easier approach to study prion replication in an *in vitro* system would be to prepare primary cultures of uninfected neonatal tissue or use cell lines and infect the cultures *ex vivo*. Unfortunately, this approach carries some drawbacks. The main concerns/obstacles for studying prion replication *in vitro* (as well as *in vivo*) is persistence of the prion inoculum. Primary cells and cell lines are cultured on coated plastic dishes that will bind proteins, including PrP^{Sc} from the inoculum. It is currently impossible to clearly distinguish between PrP^{Sc} from the original input material and *de novo* synthesized prions.

This obstacle can be overcome by using cell lines or cultures of primary cells that undergo mitosis at a rapid rate and can be serially passaged. The scrapie cell assay technique is based on the fact that cells can be passaged repeatedly after the initial inoculation, usually by splitting the cells 1:3, 3 times, followed by splits of 1:10, 3 times. This procedure dilutes out the original inoculum to an extend where it is no longer detectable and therefore all the PrP^{Sc} that can be detected must come from *de novo* replication of prions. This approach is the basis for the SCEPA (Klohn et al., 2003) and has been shown to work well for prion-infection of a number of cell lines

and for mouse neurospheres (Giri et al., 2006). The process is relatively labor-intensive and time consuming, but it can be automated. Another alternative is to use chronically infected cell lines (Solassol et al., 2003).

For primary neural cultures that are either post-mitotic (neurons) or dividing very slowly (astrocytes, microglia, oligodendrocytes) residual inoculum constitutes a major issue. Various approaches has been used to infect differentiated neural cells. Monolayers of differentiated neural stem cells was reported to be susceptible to prions (Milhavet et al., 2006). To avoid residual inoculum, the input material was solubilized using high detergent concentration and both inoculum and detergents were added to the cells. Other reports ignored the issue altogether and reported that the PrP^{Sc} signal increased over time above the signal of *Prnp*$^{o/o}$ cells treated with the same amount of input material (Cronier et al., 2004; Cronier et al., 2007). Despite the slightly crude method of the study, the authors reported that cerebellar granule neurons and astrocytes can replicate prions *in vitro*. Currently, there is no easy or robust method to infect primary neural cultures. Recently, another exciting approach on how to distinguish between inoculum and *de novo* synthesis was reported (Vorberg et al., 2004). The authors infected cells expressing a tagged version of the prion protein. PrP^{Sc} was subsequently detected with a tag-specific antibody (that did not recognize PrP^{C} in the inoculum). This method requires that the tag becomes a part of the PK-resistant portion of the prion protein upon prion replication (Vorberg et al., 2004). Unfortunately, it appears that tagging the prion protein is a very efficient method to inhibit or prevent the conversion of PrP^{C} to PrP^{Sc} *in vivo* (Barmada and Harris, 2005) and to date no transgenic animals carrying an easily convertible tag has been reported in the literature.

Prion protein deletion mutants

The normal function of the cellular prion protein and the cause of the neurological disease which develops during the conversion of PrP^{C} to PrP^{Sc} remain poorly understood. Mice expressing a deletion in the prion protein between residues 32-134 (ΔF) (Shmerling et al., 1998; Radovanovic et al., 2005) or mice with smaller C-terminal deletions lacking residues 93-134 (ΔHC) (Baumann et al., 2007) or 105-125 (Li A, 2007) develops neurological phenotypes and die at a very young age. Histological and biochemical analysis of the mice show that terminally sick ΔF and

ΔHC mice suffers from a white matter pathology involving progressive demyelination, synaptic dysfunction, and axonal degeneration. For ΔF mice and for mouse lines expressing low amounts of ΔHC, this phenotype is apparent only in the absence of full-length PrP^C expression (on a $Prnp^{o/o}$ background) (Shmerling et al., 1998). High expressing mouse lines of ΔHC mice develops pathology even on a $Prnp^{+/o}$ background, but not on a $Prnp^{+/+}$ background showing that PrP^C rescues the phenotype induced by the deletion mutants in a concentration dependent fashion (Baumann et al., 2007). Whether toxicity stems from a loss of function or a gain of function induced by the mutants is uncertain. Aged, 60 weeks old, $Prnp^{o/o}$ mice do show a similar, but much less severe white matter pathology and axonal loss (Nishida et al., 1999). It is feasible that PrP^C is part of a complex important for myelin maintenance and that pathology develops in ΔHC mice due to an accelerated loss-of-function caused by interference with this complex (Baumann et al., 2007).

In contrast, mice expressing a smaller N-terminal deleted prion protein lacking residues 69-84 (ΔA), 32-80 (ΔB) (Fischer et al., 1996) or 32-93 (ΔC) (Flechsig et al., 2000) do not develop any obvious signs of neurodegeneration. Despite lacking parts or all of the octa-peptide repeat region, both ΔB and ΔC mice replicate prions, albeit less efficient than mice expressing the full-length prion protein (Fischer et al., 1996; Flechsig et al., 2000). Prion-infected ΔC mice (*C4/C4* line) succumbs to prion disease, showing signs reminiscent of prion-infected mice expressing full-length PrP^C. Surprisingly, these prion-infected mice do not show any obvious scrapie-associated histopathological changes in the brain. In the spinal chord, pathological changes (increased GFAP expression and loss of motor neurons) are similar to what is seen in scrapie infected wild-type mice. Infectivity can be recovered from the brain (30-fold less than wild-type mice) and spinal chord (equal to wild-type mice) of terminally sick RML-infected *C4/C4* mice. Homogenates of ΔC(RML) (RML passaged in *C4/C4* mice) re-transmitted into mice expressing full-length PrP, causes prion-replication and pathology to the same extend as RML (Flechsig et al., 2000).

Outline of this work

The focus of the current study was to develop tools to study prion replication *in vitro*, specifically to overcome the problem of distinguishing between inoculum (input) and *de novo* synthesized PrP^{Sc} (output). I used ΔC(RML) (lacking the octa-peptide repeat

region) as inoculum to infect slices prepared from mice expressing full-length PrP^{C}. PrP^{Sc} synthesized from PrP^{C} contained the octa-peptide repeat region, which was absent in the inoculum. I used an antibody specific for the octa-peptide repeat region to detect PK-resistant PrP and this antibody selectively recognized newly synthesized PrP^{Sc}. This technique allows us to specifically observe prions replication *in vitro* and *in vivo* in wild type and transgenic mice. I used the technique to characterize which CNS-specific cell types replicate prion *in vitro*. I found that primary cultures of cerebellar granule neurons and astrocytes replication prions. In contrast, I could find no evidence suggesting that microglia replicate prions. A further characterization of which CNS and PNS-derived cells replicate prions is still in progress.

RESULTS

'Invisible inoculum'

In order to establish a method for the selective detection of prion replication, I took advantage of the work of Flechsig and Weissmann showing that homogenates of prion inoculated ΔC mice (*C4/C4*) inoculated with the RML strain are infectious to mice

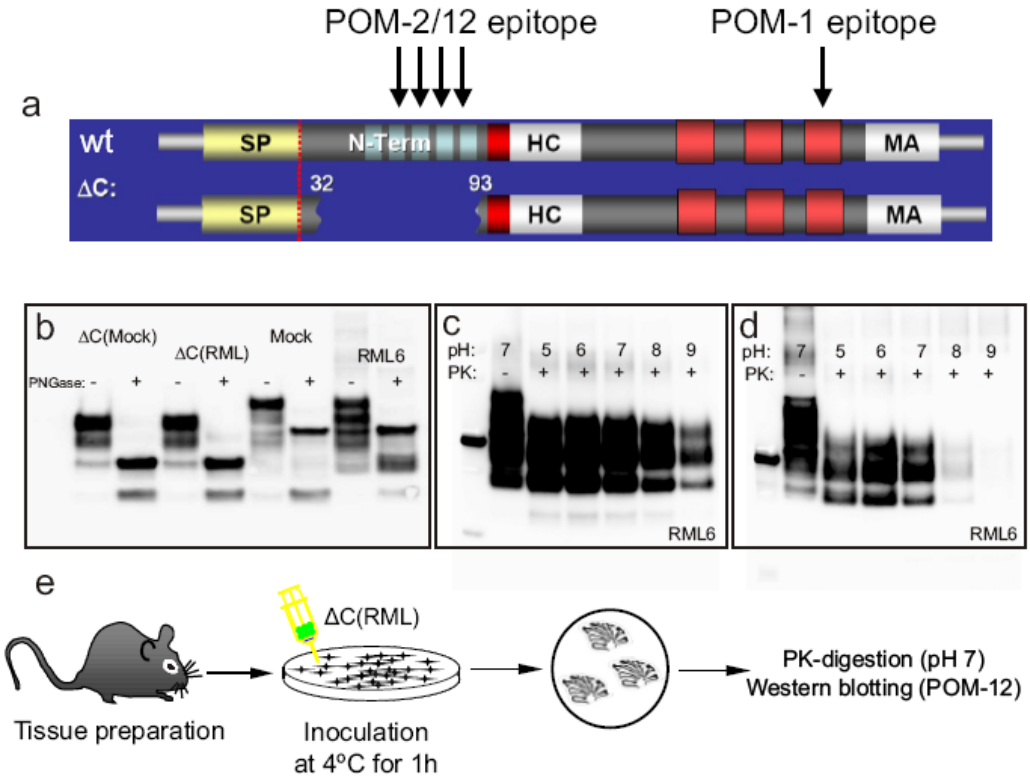

Figure 24. Parameters necessary for selectively detecting de novo prion replication in vitro

(**a**) The POM-12 monoclonal antibody recognizes an epitope in the PrP^C-octarepeat-region, which has been deleted in the PrP-deletion mutant mouse ΔC (*C4/C4*). POM-1 recognizes alpha-helix one on both PrP^C and ΔC. (**b**) PNGase treatment of *wt* mock brain homogenates, RML6, brain homogenates from ΔC mice (ΔC(mock)) or RML inoculated terminally sick ΔC mice (ΔC(RML)). (**c-d**) 20 µg RML6 was digested with 25 µg/ml PK at various pHs. Western blots were detected using mouse anti-PrP^C IgG_1 (**c**) POM-1 or (**d**) POM-12, showing that pH 6-7 is optimal for detection of PK-resistant PrP^{Sc} with POM-12. (**e**) Scheme depicting set-up for distinguishing between input and output material. ΔC(RML) lacking the POM-12 epitope is used to infect cells expressing full-length PrP^C. PK-resistant material is detected using POM-12 that should only recognize host-derived PrP^{Sc}, not ΔC(RML).

expressing full-length PrP (*tga20*$^{+/+}$) (Flechsig et al., 2000). ΔC(RML) homogenates contain high levels of PrP^{Sc}, generated from the PrP deletion-mutant, ΔC, devoid of the octa-peptide repeat region (Figure 24a). Furthermore, I took advantage of a previous observation, indicating that 2 octa-repeat region specific anti-PrP antibodies generated in the Aguzzi lab (POM-2 and POM-12), recognize PK-resistant PrP^{Sc} (Polymenidou et al., 2005). I hypothesized that if I use ΔC(RML) to infect cells expressing full-length PrP, POM2 or POM12 would selectively recognize newly synthesized PrP^{Sc} (Figure 24a). ΔC(RML) was obtained from Eckhard Flechsig and analyzed by western blotting after treatment with PNGase (a deglycosylation enzyme that removes N-linked sugar moieties). After treatment with PNGase both ΔC(RML) and ΔC(Mock) (homogenates of an uninfected *C4/C4* mouse) migrated faster than homogenates of an RML-infect or uninfected wt mice by SDS-PAGE (Figure 24b). These results confirmed that the ΔC samples only contain truncated-PrP as could be expected. I observed that the pH of the lysis buffer greatly affected detection of PrP^{Sc} with POM-12 (Figure 24d) and to some extend also with POM-1 (Figure 24c). Therefore, 100 mM Tris-HCL (pH 7.0) was added to the lysis buffer. Since the POM-12 epitope was absent in the inoculum, I predicted that we would not detect any inoculum using POM-12. I therefore skipped the washing steps normally used for removing residual inoculum. The tissue was incubated as free-floating sections in inoculum-containing buffer and after 1 h at 4 °C, the tissue was transferred to the cell culture membrane (Figure 24e).

Slices generated from *tga20*$^{+/+}$ or *Prnp*$^{o/o}$ pups were treated with RML6, ΔC(RML) and ΔC(Mock) (100 µg per 10 slices). After 5 weeks *in vitro,* slices were harvested and both slices and inoculum was analyzed by PK-western blot (Figure 25a-b). Undigested RML6, ΔC(RML) and ΔC(Mock) inoculum (10 µg per blot) were analyzed by western blot and detected with POM-1, showing faster running patterns for all ΔC-samples, indicating a smaller molecular weight as expected (Figure 25a, lane 2-4). After digestion with PK, ΔC(RML) showed a much lower PrP^{Sc} signal compared to RML6, but a clear PK-resistant PrP-signal was detected none-the-less (Figure 25a, lane 5-7). *Tga20*$^{+/+}$ slices treated with ΔC(RML) showed abundant PrP^{Sc}, whereas mock and *Prnp*$^{o/o}$ slices did not show any PK-resistant material 5 weeks post-inoculation, confirming that ΔC(RML) could replicate in *tga20*-derived slices (Figure 25a, lane 8-10).

The same samples loaded onto a replica blot were analyzed using POM-12. As predicted, POM-12 clearly detected undigested and PK-digested RML6, but no signal was detected in lanes loaded with ΔC inoculum (Figure 25b, lane 2-7). A PK-sensitive 37 kDa band was detect in RML6 and ΔC samples with POM-12, but this band is also present in *Prnp*$^{o/o}$ samples, indicating that POM-12 cross reacts with a non-PrP moiety (Figure 25b, lane 2-4, data not shown). A strong PrP^{Sc} signal was detected in *tga20*$^{+/+}$ slices infected with ΔC(RML), showing that POM-12 only recognized newly generated PrP^{Sc}, in essence rendering the inoculum 'invisible' (Figure 25b, lane 8-10).

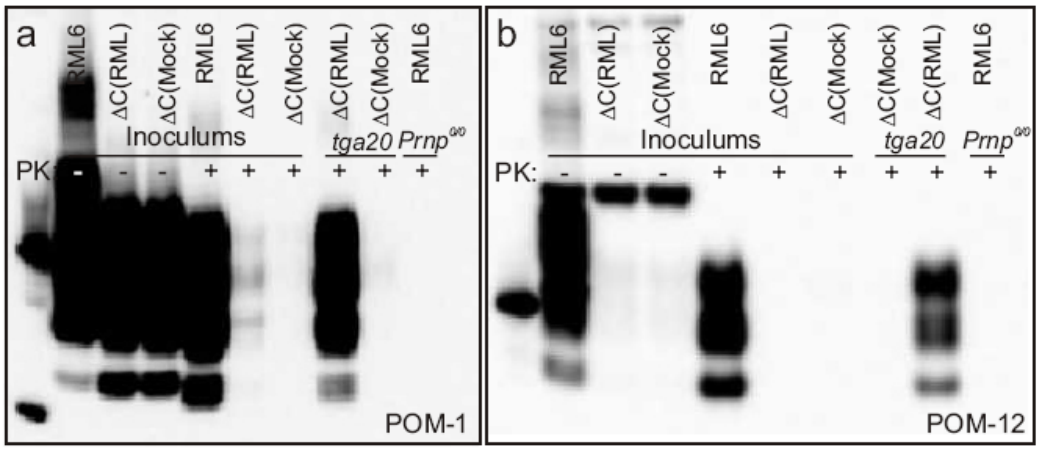

Figure 25. Selective detection of *de novo* prion replication

Cultures from *tga20*$^{+/+}$ and *Prnp*$^{o/o}$ mice were inoculated with ΔC(RML), ΔC(Mock), RML6 or mock brain homogenate and cultured for 35 days prior to harvesting the tissue in pH 7.0 lysis buffer. Western blots of PK-digested inoculum and slice culture homogenates were detected using mouse anti-PrP^{C} IgG$_1$ (**a**) POM-1 or (**b**) POM-12.

Prions replication in primary CNS cultures

Cerebellar Granule Cells

Next, I proceeded to test which CNS-derived cell populations can be infected with prions *in vitro*. Cerebellar granule cells (CGCs) make up more than 95 % of the total number of cells in the cerebellum and are easy to culture staying viable for up to 4 weeks *in vitro*. CGCs were prepared according to established methods (Leist et al., 1997). Since I previously observed that prion replication is more efficient in *ex vivo* cultures of cerebellar tissue in the absence of microglia, I first established the parameters for microglia depletion in CGC cultures using the *CD11b-HSVTK* mice (Figure 26 and 27). Cultures were prepared, treated with GCV (5 µg/ml) for 10 days, fixed and stained for various cell populations. As observed in organotypic slice cultures, GCV-mediated microglia removal was transgene-dependent (Figure 26a), without any overt effects on the neuronal axonal network of the CGCs (Figure 26b).
CGC-cultures contained about 5 % astrocytes, which showed a close physical interaction with cerebellar granule neurons (i.e. all neuronal cell bodies appeared to be in direct contact with astrocyte projections). Microglia depletion did not affect the

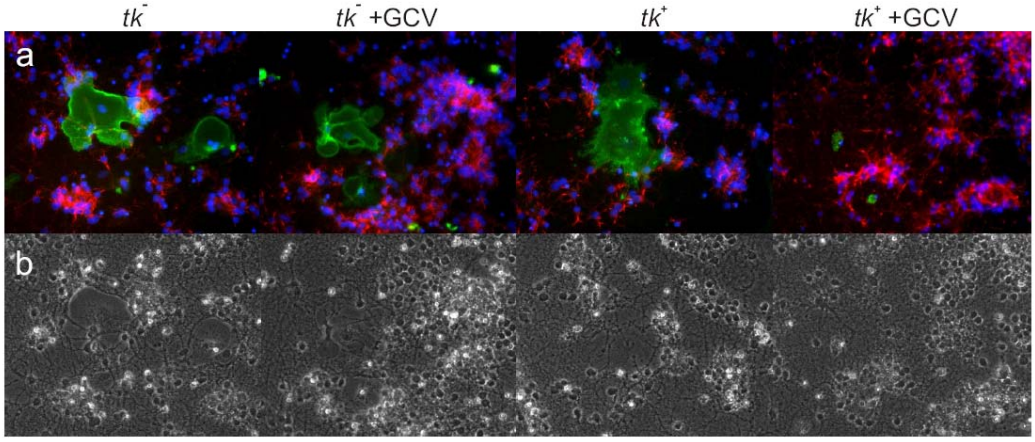

Figure 26. Microglia depletion in cerebellar granule cell cultures
Cerebellar granule cells were prepared from 7-day old *CD11b-HSVTK*$^-$ (*tk*$^-$) and *CD11b-HSVTK*$^+$ (*tk*$^+$) mice and cultured for 10 days, either untreated (-GCV) or in the presence of GCV (+GCV). (**a**) Cultures were fixed in 2 % PFA and co-stained with IB_4-Alexa^{488} (green), mouse α-β_{III}-tubulin IgG_1 (red) and dapi (blue) (**b**) Phase contrast images of the regions depicted in (**a**).

number or the morphology of astrocytes (Figure 27a). Within 10 days of GCV-treatment tk^+ microglia were completely abolished from the culture (Figure 27b). The few microglia that remained showed a condensed cytoplasm and appeared dead (Figure 28a). GCV treatment and microglia depletion also did not affect the viability

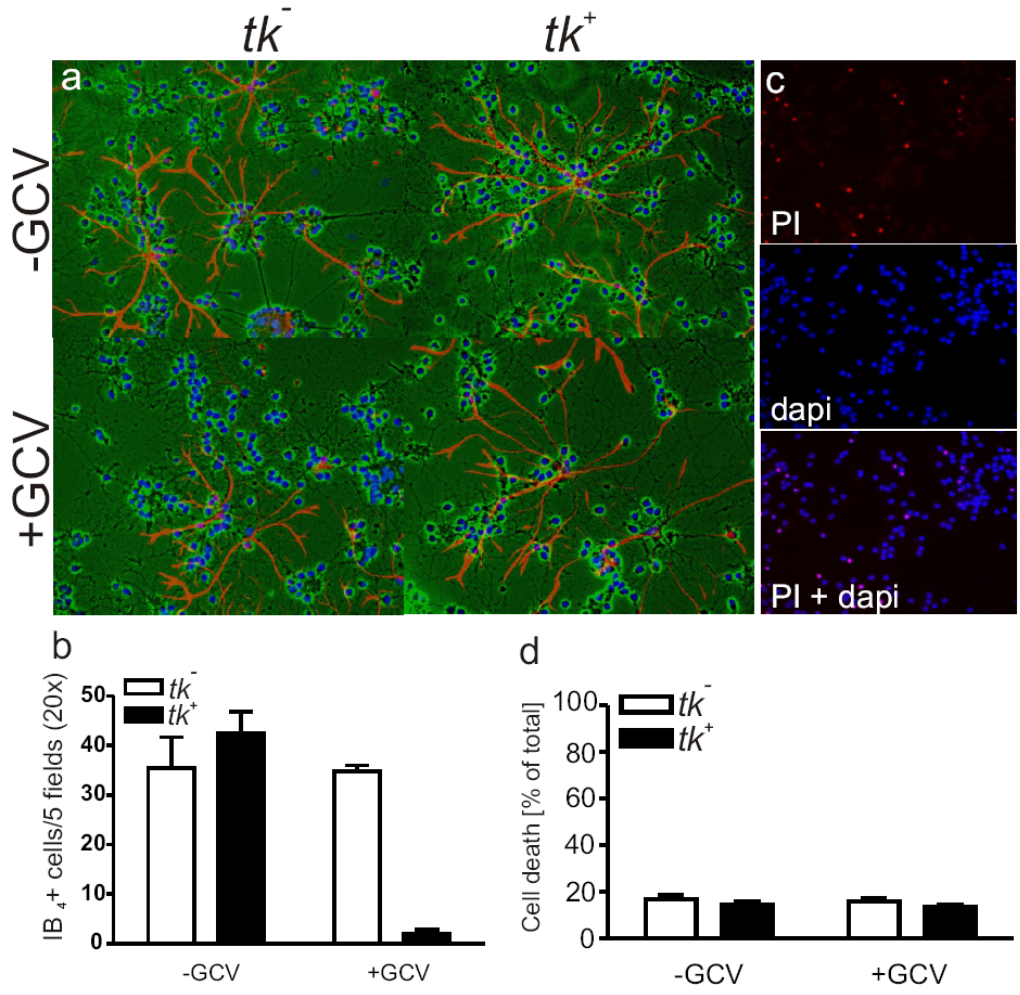

Figure 27. Microglia depletion in cerebellar granule cell cultures

Cerebellar granule cells were prepared from 7-day old *CD11b-HSVTK*$^-$ (tk^-) and *CD11b-HSVTK*$^+$ (tk^+) mice and cultured for 10 days, either untreated (-GCV) or in the presence of GCV (+GCV). (**a**) Overlay of phase contrast images (green), and cells stained with dapi (blue), and rabbit α-GFAP polyclonal antibody (red). (**b**) Images from Figure 26 (**a**) were quantified (*n = 6* biological replicas, each the added value of 5 images (20X)). Non-fixed cultures were co-stained with Dapi and PI. (**c**) Representative images of PI-positive tk^+ +GCV cultures. (**d**) Images were quantified (*n = 6* biological replicas, each the average value of 4 images (20X)).

of the cultures as measured by PI-incorporation (Figure 27c-d).

I initially tested 3 different infection regiments to prion infect CGCs. I prepared CGC cultures from *tga20*^{TK} mice and added GCV to the cultures. Cultures were either treated with 2.5 µg or 25 µg ΔC(RML) inoculum (in 250 µl medium) in the presence of 10 % FCS for 24 h before changing the medium to fresh, serum free medium. After the medium change 25 µg inoculum was added back to 1 of the cultures. Cultures were harvested 3 and 4 weeks post-inoculation and analyzed by PK-western blot. In all conditions a clear, albeit variable PrP^{Sc} signal was observed after 3 and 4 weeks, regardless of treatment regiment (Figure 28, lane 10-15). No PrP^{Sc} was found in mock treated *tga20*^{TK} or in ΔC(RML) treated *Prnp*$^{o/o}$ samples (Figure 28, lane 4, 7-9).

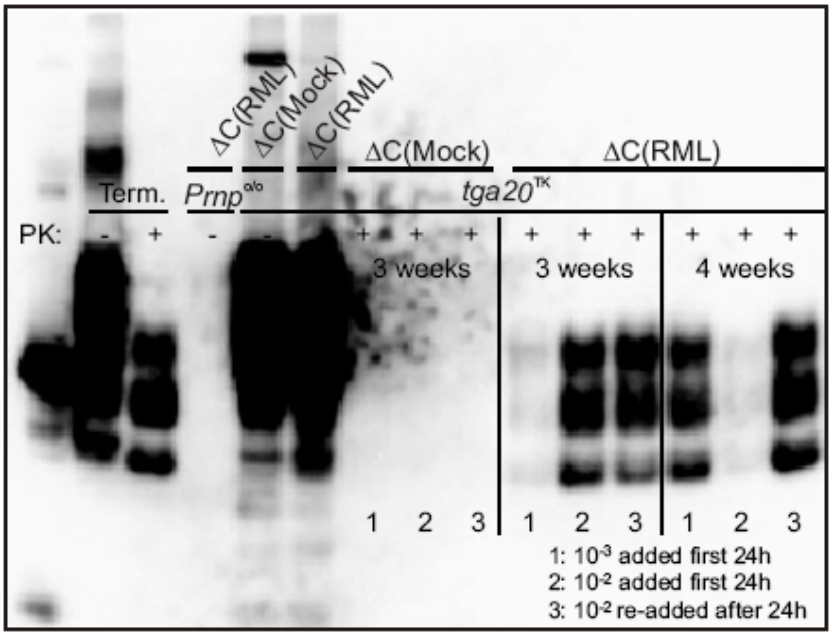

Figure 28. Prion infection of cerebellar granule cell cultures

Cerebellar granule cells were prepared from 7-day old *tga20*^{TK} mice and cultured in the presence of GCV. Cultures were inoculated with different concentrations of ΔC(RML) or ΔC(Mock) for 24 h after which the medium was exchanged to serum free medium. In some conditions the inoculum was re-added after the medium exchange After 3 or 4 weeks *in vitro*, cells were harvested, PK-digested using 5 µg/ml PK to digest 8 µg protein and samples were analyzed by western blotting.

Microglia

In a complex cellular environment the depletion of microglia led to an increase in prion replication (see PART I). This suggests that microglia are capable of removing prion, but it does not per se rule out that microglia also are capable of replicating prions. Indeed it was reported that immortalized microglia from PrP-overexpressing mice can be prion infected (Iwamaru et al., 2007). I prepared mixed glia cultures from *tga20*$^{+/+}$ and *Prnp*$^{o/oTK}$ mice and after 14 days, microglia were shaken off from the *tga20*$^{+/+}$ cultures and co-cultured with a feederlayer of *Prnp*$^{o/oTK}$ astrocytes. The cultures were treated with 10 mg ΔC(RML) or ΔC(Mock) (in 10 ml, 75 cm^2 flask) and treated with GCV for 5 weeks. After 5 weeks, the *tga20*$^{+/+}$ microglia were recovered and compared to microglia recovered from *Prnp*$^{o/o/TK}$ cultures treated with ΔC(RML). A very weak PrP^C signal was detected in *tga20* microglia, but no PK-

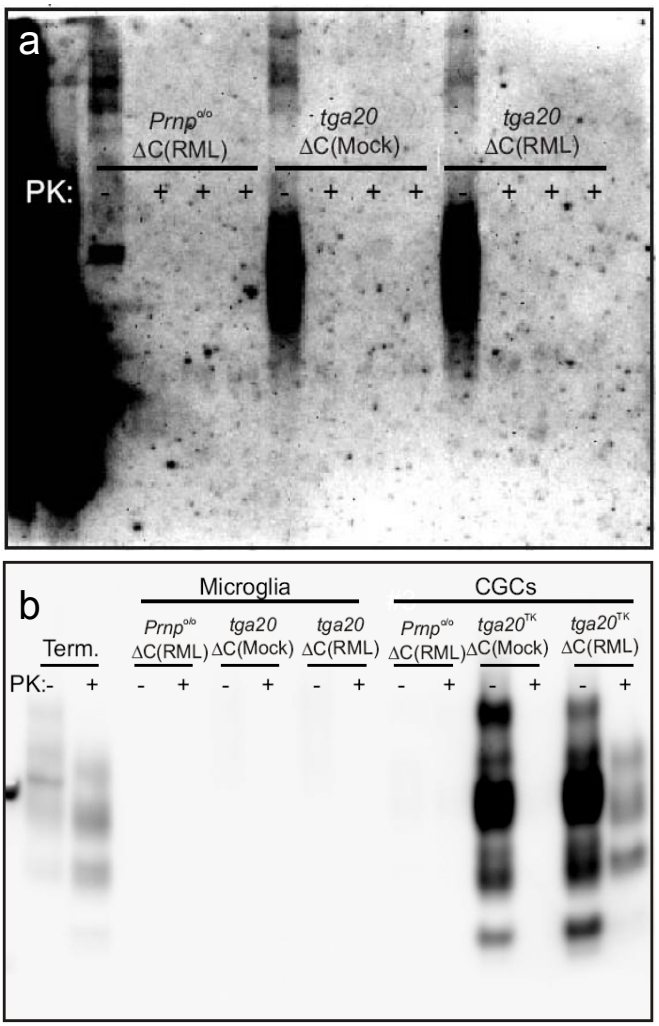

Figure 29. Prion infection of microglia

(**a**) Microglia were purified from 14-day old mixed glia cultures (prepared from 1-day old *tga20*$^{+/+}$ pups). Cells were seeded on a feeder layer of *Prnp*$^{o/o/TK+}$ astrocytes and inoculated with ΔC(RML) or ΔC(Mock) for 72 h. Cells were cultured in the presence of GCV for 5 weeks. Microglia was shaken off the feeder-layer and purified by differential adherence by letting the cells adhere to a plastic surface for 45 min (not allowing time enough for astrocytes to attach). (**b**) To qualitatively compare the PrP^C expression level of neurons to microglia, cell homogenate from Figure 26 and from (**a**) was loaded on the same blot. Microglia show a dramatically lower PrP^C expression as compared to neurons.

resistant material was found in any of the tested conditions, suggesting that microglia do not support prion replication (Figure 29a). I compared the expression level of PrP^C in CGCs and in microglia. Microglia expressed almost no PrP to as compared to cerebellar granule neurons, well in line with their apparent inability to replicate prions (Figure 29b).

Astrocytes

Finally, I tested whether microglia-depleted astrocyte cultures could be prion infected. Once again I verified that I can obtain an efficient microglia depletion in mixed glia cultures prepared from *CD11b-HSVTK* mice. Tk^+ and *wt* cultures were prepared and

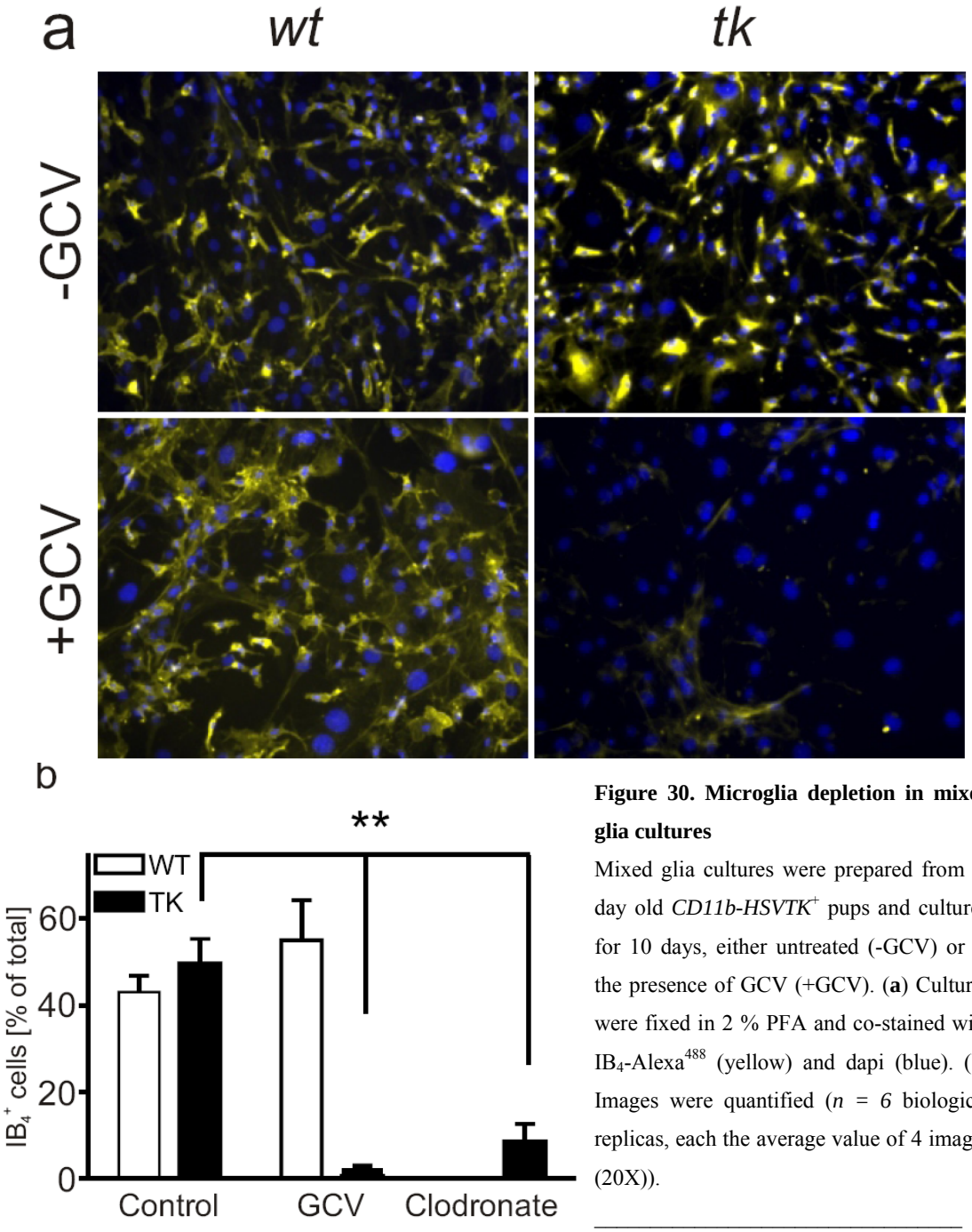

Figure 30. Microglia depletion in mixed glia cultures

Mixed glia cultures were prepared from 1-day old *CD11b-HSVTK*$^+$ pups and cultured for 10 days, either untreated (-GCV) or in the presence of GCV (+GCV). (**a**) Cultures were fixed in 2 % PFA and co-stained with IB_4-Alexa^{488} (yellow) and dapi (blue). (**b**) Images were quantified (*n = 6* biological replicas, each the average value of 4 images (20X)).

treated with GCV (5 µg/ml) for 10 days. Once again I observed an efficient, transgene-dependent depletion of microglia from the cultures (Figure 30a, b). In the same experiment I compared GCV-mediated microglia depletion to depletion with Clodronate-liposomes, a gliotoxin known to deplete microglia (Markovic et al., 2005). Although Clodronate-liposomes did lead to a decrease in the microglia numbers, the depletion was incomplete and induced a certain degree of toxicity to astrocytes (figure 30b, data not shown).

CD11b-HSVTK^{+} astrocytes expressing wild type levels of PrP^{C} were treated with ΔC(RML) (2.5 µg RML6, in 250 µl) and GCV. 5 weeks post-inoculation ΔC(RML) treated *CD11b-HSVTK* astrocytes showed a faint PrP^{Sc} signal in 2 out of 3 replicas, suggesting that astrocytes can replicate prions (Figure 31, lane 13-15). In ΔC ΔC(mock) treated *CD11b-HSVTK*$^{+}$ astrocytes and in ΔC(RML) treated *Prnp*$^{o/o}$ cultures, no PK-resistant material was detected (Figure 31, lane 7-12).

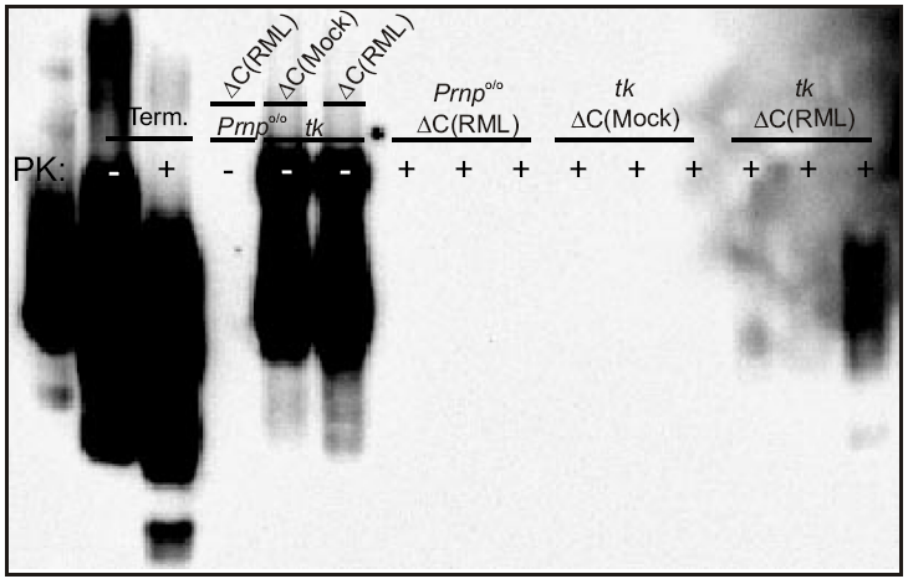

Figure 31. Prion infection of astrocyte cultures

Mixed glia cultures were prepared from 1-day old *CD11b-HSVTK*$^{+}$ and *Prnp*$^{o/o}$ pups and cultured for 10 days, in the presence of GCV. Cells were inoculated with ΔC(RML) or ΔC(Mock) for 72 h. After 5 weeks the cells were harvested, PK-digested using 5 µg/ml PK to digest 8 µg protein and samples were analyzed by western blotting.

DISCUSSION

'Invisible inoculum'

In order to study prion replication in non-dividing cells I have generated a new method that allows us to identify newly generated PrP^{Sc} in a selective manner. I am not the first group to come up with a technical setup that allows the for study of *de novo* prion replication in a stringent fashion (Vorberg et al., 1999). But whereas the previously reported method relied upon using a normal prion inoculum to infect cells expressing a tagged-PrP molecule, our method is the diametrical opposite. I use a specially modified inoculum to infect normal cells. The advantage of our method is obvious. The method devised by Vorberg et al. requires that cells that are to be infected express a tagged PrP-molecule, that are tagged in such a fashion that the tag itself is converted into the PK-resistant part of the prion molecule. It has been shown numerous times that tagging of the prion protein, using either C- or N-terminal myc, GFP or tap-tags, leads to an inhibition of the prion conversion reaction (Bian et al., 2006). Furthermore, no mice expressing a tagged, convertible versions of the prion protein are available or has been reported in the literature. Our method can be used to study prion replication in any transgenic mouse or cell type that can be infected with ΔC(RML). In essence, as long as ΔC(RML) is compatible with the host-PrP molecule (e.g. murine PrP^{C}), this technique should be applicable. Other applications for such an assay could be imagined. This setup could be used to confirm the controversial observation by Vorberg et al. suggesting that newly generated PrP^{Sc} can be detected in cells within hours after a prion infection (Vorberg et al., 1999). In addition, I speculate that the technique can be used to set up a simplified SCEPA assay, that does not require the many cell passages normally needed for a specific detection of prions. This simplified assay could be used for drug or genetic screening of factors interfering with prion infection/replication (Klohn et al., 2003; Solassol et al., 2003; Bertsch et al., 2005).

Cells supporting prion replication in the CNS

An important parameter for understanding prion replication and pathogenesis in the CNS is to assign specific functions to the various CNS cell populations. For instance,

microglia have commonly be linked to pathology, by suggesting that microglia-mediated inflammation could play a causal role in neurotoxicity (Baker and Manuelidis, 2003). Another important parameter is to understand which cells contribute to prion propagation. Different approaches has been used to characterize which cells replicate prions *in vivo*. The main approach has been to generate transgenic mouse lines expressing PrP^{C} under cell specific promoters on a $Prnp^{o/o}$ background. Mice expressing the hamster prion protein under the neuron specific enolase promoter (NSE-PrP) were susceptible to hamster prions and came down with disease only with a slight delay, showing that neuronal PrP expression is sufficient to support prion replication and prion pathogenesis (Race et al., 1995). However, similar mice expressing the hamster PrP transgene under the astrocyte specific glial fibrillary acidic promoter (GFAP), also replicated prions and developed pathology (although with a delay) upon infection with hamster prions (Raeber et al., 1997). These studies was complemented by 2 excellent studies by the Collinge group, showing that conditional neuronal deletion of the prion protein post-infection can reverse early prion pathogenesis (spongiosis) and behavioral deficits (Mallucci et al., 2003; Mallucci et al., 2007). In these mice, PrP is deleted from neurons, but not glia cells using the Cre-LoxP system, at a time post-inoculation where the mice show PrP^{Sc} accumulation and spongiosis. Despite the fact that the mice eventually develop abundant PrP^{Sc} accumulation (PrP^{Sc} replicate by glia cells) and a strong gliosis, these mice fail to develop any prion-associated pathological changes (Mallucci et al., 2003). These results, together with the results from the NSE-PrP mice, suggests that although prion replication does take place on astrocytes, prion replication in neurons are both necessary and sufficient for the development of prion pathogenesis. In contrast to these studies, PrP expression under the oligodendrocyte/Schwann cell specific promoter, the myelin basic protein (MBP), does not support prion replication (Prinz et al., 2004).

Another approach to study cell-specific prion replication is to investigate cultures of homogeneous cell populations purified from mice. Previously, only 3 groups has reported successful infections of primary post-natal CNS-derived cells (Cronier et al., 2004; Giri et al., 2006; Milhavet et al., 2006). These groups reported that dividing neural stem cells and neurospheres can be prion infected (Giri et al., 2006; Milhavet et al., 2006). Furthermore, astrocytes and CGC neurons could be infected and prion

replication induced a small increase in granule cell apoptosis, suggesting that prion induced cell death is cell autonomous (Cronier et al., 2004). While immortalized microglia from PrP-overexpressing mice was capable of supporting prion replication, primary microglia, even from *tga20*$^{+/+}$ mice failed to replicate prions (Iwamaru et al., 2007). This is possibly due to their low expression of PrP^{C} (Baker et al., 2002). In a similar fashion, it was shown that cell lines derived from peripheral glia cells (Schwann cells) are also capable of replicating prions (Follet et al., 2002; Archer et al., 2004). Whether Schwann cells themselves replicate prions is a different matter entirely, and yet to be determined.

OUTLOOK

I am currently continuing to test which CNS and PNS-derived primary cells can be infected *in vitro*. Oligodendrocytes, Schwann cells and peripheral neurons are being tested to determine their prion replication competence. In addition, other people in the Aguzzi lab are testing other peripheral cell types involved in prion transport and neuroinvasion. I plan to use the invisible inoculum to determine if early prion replication within hours does take place *in vitro* and *in vivo* (Vorberg et al., 2004). Furthermore, I plan to test if the ΔC(RML) inoculum can be used for a simplified SCEPA assay (Klohn et al., 2003). Finally, I am trying to determine if the deletion of a part of the N-terminus of the prion protein confers new strain properties by comparing the original RML inoculum to RML passaged in ΔC mice using various biochemical and biophysical tools.

Materials and Methods

Mice

All mouse experiments were performed according to Swiss federal regulations. The pups used for most experiments were F1 offspring of *tga20*$^{+/+}$ *Prnp*$^{o/o}$ males on a 129SV/BL6 background crossed to heterozygous *CD11b-HSVTK* females (*tg620*) on a C57BL/6 background (Heppner et al., 2005). I refer to the *Prnp*$^{+/o}$ *tga20*$^{+}$ *HSVTK* transgene-negative offspring as *tga20*^{TK} and the transgene-positive littermates as *tga20*$^{TK+}$. *Prnp*$^{o/o}$, *Prnp*$^{+/o}$, *Prnp*$^{o/o}$ *tga20*$^{+}$ and *CD11b-HSVTK mice* backcrossed to *Prnp*$^{o/o}$ for 6-8 generations (*Prnp*$^{o/o/TK}$) were all on a 129SV/BL6 background. *CD11b-HSVTK* (*tg620*) and *GFAP-HSVTK* mice (line 7.1) were all on a C57BL/6 background and were genotyped as previously described (Bush et al., 1998; Heppner et al., 2005).

Prion strains

Rocky Mountain Laboratory strain passage-6 (RML6) was amplified in CD-1 mice, ME7 in 129/Sv mice, 5193/1 in tga20 mice and 22F, 79A, 87A, 87V, 139V, 301V, 5192/2 and 301C (murine-adapted BSE) were all amplified in C57BL/6 mice by intracerebral inoculation of 30 µl, 10 % brain homogenate. RML passaged once into ΔC (*C4/C4*) mice were obtained (a kind gift from Eckhard Flechsig) and further transmitted for a second passage into *C4/C4* mice. The primary ΔC(RML) passage was used for all experiments.

Organotypic cerebellar slice cultures

Organotypic cerebellar slice cultures were prepared according to a modified version of a protocol by Stoppini et al (Stoppini et al., 1991). In brief, the cerebellum was obtained from 9-12-day old pups. Brain tissue was embedded in 2 % (w/v) Ultra-low melting point agarose dissolved in Gey's balanced salt solution (GBSS) (NaCl 8 g/l, KCl 0.37 g/l, Na_2HPO_4 0.12 g/l, $CaCl_2 \cdot 2H_20$ 0.22 g/l, KH_2PO_4 0.09 g/l, $MgSO_4 \cdot 7H_20$ 0.07 g/l, $MgCl_2 \cdot 6H_20$ 0.210 g/l, $NaHCO_3$ 0.227 g/l) supplemented with

the glutamate receptor antagonist kynurenic acid (1 mM) (GBSS-K). Liquid agarose (kept at a constant temperature 37 °C using a water bath) was transferred to a small container, the isolated brain tissue was submerged and the tissue block was cooled on ice until the agarose solidified (10 min). The block was mounted (glued) onto a specimen disc and 350 μm thick slices were cut on a vibratome (VT1000, Leica-microsystems) while submerged in a cooled reservoir (4 °C) containing GBSS-K. Slices were transferred in a small volume of GBSS-K to Millicell-CM Biopore^{TM} PTFE membrane inserts (Millipore), using the blunt end of a sterile Pasteur pipette. Residual GBSS was removed and the inserts were transferred to a cell culture plate and cultured for up to 5 weeks in slice culture medium (50 % MEM, 25 % BME and 25 % horse serum supplemented with 0.65 % glucose, penicillin/streptomycin (1x) and Glutamax (1x) (Invitrogen). Cultures were kept in a standard cell incubator (37 °C, 5 % CO_2 and 95 % humidity) and 80 % of the culture medium was exchanged 3 times a week.

Prion Organotypic Slice Culture Assay (POSCA)

In order to prion infect the tissue cultures, slices were prepared and transferred to 24-well plates in a small volume of GBSS-K. Cultures were treated as free-floating sections with various concentrations of prion-infected or mock brain homogenates (homogenized in PBS) diluted in 1 ml GBSS-K for 1 h at 4 ºC. Slices were washed twice by transferring the slices in a small volume of GBSS-K (approximately 0.5 ml) to a reservoir containing 6 ml fresh GBSS-K buffer. Finally, 5-10 slices were transferred to a 6-well Millicell-CM Biopore^{TM} PTFE membrane insert (Millipore) (For staining experiments, 1-2 slices were placed on a 24-well insert) and all excess buffer was removed.

Macrophage reconstitution of microglia depleted slices

For reconstitution of microglia-depleted slices, intra-peritoneal macrophages were obtained. Mice were euthanized and the abdominal skin was removed without disturbing the peritoneal cavity. 5 ml ice-cold PBS was injected into the peritoneal cavity using a 25-gauge needle. After massaging the abdomen macrophages was

recovered and cells were counted using 0.4 % Trypan blue. Organotypic cerebellar slice cultures were reconstituted immediately after preparation, by adding 250.000 macrophages to each insert (10 slices/6-well insert) and GCV-treatment was initiated. GCV was added to a final concentration of 5 μg/ml, a concentration previously shown to be optimal for microglia depletion *in vitro* (Heppner et al., 2005).

Preparation of enriched mono-cultures

Mixed glial cultures were prepared from 1-2 day old mice according to a standard protocol (Giulian D, 1986). Cells were cultured in DMEM supplemented with 20 % heat inactivated FBS, antibiotics (100 U/ml penicillin and 100 μg/ml streptomycin) and 2 mM GlutaMax. After 1 week in culture, the serum concentration was lowered to 10 % and this medium was used for all subsequent experiments. After 14 days the confluent cultures were shaken vigorously to dislodge microglia and oligodendrocyte precursor cells from the astrocytic monolayer. For infection of microglia cells, floating cells were collected and seeded onto a feeder layer of GCV-treated *Prnp*$^{o/o/TK+}$ astrocytes in a 25-cm^2 flask. 40 minutes after seeding the cells, medium was exchanged to remove oligodendrocytic-precurser cells and cultures were infected with ΔC(RML). At the time of harvest, microglia were shaken off the astrocyte and collected by differential adhesion to a plastic dish. Microglia purity > 98 % was routinely obtained as measured by staining using Alexa fluor 594 conjugated Isolectin-B_4 from *griffonia simplicifolia* (Molecular Probes). The astrocytic monolayer was washed in Ca^{2+}/Mg^{2+} free Hanks buffered saline solution and split using Trypsin/EDTA. Cells were re-seeded in 12-well plates at a density of 50.000 cells/well, infected with ΔC(RML) and cultured in the presence of GCV.

Cerebellar granule neurons were cultured from 7-day old mice according to (Leist M, 1997). In brief, 7-day old mice were decapitated and the cerebellum was collected. The cerebellar meninges were removed and the tissue was digested with trypsin and Dnase-1. After trituration, cells were counted and seeded on Poly-L-lysine (100 μg/ml) coated 24-well plates at a density of 400.000 cells/well and after 45 min, medium was exchanged to decrease the number of glia in the culture. Cells were cultured for 1 day in BME supplemented with 10 % FCS, 1 mM Glutamax, 100 U/ml penicillin and 100 μg/ml streptomycin. After 24 h, the medium was exchanged to

serum-free medium, neurobasal medium, supplemented with 1 mM Glutamax, 100 U/ml penicillin, 100 µg/ml streptomycin and B27-supplement. Cultures were infected with ΔC(RML) immediately after seeding or after the first medium exchange. Ganciclovir (5 µg/ml) was added at the time of culturing and after 7 days *in vitro*.

Western blot analyses

Cultures were washed twice in PBS, residual PBS was removed and the tissue was scraped off the membrane using 10 µl lysis buffer per slice (0.5 % sodium deoxycholate and 0.5 % Nonidet P-40) or PBS. Tissue was lysed by 3 freeze-thaw cycles and triturated using a 200 µl pipette until homogeneous. For samples that were transferred to the SCEPA, samples were harvested in PBS, triturated using a 29-G needle, followed by 30 sec sonication. Each sample consisted of a pool of 5-10 slices grown on the same insert, yielding approximately 2-350 µg protein in total. Protein concentration was determined using the bicinchoninic acid assay (Pierce) and the tissue was digested with PK (Roche) in lysis buffer for 30 minutes at 37 °C. PK-resistant material was detected as a standard by digesting 20 µg protein lysate with 25 µg/ml PK. This condition was more sensitive as compared to using higher PK concentrations, but still allowed for specific detection of PrP^{Sc}. For analysis of prion-infected mono-cultures, the lysis buffer were supplemented with 1 mM ethylenediamine tetraacetic acid (EDTA) and 100 mM 4-(2-hydroxyethyl)-1-piperazineethanesulfonic acid (HEPES, pH 7.0). 8-10 µg protein was digested with 5 µg/ml PK. PK digestion was stopped by adding loading buffer (NuPAGE, Invitrogen) and boiling the samples at 95 °C for 5 minutes. Proteins were separated on a 12 % Bis-Tris polyacrylamide gel (NuPAGE, Invitrogen) and blotted onto a nitrocellulose membrane. Membranes were blocked with 5 % Topblock (Fluka) in PBS and incubated with primary antibodies in 1 % Topblock. Primary antibodies used were mouse α-PrP^{C} IgG_1 (POM-1), mouse α-PrP^{C} IgG_1 (POM-12), 200 ng/ml, ascites fluid of mouse α-Glial Fibrillary Acidic Protein (GFAP) IgG_1 (Clone GA5) 1:3000 (Sigma-Aldrich) and goat α-human Iba1, 0.5 µg/ml (Wako). Secondary antibodies used were horse radish peroxidase-conjugated (HRP) rabbit α-mouse IgG_1, 1:10,000 (Zymed), HRP-conjugated rabbit α-goat IgG_1, 1:10,000 (Zymed) and HRP-conjugated swine α-rabbit IgG, 260 ng/ml (DAKO). The blots were developed using

SuperSignal® West Pico Chemiluminescent substrate (Pierce) and detected using the VersaDoc system (model 3000, Biorad). The molecular weight marker was spiked with recombinant PrP^C yielding a PrP-signal at 23 kDa, with a degradation product at 15 kDa. 10 µl marker were loaded in the left lane on all blots.

Cell death measurements

Propidium Iodide (PI) incorporation was measured by incubating the slices with PI (10 µg/ml, Molecular Probes) for 15 minutes. Images were acquired using a fluorescent microscope (Axiovert 200M equipped with Axiocam HRm, Zeiss) and images were analyzed using image analysis software analySIS© vs5.0 (Olympus Soft Imaging Solutions GmbH, Münster, Germany). All images were acquired using the same exposure times and analyzed using the same software settings within a region of interest (the total area of tissue present in the image). After recording fluorescent images, the tissue was washed in PBS and lysed in PBS, 0.5 % Nonidet-P40, 0.5 % DOC and 5 mM 1,4-dithiothreitol. Caspase-3 Fluorometric Correlate-Assay (Assay designs) was used to determine caspase-3 DEVDase activity according to the manufacturers instruction. In brief, protein lysates were incubated with the fluorogenic caspase-3 substrate, Ac-DEVD-7-Amino-4-methyl coumarin, and enzymatic cleavage by caspase-3 was quantitated by kinetic measurements (1 measurement every 2 minutes for 2 hours) using a fluorometer. The specific caspase activity was calculated from a standard curve generated using recombinant caspase-3 with a known enzymatic activity and normalized to the protein content. One unit of caspase-3 activity is defined as the amount of enzyme needed to convert 1 picomol of substrate per minute at 30 ºC.

Enzyme-linked immunosorbent assay (ELISA) and nitrite measurement

Organotypic hippocampal slice cultures (OHSCs) were prepared from 12 day old mice, and treated with 5 µg/ml GCV for the duration of the experiment. After 7 days, activation of microglia was initiated by adding recombinant murine IFN-γ (10 ng/ml, R&D systems) and LPS from *Salmonella abortus equi* (1 µg/ml, Bioclot). To assess nitric oxide, cytokines and chemokines, cell culture supernatant was harvested 48 h after LPS/IFN-γ stimulation except for TNF measurements, where supernatant was

taken after 8 h. Each group contained of 3–4 inserts with 4 OHSCs on each insert. Supernatants derived from OHSCs were analyzed by the use of ELISA kits for TNF-α, IFN-γ (Pharmingen) or MIP-1β (R&D systems) according to the manufacturer's instructions. Nitrite was measured with the Griess reagent. 50 µl supernatant or $NaNO_2$ standards were mixed with 25 µl N-(1-naphthyl)ethylenediamine (0.1 % in H_2O) and 25 µl sulfanilamide (1 % in 1.2 N HCl) in a 96 well plate and the optical density was assessed after 3 min at 570–690 nm. To include the contribution of the NO metabolite nitrate, 50 µl vanadium(III) chloride (8 mg/ml in 1 M HCl) was added to the Griess reagent and incubated at 37°C for 30 min (Miranda et al., 2001).

Immunohistochemistry

Histoblot analysis was performed according to a standard protocol using 50 µg/ml PK (30 min, 37 °C) (Taraboulos et al., 1992). For immunohistochemistry the tissue was fixed in 2 % PFA, o/n at 4 °C. Membrane inserts were washed and incubated for 1 h in blocking buffer (0.1 % Triton X-100 and 2 % goat serum dissolved in PBS) and incubated for 2-5 days with primary antibody diluted in blocking buffer. Primary antibodies and concentrations used were ascites fluid of mouse α-chicken calbindin IgG_1 1:2000 (Swant), rabbit α-mouse neurofilament-M polyclonal antibody 1:400 (Chemicon), rabbit α-mouse GFAP polyclonal antibody 1:1000 (DAKO), mouse α-frog parvalbumin IgG_1 antibody 1:500 (Sigma-Aldrich), mouse α-human β_{III}-tubulin IgG_1 1:1000 (Chemicon), rat α-mouse CD68 $IgG_{2a,}$ 1 µg/ml (Serotec) or ascietes fluid of rat α-bovine MBP IgG_{2a} 1:250 (Serotec). The primary antibodies were detected using Alexa-conjugated secondary antibodies (4 µg/ml) (Molecular Probes) and counterstained with dapi (1 µg/ml). Microglia were detected in fixed and in live tissue by staining with IB_4 (*Griffonia Simplicifolia*) (2-4 µg/ml) (Molecular Probes). The culture membranes were removed from the inserts and mounted directly onto a microscope slide using fluorescent mounting medium (DAKO). Images were acquired in a focal plane 35-40 µm below the tissue surface using a laser-scanning confocal microscope (SP 2, Leica), by fluorescent microscopy (Axiovert 200M, Zeiss) or for live imaging studies by using wide-field microscope (DM IRBE, Leica) equipped with a temperature controller and a CO_2 box (37 °C and 5 % CO_2). Incorporation of 5-bromodeoxyuridine (BrdU) into the tissue was assessed after a 24 h incubation with

25 μg/ml BrdU. DNA was denatured by treatment with 1 N HCl for 1 h at 37 °C, followed by 2 x 30 min neutralization steps with 0.1 M Borate (pH 8.5) and 2 washes in PBS. The tissue was subsequently stained with 15 μg/ml mouse α-bromodeoxyuridine IgG_1 (clone BU-33, Sigma) and rat anti-mouse CD68 according to normal procedures. Monocultures were stained according to a similar protocol, but with only 15 min fixation, 5 min permeabilisation, o/n incubation with primary antibody, and 1 h incubation with secondary antibody. All counting was performed manually, assisted by image analysis software analySIS© vs5.0.

Quantitative PCR

Organotypic slice cultures were prepared and incubated as previously stated. Cultures were washed once with PBS and total RNA was extracted using TRIzol reagent (Invitrogen Life Technologies) according to the manufacturer's protocol. Before cDNA synthesis residual genomic DNA was removed using the DNA-free kit (Ambion) and cDNA was synthesized from 1 μg total RNA with QuantiTect reverse transcription kit (Qiaqen) using random hexamers according to the manufacturer's protocol. Successful cDNA synthesis and contamination of total RNA with genomic DNA was tested by PCR with primers specific for *Actb*. Quantitative real-time PCR was performed using the SYBR Green PCR Master Mix (Applied Biosystems) on an ABI PRISM 7700 Sequence Detector (PerkinElmer). Fold regulation was calculated relative to untreated transgene-negative slices (*wt*) after normalization to the β-actin signal. The following primer pairs were used: *Actb* sense (NM_007393): 5'-GAC GGC CAG GTC ATC ACT AT-3', antisense: 5'-ACA TCT GCT GGA AGG TGG AC-3'. *Itgam* sense (NM_008401): 5'-GAC TCA GTG AGC CCC ATC AT-3', antisense 5'-AGATCG TCT TGG CAG ATG CT-3'. *MBP* (NM_010777) and *Nefh* (NM_010904) were detected using the commercially available QuantiTect primer assay (Qiagen).

Scrapie cell assay in endpoint format (SCEPA)

Prion-susceptible neuroblastoma cells (subclone N2a-PK1) were exposed to brain homogenates in 96-well plates for 3 days. Cells were subsequently split 3 times 1:3

every 2 days, and 3 times 1:10 every 3 days. After confluence was reached, 25.000 cells from each well were filtered onto the membrane of an ELISPOT plate, treated with PK, denatured and individual infected (PrP^{Sc}-positive) cells were detected by immunocytochemistry using alkaline phosphatase-conjugated POM-1 mouse anti-PrP antibody and alkaline phosphatase conjugate substrate kit (Biorad). Serial ten-fold dilutions were performed in cell culture medium containing healthy mouse brain homogenate. Scrapie-susceptible N2a-PK1 cells were then exposed to dilutions of experimental samples ranging from 10^{-3} to 10^{-6}, or a 10^{-3} dilution of healthy mouse brain homogenate ("mock") or RML6. Samples were quantified by total luminescence per well or in end-point format by counting positive wells according to established methods (Klohn et al., 2003).

Statistical analysis

One-way ANOVA with Bonferroni post test for selected pairs of columns was used for statistical analysis of experiments involving the comparison of 3 or more samples. Paired student T-test was used for comparing 2 samples. Results are displayed as the average of replicas ± standard deviation.

Supplementary Figure 1: Video microscopy of microglia depletion. Slices prepared from *CD11b-HSVTK*$^{+}$ mice were treated with GCV for 8 days and IB_4 was added to the cell culture medium. Images were recorded on a wide-field fluorescent microscope every 30 minutes for 5 days and the video is shown at a rate of 10 frames/s.

References

Aguzzi A (2006). Prion diseases of humans and farm animals: epidemiology, genetics, and pathogenesis. J Neurochem 97:1726-1739.

Aguzzi A, Weissmann C (1997). Prion research: the next frontiers. Nature 389:795-798.

Aguzzi A, Haass C (2003). Games played by rogue proteins in prion disorders and Alzheimer's disease. Science 302:814-818.

Aguzzi A, Polymenidou M (2004). Mammalian prion biology. One century of evolving concepts. Cell 116:313-327.

Aguzzi A, Heikenwalder M, Polymenidou M (2007). Insights into prion strains and neurotoxicity. Nat Rev Mol Cell Biol 8:552-561.

Almond JW, Brown P, Gore SM, Hofman A, Wientjens PW, Ridley RM, Baker HF, Roberts GW, Tyler KL (1995). Creutzfeldt-Jakob disease and bovine spongiform encephalopathy: any connection? BMJ 311:1415-1421.

Andreoletti O, Berthon P, Levavasseur E, Marc D, Lantier F, Monks E, Elsen JM, Schelcher F (2002). Phenotyping of protein-prion (PrPsc)-accumulating cells in lymphoid and neural tissues of naturally scrapie-affected sheep by double-labeling immunohistochemistry. J Histochem Cytochem 50:1357-1370.

Archer F, Bachelin C, Andreoletti O, Besnard N, Perrot G, Langevin C, Le Dur A, Vilette D, Baron-Van Evercooren A, Vilotte JL, Laude H (2004). Cultured peripheral neuroglial cells are highly permissive to sheep prion infection. J Virol 78:482-490.

Baker CA, Manuelidis L (2003). Unique inflammatory RNA profiles of microglia in Creutzfeldt-Jakob disease. Proc Natl Acad Sci U S A 100:675-679.

Baker CA, Martin D, Manuelidis L (2002). Microglia from Creutzfeldt-Jakob disease-infected brains are infectious and show specific mRNA activation profiles. J Virol 76:10905-10913.

Baker CA, Lu ZY, Manuelidis L (2004). Early induction of interferon-responsive mRNAs in Creutzfeldt-Jakob disease. J Neurovirol 10:29-40.

Barmada SJ, Harris DA (2005). Visualization of prion infection in transgenic mice expressing green fluorescent protein-tagged prion protein. J Neurosci 25:5824-5832.

Baumann F, Tolnay M, Brabeck C, Pahnke J, Kloz U, Niemann HH, Heikenwalder M, Rulicke T, Burkle A, Aguzzi A (2007). Lethal recessive myelin toxicity of prion protein lacking its central domain. EMBO J 26:538-547.

Bendheim PE, Barry RA, DeArmond SJ, Stites DP, Prusiner SB (1984). Antibodies to a scrapie prion protein. Nature 310:418-421.

Beringue V, Demoy M, Lasmezas CI, Gouritin B, Weingarten C, Deslys JP, Andreux JP, Couvreur P, Dormont D (2000). Role of spleen macrophages in the clearance of scrapie agent early in pathogenesis. J Pathol 190:495-502.

Bertsch U, Winklhofer KF, Hirschberger T, Bieschke J, Weber P, Hartl FU, Tavan P, Tatzelt J, Kretzschmar HA, Giese A (2005). Systematic identification of antiprion drugs by high-throughput screening based on scanning for intensely fluorescent targets. J Virol 79:7785-7791.

Bian J, Nazor KE, Angers R, Jernigan M, Seward T, Centers A, Green M, Telling GC (2006). GFP-tagged PrP supports compromised prion replication in transgenic mice. Biochem Biophys Res Commun 340:894-900.

Boche D, Cunningham C, Docagne F, Scott H, Perry VH (2006). TGFbeta1 regulates the inflammatory response during chronic neurodegeneration. Neurobiol Dis 22:638-650.

Bolton DC, McKinley MP, Prusiner SB (1982). Identification of a protein that purifies with the scrapie prion. Science 218:1309-1311.

Bolton DC, Meyer RK, Prusiner SB (1985). Scrapie PrP 27-30 is a sialoglycoprotein. J Virol 53:596-606.

Borchelt DR, Scott M, Taraboulos A, Stahl N, Prusiner SB (1990). Scrapie and cellular prion proteins differ in their kinetics of synthesis and topology in cultured cells. J Cell Biol 110:743-752.

Brandner S, Raeber A, Sailer A, Blattler T, Fischer M, Weissmann C, Aguzzi A (1996). Normal host prion protein (PrPC) is required for scrapie spread within the central nervous system. Proc Natl Acad Sci U S A 93:13148-13151.

Brown DR, Schmidt B, Kretzschmar HA (1996). Role of microglia and host protein in neurotoxicity of a prion protein fragment. Nature 380:345-347.

Büeler HR, Aguzzi A, Sailer A, Greiner RA, Autenried P, Aguet M, Weissmann C (1993). Mice devoid of PrP are resistant to scrapie. Cell 73:1339-1347.

Büeler HR, Fischer M, Lang Y, Bluethmann H, Lipp HP, DeArmond SJ, Prusiner SB, Aguet M, Weissmann C (1992). Normal development and behaviour of mice lacking the neuronal cell-surface PrP protein. Nature 356:577-582.

Bush TG, Savidge TC, Freeman TC, Cox HJ, Campbell EA, Mucke L, Johnson MH, Sofroniew MV (1998). Fulminant jejuno-ileitis following ablation of enteric glia in adult transgenic mice. Cell 93:189-201.

Cancellotti E, Wiseman F, Tuzi NL, Baybutt H, Monaghan P, Aitchison L, Simpson J, Manson JC (2005). Altered glycosylated PrP proteins can have different neuronal trafficking in brain but do not acquire scrapie-like properties. J Biol Chem 280:42909-42918.

Capobianco R, Casalone C, Suardi S, Mangieri M, Miccolo C, Limido L, Catania M, Rossi G, Di Fede G, Giaccone G, Bruzzone MG, Minati L, Corona C, Acutis P, Gelmetti D, Lombardi G, Groschup MH, Buschmann A, Zanusso G, Monaco S, Caramelli M, Tagliavini F. (2007). Conversion of the BASE prion strain into the BSE strain: the origin of BSE? PLoS Pathog 3:e31.

Carlson GA, Ebeling C, Yang SL, Telling G, Torchia M, Groth D, Westaway D, DeArmond SJ, Prusiner SB (1994). Prion isolate specified allotypic interactions between the cellular and scrapie prion proteins in congenic and transgenic mice. Proc Natl Acad Sci U S A 91:5690-5694.

Carp RI, Callahan SM (1982). Effect of mouse peritoneal macrophages on scrapie infectivity during extended in vitro incubation. Intervirology 17:201-207.

Casalone C, Zanusso G, Acutis P, Ferrari S, Capucci L, Tagliavini F, Monaco S, Caramelli M (2004). Identification of a second bovine amyloidotic spongiform encephalopathy: molecular similarities with sporadic Creutzfeldt-Jakob disease. Proc Natl Acad Sci U S A 101:3065-3070.

Caughey B, Race RE, Ernst D, Buchmeier MJ, Chesebro B (1989). Prion protein biosynthesis in scrapie-infected and uninfected neuroblastoma cells. J Virol 63:175-181.

Chesebro B, Trifilo M, Race R, Meade-White K, Teng C, LaCasse R, Raymond L, Favara C, Baron G, Priola S, Caughey B, Masliah E, Oldstone M (2005). Anchorless prion protein results in infectious amyloid disease without clinical scrapie. Science 308:1435-1439.

Collinge J (2005). Molecular neurology of prion disease. J Neurol Neurosurg Psychiatry 76:906-919.

Collinge J, Sidle KC, Meads J, Ironside J, Hill AF (1996). Molecular analysis of prion strain variation and the aetiology of 'new variant' CJD. Nature 383:685-690.

Collinge J, Whittington MA, Sidle KC, Smith CJ, Palmer MS, Clarke AR, Jefferys JG (1994). Prion protein is necessary for normal synaptic function. Nature 370:295-297.

Collinge J, Whitfield J, McKintosh E, Beck J, Mead S, Thomas DJ, Alpers MP (2006). Kuru in the 21st century--an acquired human prion disease with very long incubation periods. Lancet 367:2068-2074.

Cronier S, Beringue V, Bellon A, Peyrin JM, Laude H (2007). Prion strain- and species-dependent effects of anti-prion molecules in primary neuronal cultures. J Virol. In Press.

Cronier S, Laude H, Peyrin JM (2004). Prions can infect primary cultured neurons and astrocytes and promote neuronal cell death. Proc Natl Acad Sci USA 101:12271-12276.

Cuille J, Chelle PL (1939). Experimental transmission of trembling to the goat. C R Seances Acad Sci 208:1058-1160.

Dandoy-Dron F, Guillo F, Benboudjema L, Deslys JP, Lasmezas C, Dormont D, Tovey MG, Dron M (1998). Gene expression in scrapie. Cloning of a new scrapie-responsive gene and the identification of increased levels of seven other mRNA transcripts. J Biol Chem 273:7691-7697.

DeArmond SJ (1993). Alzheimer's disease and Creutzfeldt-Jakob disease: overlap of pathogenic mechanisms. Curr Opin Neurol 6:872-881.

DeArmond SJ, McKinley MP, Barry RA, Braunfeld MB, McColloch JR, Prusiner SB (1985). Identification of prion amyloid filaments in scrapie-infected brain. Cell 41:221-235.

DeArmond SJ, Yang SL, Lee A, Bowler R, Taraboulos A, Groth D, Prusiner SB (1993). Three scrapie prion isolates exhibit different accumulation patterns of the prion protein scrapie isoform. Proc Natl Acad Sci U S A 90:6449-6453.

Deleault NR, Harris BT, Rees JR, Supattapone S (2007). Formation of native prions from minimal components in vitro. Proc Natl Acad Sci U S A 104:9741-9746.

Dodelet VC, Cashman NR (1998). Prion protein expression in human leukocyte differentiation. Blood 91:1556-1561.

Falsig J, Julius C, Margalith I, Schwarz P, Heppner FL, and Aguzzi A. 2008. A versatile prion replication assay in organotypic brain slices. *Nat. Neurosci*. 11(1):109-117

Fischer M, Rülicke T, Raeber A, Sailer A, Moser M, Oesch B, Brandner S, Aguzzi A, Weissmann C (1996). Prion protein (PrP) with amino-proximal deletions restoring susceptibility of PrP knockout mice to scrapie. EMBO J 15:1255-1264.

Flechsig E, Shmerling D, Hegyi I, Raeber AJ, Fischer M, Cozzio A, von Mering C, Aguzzi A, Weissmann C (2000). Prion protein devoid of the octapeptide repeat region restores susceptibility to scrapie in PrP knockout mice. Neuron 27:399-408.

Floden AM, Combs CK (2006). Beta-amyloid stimulates murine postnatal and adult microglia cultures in a unique manner. J Neurosci 26:4644-4648.

Follet J, Lemaire-Vieille C, Blanquet-Grossard F, Podevin-Dimster V, Lehmann S, Chauvin JP, Decavel JP, Varea R, Grassi J, Fontes M, Cesbron JY (2002). PrP expression and replication by Schwann cells: implications in prion spreading. J Virol 76:2434-2439.

Ford MJ, Burton LJ, Morris RJ, Hall SM (2002). Selective expression of prion protein in peripheral tissues of the adult mouse. Neuroscience 113:177-192.

Gajdusek DC (1977). Unconventional viruses and the origin and disappearance of kuru. Science 197:943-960.

Gajdusek DC, Gibbs CJ, Alpers M (1966). Experimental transmission of a Kuru-like syndrome to chimpanzees. Nature 209:794-796.

Gajdusek DC, Gibbs CJ, Jr., Rogers NG, Basnight M, Hooks J (1972). Persistence of viruses of kuru and Creutzfeldt-Jakob disease in tissue cultures of brain cells. Nature 235:104-105.

Gibbs CJ, Jr., Gajdusek DC, Asher DM, Alpers MP, Beck E, Daniel PM, Matthews WB (1968). Creutzfeldt-Jakob disease (spongiform encephalopathy): transmission to the chimpanzee. Science 161:388-389.

Giri RK, Young R, Pitstick R, DeArmond SJ, Prusiner SB, Carlson GA. (2006). Prion infection of mouse neurospheres. Proc Natl Acad Sci USA 103:3875-3880.

Giulian D, Baker T (1986). Characterization of ameboid microglia isolated from developing mammalian brain. J Neurosci 6:2163-2178.

Griffith JS (1967). Self-replication and scrapie. Nature 215:1043-1044.

Harris DA, Lele P, Snider WD (1993). Localization of the mRNA for a chicken prion protein by in situ hybridization. Proc Natl Acad Sci U S A 90:4309-4313.

Heikenwalder M, Zeller N, Seeger H, Prinz M, Klohn PC, Schwarz P, Ruddle NH, Weissmann C, Aguzzi A (2005). Chronic lymphocytic inflammation specifies the organ tropism of prions. Science 307:1107-1110.

Heneka MT, O'Banion MK (2007). Inflammatory processes in Alzheimer's disease. J Neuroimmunol 184:69-91.

Heppner FL, Greter M, Marino D, Falsig J, Raivich G, Hovelmeyer N, Waisman A, Rulicke T, Prinz M, Priller J, Becher B, Aguzzi A (2005). Experimental autoimmune encephalomyelitis repressed by microglial paralysis. Nat Med 11:146-152.

Herms JW, Kretzchmar HA, Titz S, Keller BU (1995). Patch-clamp analysis of synaptic transmission to cerebellar purkinje cells of prion protein knockout mice. Eur J Neurosci 7:2508-2512.

Hope J, Ritchie L, Farquhar C, Somerville R, Hunter N (1989). Bovine spongiform encephalopathy: a scrapie-like disease of British cattle. Prog Clin Biol Res 317:659-667.

Hosszu LL, Baxter NJ, Jackson GS, Power A, Clarke AR, Waltho JP, Craven CJ, Collinge J (1999). Structural mobility of the human prion protein probed by backbone hydrogen exchange. Nat Struct Biol 6:740-743.

Iwamaru Y, Takenouchi T, Ogihara K, Hoshino M, Takata M, Imamura M, Tagawa Y, Hayashi-Kato H, Ushiki-Kaku Y, Shimizu Y, Okada H, Shinagawa M, Kitani H, Yokoyama T (2007). Microglial cell line established from prion protein-overexpressing mice is susceptible to various murine prion strains. J Virol 81:1524-1527.

James TL, Liu H, Ulyanov NB, Farr-Jones S, Zhang H, Donne DG, Kaneko K, Groth D, Mehlhorn I, Prusiner SB, Cohen FE (1997). Solution structure of a 142-residue recombinant prion protein corresponding to the infectious fragment of the scrapie isoform. Proc Natl Acad Sci U S A 94:10086-10091.

Jarrett JT, Lansbury PT, Jr. (1993). Seeding "one-dimensional crystallization" of amyloid: a pathogenic mechanism in Alzheimer's disease and scrapie? Cell 73:1055-1058.

Kaerber G (1931). Beitrag zur kollektiven Behandlung pharmakologischer Reihenversuche. Arch Exp Pathol Pharmakol 162:480–483.

Kercher L, Favara C, Striebel JF, Lacasse R, Chesebro B (2007). Prion protein (PrP) expression differences in microglia and astroglia influence scrapie-induced neurodegeneration in retina and brain of transgenic mice. J Virol 81:10340-10351.

Khoury JE, Toft M, Hickman SE, Means TK, Terada K, Geula C, Luster AD (2007). Ccr2 deficiency impairs microglial accumulation and accelerates progression of Alzheimer-like disease. Nat Med 13:432-438.

Klohn PC, Stoltze L, Flechsig E, Enari M, Weissmann C (2003). A quantitative, highly sensitive cell-based infectivity assay for mouse scrapie prions. Proc Natl Acad Sci U S A 100:11666-11671.

Leist M, Volbracht C, Kühnle S, Fava E, Ferrando-May E, Nicotera P (1997). Caspase-mediated apoptosis in neuronal excitotoxicity triggered by nitric oxide. Mol Med 3:750-764.

Li A, Christensen HM, Stewart LR, Roth KA, Chiesa R, Harris DA (2007). Neonatal lethality in transgenic mice expressing prion protein with a deletion of residues 105-125. EMBO J 26:548-558.

Ligios C, Sigurdson CJ, Santucciu C, Carcassola G, Manco G, Basagni M, Maestrale C, Cancedda MG, Madau L, Aguzzi A (2005). PrPSc in mammary glands of sheep affected by scrapie and mastitis. Nat Med 11:1137-1138.

Lledo PM, Tremblay P, Dearmond SJ, Prusiner SB, Nicoll RA (1996). Mice Deficient For Prion Protein Exhibit Normal Neuronal Excitability and Synaptic Transmission in the Hippocampus. Proc Natl Acad Sci U S A 93:2403-2407.

Llewelyn CA, Hewitt PE, Knight RS, Amar K, Cousens S, Mackenzie J, Will RG (2004). Possible transmission of variant Creutzfeldt-Jakob disease by blood transfusion. Lancet 363:417-421.

Lu X, Wintrode P, Surewicz WK (2007). Beta-sheet core of human prion protein amyloid fibrils as determined by hydrogen/deuterium exchange. Proc Natl Acad Sci U S A 104:1510-1515.

Ma L, Morton AJ, Nicholson LF (2003). Microglia density decreases with age in a mouse model of Huntington's disease. Glia 43:274-280.

Mallucci G, Dickinson A, Linehan J, Klohn PC, Brandner S, Collinge J (2003). Depleting neuronal PrP in prion infection prevents disease and reverses spongiosis. Science 302:871-874.

Mallucci GR, Ratte S, Asante EA, Linehan J, Gowland I, Jefferys JG, Collinge J (2002). Post-natal knockout of prion protein alters hippocampal CA1 properties, but does not result in neurodegeneration. EMBO J 21:202-210.

Mallucci GR, White MD, Farmer M, Dickinson A, Khatun H, Powell AD, Brandner S, Jefferys JG, Collinge J (2007). Targeting cellular prion protein reverses early cognitive deficits and neurophysiological dysfunction in prion-infected mice. Neuron 53:325-335.

Manuelidis L, Fritch W (1996). Infectivity and host responses in Creutzfeldt-Jakob disease. Virology 216:46-59.

Manuelidis L, Sklaviadis T, Manuelidis EE (1987). Evidence suggesting that PrP is not the infectious agent in Creutzfeldt-Jakob disease. EMBO J 6:341-347.

Manuelidis L, Fritch W, Xi YG (1997). Evolution of a strain of CJD that induces BSE-like plaques. Science 277:94-98.

Markovic DS, Glass R, Synowitz M, Rooijen N, Kettenmann H (2005). Microglia stimulate the invasiveness of glioma cells by increasing the activity of metalloprotease-2. J Neuropathol Exp Neurol 64:754-762.

Marsh RF, Hadlow WJ (1992). Transmissible mink encephalopathy. Rev Sci Tech 11:539-550.

Mathiason CK, Powers JG, Dahmes SJ, Osborn DA, Miller KV, Warren RJ, Mason GL, Hays SA, Hayes-Klug J, Seelig DM, Wild MA, Wolfe LL, Spraker TR, Miller MW, Sigurdson CJ, Telling GC, Hoover EA (2006). Infectious prions in the saliva and blood of deer with chronic wasting disease. Science 314:133-136.

McGeer PL, Rogers J, McGeer EG (2006). Inflammation, anti-inflammatory agents and Alzheimer disease: the last 12 years. J Alzheimers Dis 9:271-276.

McKinley MP, Bolton DC, Prusiner SB (1983). A protease-resistant protein is a structural component of the scrapie prion. Cell 35:57-62.

Mead S, Stumpf MP, Whitfield J, Beck JA, Poulter M, Campbell T, Uphill JB, Goldstein D, Alpers M, Fisher EM, Collinge J (2003). Balancing selection at the prion protein gene consistent with prehistoric kurulike epidemics. Science 300:640-643.

Medori R, Tritschler HJ, LeBlanc A, Villare F, Manetto V, Chen HY, Xue R, Leal S, Montagna P, Cortelli P, et al (1992). Fatal familial insomnia, a prion disease with a mutation at codon 178 of the prion protein gene. New England Journal of Medicine 326:444-449.

Meyer RK, McKinley MP, Bowman KA, Braunfeld MB, Barry RA, Prusiner SB (1986). Separation and properties of cellular and scrapie prion proteins. Proc Natl Acad Sci U S A 83:2310-2314.

Michel B, Tamalet J, Bongrand P, Gambarelli D, Gastaut JL (1987). Role of phagocytes in experimental scrapie in hamsters. Rev Neurol Paris 143:526-531.

Milhavet O, Casanova D, Chevallier N, McKay RD, Lehmann S (2006). Neural stem cell model for prion propagation. Stem Cells 24(10):2284-91 (2006).

Miranda KM, Espey MG, Wink DA (2001). A rapid, simple spectrophotometric method for simultaneous detection of nitrate and nitrite. Nitric Oxide 5:62-71.

Moser M, Colello RJ, Pott U, Oesch B (1995). Developmental expression of the prion protein gene in glial cells. Neuron 14:509-517.

Nimmerjahn A, Kirchhoff F, Helmchen F (2005). Resting microglial cells are highly dynamic surveillants of brain parenchyma in vivo. Science 308:1314-1318.

Nishida N, Tremblay P, Sugimoto T, Shigematsu K, Shirabe S, Petromilli C, Erpel SP, Nakaoke R, Atarashi R, Houtani T, Torchia M, Sakaguchi S, DeArmond SJ, Prusiner SB, Katamine S (1999). A mouse prion protein transgene rescues mice deficient for the prion protein gene from purkinje cell degeneration and demyelination. Lab Invest 79:689-697.

Nonno R, Bari MA, Cardone F, Vaccari G, Fazzi P, Dell'omo G, Cartoni C, Ingrosso L, Boyle A, Galeno R, Sbriccoli M, Lipp HP, Bruce M, Pocchiari M, Agrimi U (2006). Efficient transmission and characterization of creutzfeldt-jakob disease strains in bank voles. PLoS Pathog 2:e12.

Oesch B, Westaway D, Walchli M, McKinley MP, Kent SB, Aebersold R, Barry RA, Tempst P, Teplow DB, Hood LE, Weissmann C (1985). A cellular gene encodes scrapie PrP 27-30 protein. Cell 40:735-746.

Polymenidou M, Stoeck K, Glatzel M, Vey M, Bellon A, Aguzzi A (2005). Coexistence of multiple PrPSc types in individuals with Creutzfeldt-Jakob disease. Lancet Neurol 4:805-814.

Priller J, Prinz M, Heikenwalder M, Zeller N, Schwarz P, Aguzzi A (2006). Early and rapid engraftment of bone marrow-derived microglia in scrapie. Journal of Neuroscience 26(45):11753-62.

Prinz M, Montrasio F, Furukawa H, van der Haar ME, Schwarz P, Rülicke T, Giger O, Häusler KG, Glatzel M, Aguzzi A (2004). Intrinsic resistance of oligodendrocytes to prion infection. J Neurosci 24:5974-5981.

Priola SA, Chesebro B, Caughey B (2003) Biomedicine. A view from the top--prion diseases from 10,000 feet. Science 300:917-919.

Prusiner SB (1982). Novel proteinaceous infectious particles cause scrapie. Science 216:136-144.

Prusiner SB (1991). Molecular biology of prion diseases. Science 252:1515-1522.

Prusiner SB, Scott MR, DeArmond SJ, Cohen FE (1998). Prion protein biology. Cell 93:337-348.

Prusiner SB, Cochran SP, Groth DF, Downey DE, Bowman KA, Martinez HM (1982). Measurement of the scrapie agent using an incubation time interval assay. Ann Neurol 11:353-358.

Race RE, Priola SA, Bessen RA, Ernst D, Dockter J, Rall GF, Mucke L, Chesebro B, Oldstone MB (1995). Neuron-specific expression of a hamster prion protein minigene in transgenic mice induces susceptibility to hamster scrapie agent. Neuron 15:1183-1191.

Radovanovic I, Braun N, Giger OT, Mertz K, Miele G, Prinz M, Navarro B, Aguzzi A (2005). Truncated Prion Protein and Doppel Are Myelinotoxic in the Absence of Oligodendrocytic PrPC. J Neurosci 25:4879-4888.

Raeber AJ, Race RE, Brandner S, Priola SA, Sailer A, Bessen RA, Mucke L, Manson J, Aguzzi A, Oldstone MB, Weissmann C, Chesebro B (1997). Astrocyte-specific expression of hamster prion protein (PrP) renders PrP knockout mice susceptible to hamster scrapie. EMBO J 16:6057-6065.

Riek R, Hornemann S, Wider G, Billeter M, Glockshuber R, Wuthrich K (1996). NMR Structure of the Mouse Prion Protein Domain Prp(121-231). Nature 382:180-182.

Rivera-Milla E, Stuermer CA, Malaga-Trillo E (2003). An evolutionary basis for scrapie disease: identification of a fish prion mRNA. Trends Genet 19:72-75.

Rubsam LZ, Boucher PD, Shewach DS (1998). Superior cytotoxicity with ganciclovir compared with acyclovir and 1-beta-D-arabinofuranosylthymine in herpes simplex virus-thymidine kinase-expressing cells: a novel paradigm for cell killing. Cancer Res 58:3873-3882.

Safar J, Wille H, Itri V, Groth D, Serban H, Torchia M, Cohen FE, Prusiner SB (1998). Eight prion strains have PrP^{Sc} molecules with different conformations. Nature Medicine 4:1157-1165.

Safar JG, DeArmond SJ, Kociuba K, Deering C, Didorenko S, Bouzamondo-Bernstein E, Prusiner SB, Tremblay P (2005). Prion clearance in bigenic mice. J Gen Virol 86:2913-2923.

Safar JG, Scott M, Monaghan J, Deering C, Didorenko S, Vergara J, Ball H, Legname G, Leclerc E, Solforosi L, Serban H, Groth D, Burton DR, Prusiner SB, Williamson RA (2002). Measuring prions causing bovine spongiform encephalopathy or chronic wasting disease by immunoassays and transgenic mice. Nat Biotechnol 20:1147-1150.

Schultz J, Schwarz A, Neidhold S, Burwinkel M, Riemer C, Simon D, Kopf M, Otto M, Baier M (2004). Role of interleukin-1 in prion disease-associated astrocyte activation. Am J Pathol 165:671-678.

Schwartz M, Butovsky O, Brück W, Hanisch UK (2006). Microglial phenotype: is the commitment reversible? Trends Neurosci 29:68-74.

Seeger H, Heikenwalder M, Zeller N, Kranich J, Schwarz P, Gaspert A, Seifert B, Miele G, Aguzzi A (2005). Coincident scrapie infection and nephritis lead to urinary prion excretion. Science 310:324-326.

Shmerling D, Hegyi I, Fischer M, Blattler T, Brandner S, Gotz J, Rulicke T, Flechsig E, Cozzio A, von Mering C, Hangartner C, Aguzzi A, Weissmann C (1998). Expression of amino-terminally truncated PrP in the mouse leading to ataxia and specific cerebellar lesions. Cell 93:203-214.

Sigurdson CJ, Aguzzi A (2007). Chronic wasting disease. Biochim Biophys Acta 1772:610-618.

Sigurdson CJ, Manco G, Schwarz P, Liberski P, Hoover EA, Hornemann S, Polymenidou M, Miller MW, Glatzel M, Aguzzi A (2006). Strain fidelity of chronic wasting disease upon murine adaptation. J Virol 80:12303-12311.

Silveira JR, Raymond GJ, Hughson AG, Race RE, Sim VL, Hayes SF, Caughey B (2005). The most infectious prion protein particles. Nature 437:257-261.

Simard AR, Soulet D, Gowing G, Julien JP, Rivest S (2006). Bone marrow-derived microglia play a critical role in restricting senile plaque formation in Alzheimer's disease. Neuron 49:489-502.

Simonic T, Duga S, Strumbo B, Asselta R, Ceciliani F, Ronchi S (2000). cDNA cloning of turtle prion protein. FEBS Lett 469:33-38.

Solassol J, Crozet C, Lehmann S (2003). Prion propagation in cultured cells. Br Med Bull 66:87-97.

Stahl N, Borchelt DR, Hsiao K, Prusiner SB (1987). Scrapie prion protein contains a phosphatidylinositol glycolipid. Cell 51:229-240.

Stahl N, Baldwin MA, Teplow DB, Hood L, Gibson BW, Burlingame AL, Prusiner SB (1993). Structural studies of the scrapie prion protein using mass spectrometry and amino acid sequencing. Biochemistry 32:1991-2002.

Steele AD, Emsley JG, Ozdinler PH, Lindquist S, Macklis JD (2006). Prion protein (PrPc) positively regulates neural precursor proliferation during developmental and adult mammalian neurogenesis. Proc Natl Acad Sci U S A 103:3416-3421.

Stoppini L, Buchs PA, Muller D (1991). A simple method for organotypic cultures of nervous tissue. J Neurosci Methods 37:173-182.

Strumbo B, Ronchi S, Bolis LC, Simonic T (2001). Molecular cloning of the cDNA coding for Xenopus laevis prion protein. FEBS Letters 508:170-174.

Taraboulos A, Jendroska K, Serban D, Yang SL, DeArmond SJ, Prusiner SB (1992). Regional mapping of prion proteins in brain. Proc Natl Acad Sci U S A 89:7620-7624.

Telling GC, Scott M, Mastrianni J, Gabizon R, Torchia M, Cohen FE, DeArmond SJ, Prusiner SB (1995). Prion propagation in mice expressing human and chimeric PrP transgenes implicates the interaction of cellular PrP with another protein. Cell 83:79-90.

Tobler I, Gaus SE, Deboer T, Achermann P, Fischer M, Rülicke T, Moser M, Oesch B, McBride PA, Manson JC (1996). Altered circadian activity rhythms and sleep in mice devoid of prion protein. Nature 380:639-642.

Vorberg I, Raines A, Priola SA (2004). Acute formation of protease-resistant prion protein does not always lead to persistent scrapie infection in vitro. J Biol Chem 279:29218-29225.

Vorberg I, Buschmann A, Harmeyer S, Saalm ller A, Pfaff E, Groschup MH (1999). A novel epitope for the specific detection of exogenous prion proteins in transgenic mice and transfected murine cell lines. Virology 255:26-31.

Wadsworth JD, Asante EA, Desbruslais M, Linehan JM, Joiner S, Gowland I, Welch J, Stone L, Lloyd SE, Hill AF, Brandner S, Collinge J (2004). Human prion protein with valine 129 prevents expression of variant CJD phenotype. Science 306:1793-1796.

Weissmann C (1991). A 'unified theory' of prion propagation. Nature 352:679-683.

Weissmann C (2004). The state of the prion. Nat Rev Microbiol 2:861-871.

Wilesmith JW (1988). Bovine spongiform encephalopathy. Vet Rec 122:614.

Williams A, Lucassen PJ, Ritchie D, Bruce M (1997). PrP deposition, microglial activation, and neuronal apoptosis in murine scrapie. Exp Neurol 144:433-438.

Williams ES, Young S (1980). Chronic wasting disease of captive mule deer: a spongiform encephalopathy. J Wildl Dis 16:89-98.

Wroe SJ, Pal S, Siddique D, Hyare H, Macfarlane R, Joiner S, Linehan JM, Brandner S, Wadsworth JD, Hewitt P, Collinge J (2006). Clinical presentation and pre-mortem diagnosis of variant Creutzfeldt-Jakob disease associated with blood transfusion: a case report. Lancet 368:2061-2067.

Yull HM, Ritchie DL, Langeveld JP, van Zijderveld FG, Bruce ME, Ironside JW, Head MW (2006). Detection of type 1 prion protein in variant Creutzfeldt-Jakob disease. Am J Pathol 168:151-157.

Zanusso G, Farinazzo A, Prelli F, Fiorini M, Gelati M, Ferrari S, Righetti PG, Rizzuto N, Frangione B, Monaco S (2004). Identification of distinct N-terminal truncated forms of prion protein in different Creutzfeldt-Jakob disease subtypes. J Biol Chem 279:38936-38942.

Zhang CC, Steele AD, Lindquist S, Lodish HF (2006). Prion protein is expressed on long-term repopulating hematopoietic stem cells and is important for their self-renewal. Proc Natl Acad Sci U S A 103:2184-2189.

ACKNOWLEDGEMENTS

I would like to express my gratitude to Professor Adriano Aguzzi for his support, brilliant ideas and guidance throughout my Ph.D. thesis.

Furthermore, I would like to express my gratitude to a number of people who have helped me throughout:

Dr. Frank L. Heppner deserved many thanks for allowing me to work with the *CD11b-HSVTK* mice and for getting me started with the organotypic slice cultures. Both Frank and Denis Marino has been a big help throughout the first part of my thesis. On the same note I would like to thank Beat Gähwiler and Lotty Rietschin for teaching me how to prepare organotypic slice cultures.

A big thank you goes out to Li-Chun Infanger, Dimitri Goriounov and the BZL-team for taking care of my mice and for helping with the genotyping of the mice.

I would also like to thank all my current and former colleagues at the institute of neuropathology. Especially I would like to thank Petra Schwarz for performing histoblots, Ilan Margalith for collaborating on the transmission experiments in figure 12 and for helping me with the occasional westernblot or medium change, Anna Maria Calella for performing PNGase treatments and Christian Julius and Audrey Marcel for performing all scrapie cell assays.

I would also like to extend my gratitude to Zentrum für Neurowissenschaften Zurich (ZNZ), the Center for Transgenic excellence, the Desiree and Niels Yde foundation, Henny Sophie Clausen og møbelarkitekt Axel Clausens Foundation and the Ivan Nielsens Foundation for financial support throughout my Ph.D.

Finally, I would like to express my outmost gratitude to my father, Jane, Rasmus, Lasse, Marcel Leist and my fantastic friends whose support has been there throughout.

CURRICULUM VITAE

Jeppe Falsig Pedersen
Date of Birth: October 5th, 1976
Place of birth: Copenhagen, Denmark

Education and Training

Institution	Degree or Position	Year(s)	Subject of study
University Hospital of Zürich, Switzerland. Supervisor: Professor. Adriano Aguzzi	Ph.D. Student	Apr.2004 - Dec. 2007	Prion Diseases
H. Lundbeck A/S, Valby, Denmark and Copenhagen University, Denmark Supervisor: Dr. Marcel Leist	Master's Degree	2001-2004 (27 months)	Neuroinflammation
Biochemistry Studies, Copenhagen University (Copenhagen, Denmark)	Master of Science	2001-2004	Molecular and Cellular Biology
Ontario Cancer Institute, University of Toronto (Ontario, Canada). Supervisor: Dr. Emil Pai	Summer Internship	Summer 2001	Protein Chemistry and X-ray Crystallography
Sanct Hans Hospital (Roskilde, Denmark). Supervisor: Thomas Werge	Summer Internship	Summer 2000	Cell biology and Electrophysiology
Biochemistry Studies, Copenhagen University (Copenhagen, Denmark)	Bachelor of Science	1998-2001	Chemistry, Math, Physics, Biology and Biochemistry
Royal Danish Engineering Core (Farum, Denmark).	Sergeant	1996-1998	Communication and Basic Training
Highschool, Alberstlund Gymnasium (Albertslund, Denmark)	Student	1993-1996	Natural sciences

Publications

Falsig J. and Aguzzi A. 2008. The prion organotypic slice culture assay - POSCA. *Nat. Protocols*, In Press.

Falsig J., Julius C., Margalith I., Schwarz P., Heppner F.L., and Aguzzi A. 2008. A versatile prion replication assay in organotypic brain slices. *Nat. Neurosci.*, 11(1):109-117.

Falsig J., van Beek J., Hermann C., and Leist M. 2007. Molecular basis for detection of invading pathogens in the brain (Review). *J. Neurosci. Res.* In press.

Geist M.A., Volbracht C., Podhorna J., **Falsig J.**, and Leist M. 2007. Wide spectrum modulation by KP-544 in models relevant for neuronal survival. *Neuroreport.* 18(6):571-5.

Lund S., Christensen K.V., Hedtjarn M., Mortensen A.L., Hagberg H., **Falsig J.**, Hasseldam H., Schrattenholz A., Porzgen P., and Leist M. 2006. The dynamics of the LPS triggered inflammatory response of murine microglia under different culture and in vivo conditions. *J Neuroimmunol.* 180(1-2):71-87.

Falsig J., Porzgen P., Lund S., Schrattenholz A., and Leist M. 2006. The inflammatory transcriptome of reactive murine astrocytes and implications for their innate immune function. *J Neurochem.* 96(3):893-907.

Lotharius J., **Falsig J.**, van Beek J., Payne S., Dringen R., Brundin P., and Leist M. 2005. A novel human model of parkinsonian neurodegeneration and its modulation by the pan-mixed lineage kinase inhibitor CEP1347. *J. Neurosci.* 25(27):6329-42.

Heppner F.L., Greter M., Marino D., **Falsig J.**, Raivich G., Hövelmeyer N., Waisman A., Rülicke T., Becher B., and Aguzzi A. 2005. Experimental autoimmune encephalomyelitis repressed by microglial paralysis. *Nature Medicine* 11(2):146-52

Falsig J., Christiansen S.H., Feuerhahn S., Bürkle A., Oei S.L., Keil C., and Leist M. 2004. PARG as a target for neuroprotective intervention: Investigation of currently available tool compounds. *Eur. J. Pharmacol.* 497(1) :7-16

Falsig J., Pörzgen P., Leist M. 2004. Specific modulation of astrocyte inflammation by inhibition of mixed lineage kinases by CEP-1347. *J. Immunol.* 173(4):2762-70

Falsig J., Pörzgen P., Leist M. 2004. Cytokine treatment of astrocytes affects the expression pattern of apoptosis-related genes and increases the sensitivity towards CD95-driven apoptosis. *Signal Transduction* 4(1-2):17-28

Falsig J., Latta M., Leist M. 2004. Defined inflammatory states in astrocyte cultures: Correlation with susceptibility towards CD95-driven apoptosis. *J. Neurochem.* 88(1):181-93

Jeppe Matzen and **Jeppe Falsig Pedersen**. Hjortegalskaben haerger I USA. (Chronic Wasting Disease ravages the US). *Politiken* (second largest daily DK newspaper), ¾ of the front page of the Science and Debate section, 26. December 2005.